In presenting the dissertation as a partial fulfillment of the requirements for an advanced degree from the Georgia Institute of Technology, I agree that the Library of the Institution shall make it available for inspection and circulation in accordance with its regulations governing materials of this type. I agree that permission to copy from, or to publish from, this dissertation may be granted by the professor under whose direction it was written, or, in his absence, by the dean of the Graduate Division when such copying or publication is solely for scholarly purposes and does not involve potential financial gain. It is understood that any copying from, or publication of, this dissertation which involves potential financial gain will not be allowed without written permission.

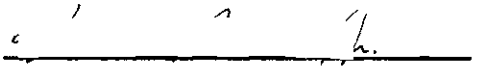

THE ADSORPTION OF POLYMERS BY POROUS AND NON-POROUS ADSORBENTS

A THESIS

Presented to

The Faculty of the Graduate Division

by

Harris Burns, Jr.

In Partial Fulfillment

of the Requirements for the Degree

Doctor of Philosophy

in the School of Chemistry

Georgia Institute of Technology

June, 1964

THE ADSORPTION OF POLYMERS

BY POROUS AND NON-POROUS ADOSRBENTS

Approved:

Chairman

Date Approved by Chairman: June 4, 1964

ACKNOWLEDGMENTS

I wish to express my deepest appreciation to all those who have helped me in the course of this work. I am particularly indebted to Dr. Dewey K. Carpenter for suggesting the problem and for guiding my progress throughout; to the members of my Reading Committee, Drs. Robert A. Pierotti and H. Clay Lewis, for many helpful discussions and suggestions; to Dr. Clyde Orr, Jr., Mr. William J. Corbett, and Mr. John H. Burson for their assistance in making surface area and particle size measurements and for their generosity in allowing me to use their equipment; and to Mr. Donald E. Lillie and Mr. Malcolm Rucker for their assistance in constructing my apparatus. I am also indebted to the United States Steel Corporation and the National Science Foundation for financial support during the course of my studies. Finally, I am most grateful to my wife, Priscilla Goree Burns, for her patience and forebearance during a long, trying, and often lonely ordeal.

TABLE OF CONTENTS

LIST OF TABLES

Page

LIST OF ILLUSTRATIONS

Figure

Figure Page

NOMENCLATURE

A	specific adsorption.
A_o	specific adsorption at zero concentration.
a	working-standard constant in light scattering; exponent in empirical relation between molecular weight and adsorption; exponent in Mark-Houwink equation.
a_o	area of an adsorption site; area occupied by an adsorbed molecule or segment.
B	second virial coefficient.
C	third virial coefficient; concentration; empirical constant.
c	concentration.
D	diameter.
d	deflection of refractometer beam.
F	distribution function; transmittance of optical filters.
G	galvanometer reading.
h	osmotic head; beam width in light scattering.
I_o	intensity of incident light.
i_θ	intensity of scattered light.
K	empirical constant; equilibrium constant.
K'	optical constant in light-scattering equation; empirical constant.
k	empirical constant.
L	distance between ends of a polymer chain.
M	molecular weight.
M_n	number-average molecular weight.
M_w	weight-average molecular weight.

M_o molecular weight of a polymer segment.

N number (of molecules, particles, etc.)

N_A Avogadro's number.

n refractive index.

$P(\theta)$ $\text{Lim}_{c \to 0} R(\theta)/R_o(\theta)$.

p fraction of segments in adsorbed polymer molecule actually adhering to the adsorbing surface; pressure.

p_s saturation pressure.

R radius; gas constant.

$R(\theta)$ reduced scattering intensity.

r radius.

S specific surface area.

T absolute temperature.

TD reference-standard constant in light scattering.

t total number of segments in a polymer molecule; time, film thickness.

V volume.

v volume.

w weight of adsorbent.

α expansion factor.

β effective bond length.

Γ form of second virial coefficient; number of segments adsorbed per adsorption site.

δ small difference between two measurements.

ε constant in Beer-Lambert relation between absorbance and concentration.

η viscosity.

$[\eta]$ intrinsic viscosity.

η_{sp}	specific viscosity
θ	thermodynamic ideal temperature for polymer solutions; fraction of adsorbent surface covered; scattering angle.
π	osmotic pressure.
λ	wavelength of light.
ρ	depolarization; density.
σ	surface tension.
Φ	Flory-Fox parameter.

SUMMARY

A study was made of the adsorption of polystyrene from cyclohexane solution onto aluminum and aluminum oxide surfaces. Four polystyrene fractions were obtained, ranging in molecular weight from 67,000 to 1,800,000. The weight-average molecular weights of the fractions were determined by light scattering and the number-average molecular weights by osmometry, except in the case of the fraction of highest molecular weight. Osmotic pressure could not be used to measure so high a molecular weight, and the molecular weight distribution was determined by fractionation. A very brief study was made of the adsorption of unfractionated polyisobutylene from benzene solution onto aluminum for comparison.

The surface areas of the two adsorbents were measured by the BET technique, and the pore-size distribution of the aluminum oxide was determined by low-temperature nitrogen adsorption. The aluminum appeared to be essentially non-porous.

The adsorption measurements were made by shaking aliquots of polymer solution of known initial concentration with weighed portions of adsorbent; then measuring the concentration of the solution afterward. The amount of polymer adsorbed per gram of adsorbent (specific adsorption) was determined from the initial and final concentrations, the amount of solution, and the amount of adsorbent used. Solutions were analyzed spectrophotometrically in the case of polystyrene, but a gravimetric technique had to be used for analysis of polyisobutylene

solutions. The adsorption of ethylbenzene was also studied briefly as a monomeric analog to polystyrene.

Adsorption rates were determined by measuring specific adsorption as a function of time. Adsorption appeared to be completed very quickly, at least within a matter of hours, on aluminum, but continued at a measurable rate for many days on aluminum oxide. It was doubtful whether true equilibrium was ever established, even after 25 days, in the adsorption on aluminum oxide.

Adsorption isotherms were plotted as specific adsorption versus final concentration in solution. The range of concentration studied was from zero to about 100 milligrams of polymer per 100 grams of solution. The isotherms for adsorption on aluminum powder were nearly horizontal straight lines in three out of the four cases at both 34.8° and 50° C. The fraction of highest molecular weight showed anomalous behavior in that its isotherm had a steep slope at both temperatures although its intercept was in good agreement with that expected from the trend shown by the other fractions. The intercepts of the aluminum isotherms were found to be related to molecular weight by the empirical equation

$$A_o = K\bar{M}_w^{\,a}$$

where A_o = specific adsorption at zero concentrations;

$\bar{M}_w$ = weight-average molecular weight;

K,a = constants.

Adsorption on aluminum increased with increasing molecular weight and decreased slightly with increasing temperature.

Adsorption on aluminum oxide showed a reversal of the molecular weight dependence, with the low-molecular-weight fractions being much more strongly adsorbed. This behavior was attributed to the ability of the smaller molecules to penetrate the pore structure of the porous adsorbent more deeply than the larger molecules. Assuming that a given quantity of polymer is adsorbed in a film of the same area on either aluminum or aluminum oxide, it was possible to estimate the radius of the smallest pores penetrated by each fraction by calculating the area of the film on aluminum oxide from that on aluminum and determining the corresponding pore radius from the measured distribution of surface area within pores. This radius was found to be in reasonable agreement with the radius of gyration of the polymer molecule in solution. The agreement appeared to be sufficiently good to make possible the use of adsorption on porous adsorbents as a semi-quantitative measure of molecular dimensions of well-fractionated samples and as a method of selective fractionation.

Polyisobutylene was not adsorbed on aluminum from benzene, even though benzene is a poor solvent for this polymer. This result was attributed to preferential adsorption of the solvent.

The adsorption of ethylbenzene from cyclohexane was studied briefly in order to estimate the magnitude of the heat of adsorption per segment of polystyrene. No measurable adsorption of ethylbenzene on aluminum was found. Isotherms for the adsorption of ethylbenzene on aluminum oxide were measured at 35° and 50° C. and the heat of adsorption per mole calculated from their slopes. This was found to be about 4220 calories per mole or about 3.3 RT. Although this is

a crude estimate of the actual heat of adsorption of polystyrene segments, it does indicate that the segment-surface interaction is probably quite strong.

CHAPTER I

INTRODUCTION

The physico-chemical behavior of macromolecules is, of course, governed by the laws of thermodynamics as is that of small molecules. Yet in such properties as vapor pressure and osmotic pressure, polymer solutions show far greater deviations from "ideal" behavior than do solutions of small molecules. These deviations are explained by the large entropies of mixing that result from the great difference in size and flexibility between solute and solvent molecules.

Similarly, large configurational entropies affect the adsorption of polymers on solid surfaces. The number of possible configurations of a polymer molecule at a surface is many times larger than that of a small molecule, and the polymer chain may have many points of attachment to the surface. It is not surprising, then, that the behavior of adsorbed polymeric materials is quite different from that of smaller molecules.

Considerable differences are also found in the adsorption behavior of various kinds of polymers. Thus, a study of the adsorption of a given polymer sample should provide a tool for its characterization. The analysis of adsorption data is, however, complex; and a great deal of effort is necessary to ascertain the factors responsible for the results.

Properties of Polymers in Solution

The chemical potential, μ_1, of a solvent in which any nonelectrolyte

is dissolved is given by the equation

$$\mu_1 - F_1^o = (RTV_1^o/M)c_2(1 + Bc_2 + Cc_2^2 + \ldots) \qquad (1)$$

where F_1^o = molar free energy of pure solvent;

R = gas constant;

T = absolute temperature;

V_1^o = molar volume of pure solvent;

M = molecular weight of solute;

c_2 = concentration of solute (weight per unit volume);

B, C = constants which are determined by the solvent, the solute, and the temperature (1). Equation 1 is called a "virial equation" by analogy with the power-series representation of the equation of state of an imperfect gas.

When the solute is a polymer which is not homogeneous with respect to molecular weight, M represents the number average molecular weight.

The constant B, known as the second virial coefficient, is found to increase with increasing temperature. In poor solvents there exists a temperature, θ, at which B is equal to zero. At this temperature dilute solutions of the polymer exhibit ideal behavior over a fairly wide range of concentration (2).

Certain properties of ideal (or "theta") solutions of polymers are of particular interest: Molecular dimensions of the dissolved molecules are those of an unperturbed random coil. The dissolved polymer molecules interpenetrate each other freely, showing neither mutual attraction nor

repulsion (2). The theta temperature for a given solvent is the critical precipitation temperature for a polymer of infinite molecular weight; for polymers of finite molecular weight, phase separation occurs somewhat below this temperature (3).

Polymer Adsorption: Experimental Background

The earliest experimental studies of polymer adsorption were those of Mark and Saito (4), who tried to develop a chromatographic method of polymer fractionation. Similar work was done by the Claessons (5,6) and Landler (7). Since 1950 the number of investigations has increased considerably, and a fairly consistent picture of adsorption behavior of polymers has begun to develop.

The Adsorption Isotherm

The form of the adsorption isotherm was established for a variety of polymers, solvents, and adsorbents by Jenckel and Rumbach (8) and has been found to be followed, with only small variations, by practically all systems studied subsequently in which non-porous adsorbents were used. Characteristically the amount of polymer adsorbed per gram of adsorbent rose very sharply with increasing concentration at low concentration, then leveled off to form a plateau, which persisted over a wide range of concentration.

In order to obtain thermodynamic data it is desirable to measure the slope of the isotherm as the concentration of polymer in the supernatant solution approaches zero. In some cases this appears to be possible; in others it does not. Binford and Gessler (9) obtained isotherms for the adsorption of polyisobutylene and butyl rubber on carbon blacks. Except for the fractions of highest molecular weight, all showed

rather gentle initial slopes, approaching the plateau at fairly high concentrations. Patat and co-workers (10-12) measured the adsorption of various polymers on metal and polymeric foils and obtained isotherms that had quite small slopes at low concentration and approached the plateau very slowly. The initial slopes of isotherms for the adsorption of polydimethyl siloxane fractions on iron and glass were measurable and increased regularly with increasing molecular weight (13).

Other investigators, however, have found that at the lowest concentrations that can be determined experimentally, the adsorption appears to be at or near its maximum value. The adsorption of polyvinyl acetate on iron and glass powders was appreciable at the lowest concentrations that could be measured, even in very good solvents (14). The adsorption of polystyrene from toluene on carbon black showed similar behavior (15), as did the adsorption of polymethyl methacrylate on iron and glass (16).

The adsorption isotherm for polyvinyl acetate on porous carbon, measured by Kangle and Pacsu (17), also showed no sign of approaching zero adsorption at low concentration. It differed from those previously discussed by not having a flat plateau. Rather it showed adsorption increasing linearly with concentration up to a concentration of more than ten grams per liter. The difference may be ascribed either to the use of a polymer sample having a much broader molecular weight distribution than those used in other studies or to the use of a porous adsorbent.

The Adsorbed Film

The direct investigation of the surface film is a formidable problem that has only recently begun to yield a solution. Certain inferences may be drawn from equilibrium measurements concerning the nature of the

polymer at the surface. A comparison of the amount of polymer absorbed per square meter of surface with the cross-sectional area of a polymer segment led Jenckel and Rumbach (8) to conclude that only a small percentage of polymer segments are adsorbed, the rest being in long pendant loops away from the surface but anchored to it by the adsorbed segments. Koral, Ullman, and Eirich (14) compared adsorption data with the area of polyvinyl acetate monolayer determined by a spread-film experiment and concluded that the adsorbed film had a thickness corresponding to 10-20 layers of monomer units. Similar results were reported for polydimethyl siloxane (13).

However, the calculations of the film thickness of adsorbed polymethyl methacrylate led to ambiguous results and suggested the adsorption of a single monolayer or even less (16). Binford and Gessler (9) concluded that the elastomers they studied lay flat on the surface, whereas the work of Kolthoff, Gutmacher, and Kahn (18) and Kolthoff and Gutmacher (19) showed no relation between specific surface area of various carbon blacks and their capacity for adsorbing synthetic rubber.

It is natural to suppose that polymers that contain polar functional groups will be adsorbed by attachment of these polar groups to a polar surface. This idea receives support from the fact that adsorption of polar polymers such as polyvinyl acetate (14) and polymethyl methacrylate (16) appears to be greater than that of polyisobutylene (9) and synthetic rubber (18,19). However, there are great differences in the experiments on these materials that have been reported; and any comparison of the results is necessarily tentative. More reliable evidence is the greatly enhanced adsorption of polymethyl

methacrylate when a very small percentage of the ester linkages in the chain were hydrolyzed (16). Recent work by Fontana (20) has shown that adsorption of carbonyl groups in polyalkyl methacrylates is completely excluded by addition of a small percentage of more highly polar ether linkages in polyethylene glycol side chains.

Apparently competition between solvent and polymer for surface sites has a major effect on adsorption. Koral, Ullman, and Eirich (14) found that no polyvinyl acetate was adsorbed from acetonitrile onto tin, even though acetonitrile is a relatively poor solvent. Acetonitrile is a non-solvent for polymethyl methacrylate; yet addition of a small quantity to benzene was found to cause a dramatic reduction in the amount of this polymer adsorbed on iron (16). Adsorption of polymethyl methacrylate is greater from trans-1, 2-dichloroethylene than from the more polar cis isomer. Because of the high polarities of acetonitrile and cis-1, 2-dichloroethylene, it seems likely that they are preferentially adsorbed, leaving little or no surface available for the adsorption of the polymer. Fontana has also shown that "goodness" of solvent as indicated by intrinsic viscosity measurements is of less importance in adsorption than is competition between solvent and polymer for sites on the surface (20).

Fontana and Thomas (21) measured the fraction of the carbonyl groups in polylauryl methacrylate adsorbed on silica via the shift in the characteristic vibration frequency of the carbonyl which occurs on adsorption. Assuming that all adsorption occurs in this way, they calculated the fraction of segments attached to the surface as 0.36. They concluded that the adsorbed polymer is considerably flattened on the surface and not randomly coiled as in solution. Addition of ether

linkages in polyethylene glycol side chains practically eliminated adsorption through the carbonyl, even though the ratio of ether linkages to carbonyl groups was only about one to twenty (20). Addition of the ether linkages probably had the effect of thickening the film by excluding most of the segments from the surface and keeping them in long loops extending into the solution.

Stromberg, Passaglia and Tutas (22), studying the thickness of a film of polystyrene adsorbed from cyclohexane on chrome ferrotype plate by ellipsometry, obtained different results. Their method enabled them to measure both the film thickness and the polymer concentration in the film. The film was found to be about 210 Angstroms thick and to have a polymer concentration of about 12 grams per 100 milliliters. This result is consistent with the model of long pendant loops and relatively few points of attachment. It also appears that in this system the polymer molecules interpenetrate almost completely. This result is not surprising in view of the fact that the experiment was carried out somewhat below the theta temperature.

Reversibility

The question of whether or not a polymer film, once absorbed, can be quantitatively removed seems to depend on the system under consideration. Polyvinyl acetate, after being adsorbed from carbon tetrachloride, was desorbed almost quantitatively in one washing from iron and tin powders by acetonitrile and 1,2-dichloroethane, and partially desorbed by carbon tetrachloride (14). Binford and Gessler (9) were able to remove 39 percent of a butyl rubber fraction with a molecular weight of 8,800 from carbon by prolonged extraction with a good solvent

in a Soxhlet extractor. Only three percent of a fraction with a molecular weight of 325,000 could be removed by the same procedure. Frisch, Hellman, and Lundberg (15) were unable to remove any detectable quantity of adsorbed polystyrene from carbon by shaking the carbon with freshly distilled toluene for several weeks. Extraction with boiling toluene in a Soxhlet extractor removed only about ten percent of adsorbed polystyrene after three days. Adsorption of polymethyl methacrylate on iron and glass appeared to be irreversible when the solvent was pure benzene, but completely reversible if a small percentage of acetonitrile was added (16). Again, preferential adsorption of acetonitrile seems to be of importance.

Kangle and Pacsu (17) found that adsorbed polyvinyl acetate could not be eluted from carbon by acetone, a poor solvent. When a good solvent, chloroform, was used, about 80 percent of the adsorbed polymer was removed. The remainder was assumed to be irreversibly bound to the adsorbent.

Molecular Weight Dependence

The earliest investigationsof polymer adsorption phenomena consistently obtained results indicating preferential adsorption of low molecular weight molecules (4-7). In all of these investigations the adsorbents used were highly porous charcoals, and Claesson (3) speculated that the observed molecular weight dependence might be due to failure of large molecules to penetrate small pores. Heller and Tanaka (23) observed a reversal of this behavior when polyethylene glycols with molecular weights between 600 and 6,000 were adsorbed on carbon black and alumina.

Kolthoff, Gutmacher, and Kahn (18) discerned no appreciable relation between adsorption of GR-S rubber on carbon black and molecular weight over a molecular weight range of 32,000 to 230,000. Similar results were later reported from the same system by Kolthoff and Gutmacher (19), except that they observed a decrease in the intrinsic viscosity of the supernatant solution with time, despite constant concentration of total polymer. Their conclusion was that low molecular weight material is adsorbed rapidly but subsequently replaced in the adsorbed film by polymer of higher molecular weight.

Treiber and co-workers (24) found only a very slight increase in adsorption of polystyrene from cyclohexane on charcoal with increasing molecular weight. Hobden and Jellinek (25) found that adsorption of polystyrene from methylethyl ketone onto charcoal decreased with molecular weight. The adsorption at saturation was found to be a linear function of the reciprocal of the intrinsic viscosity of the polymer in the solvent used.

Koral, Ullman, and Eirich (14) found that maximum adsorption of polyvinyl acetate on non-porous adsorbents increased markedly with increasing molecular weight if the solvent were a poor one, and increased to a lesser extent if the solvent were good. On the other hand, porous alumina adsorbed more of a low molecular weight fraction, suggesting that access to the interior surface is an important factor in adsorption by porous solids.

The adsorption of polydimethyl siloxane on non-porous adsorbents was shown by Perkel and Ullman (13) to fit the empirical equation

$$A_s = K\bar{M}_w^a \qquad (2)$$

where A_s = amount adsorbed per gram of adsorbent at saturation;

$\bar{M}_w$ = weight-average molecular weight;

K, a = empirical constants.

The same type of equation also described the adsorption of polymethyl methacrylate (16).

Gilliland and Gutoff (26) were able to fractionate polyisobutylene and butyl rubber samples by adsorption using various carbon blacks as adsorbents. Adsorption of high molecular weight species was greatly favored in these studies. On the other hand, Kangle and Pacsu (17) studied the fractionation of polyvinyl acetate by adsorption onto porous charcoal and found that smaller molecules were preferentially adsorbed. A molecular weight distribution was determined by measuring the intrinsic viscosity of the polymer remaining in solution after adsorption using various carbon-to-polymer ratios. The intrinsic viscosity of the unadsorbed material increased as the ratio of adsorbent to polymer increased.

Adsorption Kinetics

Relatively few detailed studies of the kinetics of polymer adsorption have been made. Hobden and Jellinek (25) studied the rate of adsorption of polystyrene on charcoal from methylethyl ketone. The process took place in two stages. Both stages appeared to obey first-order kinetics. Addition of one percent methanol to the solvent had the effect of decreasing the rate of the first step but had little effect on the second. Total adsorption at saturation was slightly enhanced by addition of methanol. Jellinek and Northey (27) subsequently found that when moisture was excluded, only one step was

observed. Apparently either water or methanol is adsorbed more rapidly than is polystyrene but less strongly bound to the surface. In the first stage, both water (or methanol) and polystyrene are being adsorbed. In the second stage, polystyrene is displacing the water already adsorbed.

Yurzhenko and Malyev (28) found that adsorption of low molecular weight fractions of polystyrene and polymethacrylate esters on alumina was more rapid than that of high molecular weight fractions.

Rate curves for the adsorption of polyvinyl acetate on porous carbon, obtained by Kangle and Pacsu (17), showed very rapid adsorption initially, followed by a slow increase in adsorption that persisted for at least 90 hours, the duraction of the experiment.

Peterson and Kwei (29) studied the kinetics of the adsorption of polyvinyl acetate from benzene onto chrome plate using a radiotracer technique. They assumed that the adsorption kinetics could be described by the equation

$$d\theta/dt = k_1(1 - \theta)c - k_{-1} \qquad (3)$$

where θ = fraction of surface covered;

t = time (seconds)

k_1 = rate constant for adsorption;

k_{-1} = rate constant for desorption;

c = polymer concentration (base moles per liter)

Their data fitted Equation 3 well. Typical values for k_1 and k_{-1} were 1.98×10^2 and 4.95×10^{-5}, respectively. The adsorption appeared to take place in two stages. The data were interpreted as representing

a reversible stage in which polymer molecules adhere to the surface at a small number of sites and can be easily desorbed, followed by an irreversible stage in which the adsorbed polymer molecules collapse into the surface, and nearly all segments are adsorbed.

Polymer Adsorption: Theoretical Background

Several efforts have been made to explain the experimental facts in terms of statistical mechanics. Mackor and van der Waals (30) derived an isotherm for the adsorption of rods, and Sarolea (31) developed a theory applicable to stiff or flexible polymers with all segments in the surface.

The first theoretical treatment of polymer adsorption based on a three-dimensional model of the surface film was that of Simha, Frisch, and Eirich (32). These workers assumed the polymer was coiled near the surface and described it in terms of a three-dimensional random flight in the presence of a reflecting barrier, according to the method of Chandrasekhar (33). The fraction p of segments deposited in the surface by a molecule containing a total of t segments was calculated, the entropy and free energy of mixing of segments with surface sites and solvent molecules were determined, and a theoretical equation for the adsorption isotherm was obtained, applicable chiefly to low surface coverage.

A subsequent paper by Frisch and Simha (34) extended the treatment to apply to higher surface coverage and multilayer adsorption, and another paper by the same authors (35) corrected some errors in the original derivation and gave a new derivation for the isotherm, which differed somewhat from the original.

The results of these derivations are mathematically complex. Because the derivations involve primarily consideration of an isolated molecule at the surface and treat chain interference only approximately, the results are expected to apply quantitatively only to rather low surface coverages. Certain consequences, however, are of interest insofar as they are qualitatively related to experimental results. The theory predicts that the fraction p of segments adsorbed will be small and proportional to the square root of t, the degree of polymerization. Most segments appear in long pendant loops extending into the solution and giving rise to a rather thick surface film. This conclusion is modified by treatments of Frisch (36) and Higuchi (37), who showed that strong, short-range interactions between polymer segments and the surface ($>4kT$) could lead to collapse of the surface film, so that essentially all segments would be adsorbed.

The Simha-Frisch-Eirich theory also predicts preferential adsorption of high molecular weight polymers, the effect being large at low surface coverage and smaller as saturation is approached. Either positive or negative temperature coefficients of adsorption are possible. Positive coefficients result from desorption of solvent at high temperatures, making more sites available for polymer adsorption.

The form of the isotherm is similar to the typical experimental curves. The initial slope is considerably larger than that of the Langmuir isotherm, but the curve approximates the Langmuir isotherm at high concentration.

Gilliland and Gutoff (38) applied a similar treatment to the adsorption of heterogeneous polymers in a theta solvent. Their theory

predicts the correct form of the isotherm with the initial slope increasing with molecular weight. Preferential adsorption of either high or low molecular weight molecules is possible. High heats of adsorption favor the former because of the increase of the fraction of segments adsorbed with increasing degree of polymerization. Normally adsorption decreases with increasing temperature, but the opposite behavior is not necessarily ruled out.

Forsman and Hughes (39-41) applied chain statistics and a random-flight model to the determination of molecular dimensions at a solution-solid interface. The isotherm derived from their model predicts that the amount of polymer adsorbed at saturation is independent of molecular weight and increases with increasing temperature.

A different formulation of the problem by Silberberg (42,43) used lattice statistics and took into account the enhanced probability of adsorption of a segment that is adjacent on the chain to an adsorbed segment. The principal difference between the Silberberg and the Simha-Frisch-Eirich treatments is that the former abandons the random-flight model and, using a lattice model for the solution, counts the number of possible configurations for pendant loops of various lengths, determines the configurational entropy and the heat of adsorption, and minimizes the free energy with respect to the number of segments adsorbed. The adsorption isotherm obtained in this manner is too complex to be of general utility in evaluating experimental results, but again the qualitative results are of interest.

The Silberberg theory predicts that when all sites on the surface are available for adsorption, p has a value of 0.7. In this case, the

film would be largely collapsed and only a few Angstroms thick. On the other hand, p is much smaller where available adsorption sites are widely separated. The loops are longer and the film thicker in this case. Adsorption increases with increasing molecular weight at low molecular weights and approaches a limit as the molecular weight increases. Molecular weight dependence is more pronounced in poor solvents than in good ones.

Purpose and Scope

The aim of the present investigation has been to study the adsorption of polystyrene from a theta solvent on two adsorbents, one porous, the other non-porous, that are otherwise similar. The adsorbents chosen were aluminum powder and activated aluminum oxide. The amount of polystyrene adsorbed was studied as a function of temperature, molecular weight, and concentration. The rate of approach to equilibrium was also studied. Another theta system, polyisobutylene in benzene, was also studied briefly as a test of the effect of solvent-surface interaction on polymer adsorption.

CHAPTER II

POLYMER AND ADSORBENT CHARACTERIZATION

Before meaningful conclusions can be drawn regarding the results of the adsorption studies, certain information must be obtained about the polymer samples and the adsorbent surfaces used. The molecular weights and molecular weight distributions of the polymer samples must be known, as must the specific surface area and porosity of the adsorbents.

Polymer Preparation

The polystyrene used in this study was obtained from two sources. The high molecular weight material came from a styrene sample that had polymerized while standing. The formation of polymer in this manner proceeds very slowly by a free-radical mechanism. Since relatively few free radicals are formed spontaneously at room temperature, the probability of chain termination is quite small. Hence, the polymerization process, once initiated, goes on for quite a long time, resulting in formation of molecules of very high molecular weight.

To prepare the polystyrene for use, small pieces were dissolved in enough benzene to yield a solution of less than five percent polymer. The solution was stirred gently from time to time during the dissolution process, which required several days for completion. When the polymer appeared to be completely dissolved, it was precipitated by pouring portions of approximately 50 milliliters each into two-hundred milliliter

portions of methanol that were being violently agitated in a Waring blender. The solid polymer was separated from the supernatant liquid by filtration and washed at least three times with methanol while being agitated in the blender. It was then heated to 80° C. in an air bath until the odor of methanol had disappeared, and finally dried under vacuum at one hundred degrees for 24 hours. The final product was a rather hard, coarse, granular, odorless powder with no trace of gumminess.

The polystyrene sample of lower molecular weight was prepared by polymerization of freshly distilled styrene by benzoyl peroxide initiation. Eastman White Label styrene was shaken with aqueous sodium hydroxide to remove the tert-butyl catechol inhibitor, dried over calcium chloride, and distilled from sodium wire at a pressure of 100 millimeters of mercury.

A very small quantity of benzoyl peroxide was added to 90 milliliters of distilled styrene, and the solution was shaken thoroughly to ensure uniform mixing. Since the polymerization is strongly exothermic, it was carried out in four test tubes instead of a flask in order to increase the surface area for heat dissipation. The test tubes were filled almost to the top and were tightly stoppered. They were immersed in a thermostat at 45° C. for five days.

At the end of this time, the test tubes were broken, and the polymer remained in the form of hard rods which shattered like glass at a blow. The rods were broken into small pieces, dissolved in benzene, and precipitated in the same manner as the thermally initiated polymer described above.

"Vistanex" polyisobutylene was cut into small pieces, dissolved in cyclohexane, and precipitated by pouring into acetone in the blender. The procedure used was the same as that for polystyrene.

Fractionation

Any sample of polystyrene prepared by thermal or peroxide initiation has a wide range of molecular weights. Ideally, one would like to obtain polymer of a single molecular weight for adsorption studies, but it is necessary to be satisfied with obtaining as narrow a distribution of molecular weights as practicable. This may be done by any of the numerous fractionation techniques that are available.

Theory

Almost all methods of polymer fractionation depend on the molecular weight dependence of the distribution of polymer between phases in a two-phase system. The theory of polymer fractionation is summarized by Tompa (44). Briefly, if a sample of polydisperse polymer is dissolved in enough poor solvent to give a dilute solution, and the temperature is subsequently lowered below the theta temperature, phase separation will eventually take place. Both phases will be dilute solutions, although one phase will be richer in polymer than the other. The average molecular weight of the polymer in the polymer-rich phase will be higher than that in the polymer-poor phase.

More commonly the polymer is dissolved in a good solvent, which is then made poorer by addition of a non-solvent until phase separation occurs. Once again the polymer-rich phase at equilibrium contains polymer of higher average molecular weight than that in the polymer-poor phase.

If the polymer-rich phase is removed after each addition of non-solvent, a series of polymer samples may be recovered, each of which has a lower average molecular weight than its predecessor.

It is important to note that it is theoretically impossible by a single fractionation step to obtain two fractions, one of which has no molecules of molecular weight greater than a certain value and the other of which has no molecules of molecular weight less than the same value. In other words, the fractions obtained in any fractionation are not only not perfectly monodisperse, but also some overlap of adjacent fractions is inevitable (45).

By using proper technique and subjecting the fractions to repeated refractionation, fractions of any desired sharpness may be obtained. However, the labor involved in preparing very sharp fractions in this manner is prohibitive. Continuous fractionation methods using columns can be used to alleviate some of the difficulties encountered in stepwise processes, but these methods, too, are subject to serious limitations, particularly when used as preparative methods. Therefore, substantial polydispersity must be accepted if polymer fractions of practical size are to be obtained within a reasonable time.

Column fractionation depends for its effectiveness upon the different mobilities of the polymer-rich and polymer-poor phases. In most procedures, polymer is deposited upon a portion of the packing material at the top of the column and eluted by a mixture of solvent and non-solvent. Initially, the composition of the elutant is such that the polymer is wholly insoluble. The elutant passes over the polymer, down the column, and out at the bottom. The elutant entering the column

is continuously enriched with solvent. The elutant composition at which the low molecular weight polymer begins to dissolve is still too poor in solvent to dissolve material of higher molecular weight. However, the "undissolved" polymer is swollen by the elutant and becomes a viscous liquid like the polymer-rich phase of the fractional precipitation method. Thus it is not truly a stationary phase but moves much more slowly through the packing material than does the polymer-poor phase because of the much higher viscosity of the former.

As the elutant becomes progressively richer in solvent, larger and larger molecules can be dissolved in the polymer-poor phase. If no vertical mixing occurs, the molecular weight of polymer in each increment of solution withdrawn from the bottom of the column should be higher than that of the preceding increment.

If the temperature in the column is constant throughout, fractionation occurs in a single stage. A procedure for constant-temperature elution fractionation was developed by Desreux (46). Fractionation is effected because the smaller molecules are dissolved from the polymer-rich phase more rapidly than the larger ones.

An alternative procedure is to use thermal-gradient elution. This procedure was developed by Baker and Williams (47) and later refined by Schneider and co-workers (48). If a thermal gradient is maintained through the column such that the top of the column is at a considerably higher temperature than the bottom, the solvent power of elutant of a given composition decreases as the solution moves down the column. Theoretically the dissolved polymer precipitates as it moves into the cooler part of the column, is redissolved as the elutant in its vicinity becomes

richer in solvent, reprecipitates further down the column, and so on until it finally reaches the bottom of the column and is removed. Thus fractionation takes place in a series of equilibrium stages instead of in one step, and fractionation efficiency should be much improved over that in the constant temperature case. In practice, some improvement is observed, but far less than is predicted by theory (49). This may be caused by channeling in the column, vertical mixing, lateral thermal gradients within the column, failure to achieve equilibrium between the phases, or too high mobility of the polymer-rich phase, particularly at the higher temperatures.

Preferential adsorption of the high molecular weight polymer by the packing material may contribute somewhat to the fractionation. However, since polymer adsorption is frequently highly irreversible, it is usual to select non-adsorptive packings, such as glass beads or sand in order to avoid undue loss of polymer (50).

The principles of operation of a thermal-gradient elution column for large-scale fractionation have been discussed by Pepper and Rutherford (51) and by Schneider, Loconti, and Holmes (52).

Polymer fractionation techniques are summarized by Hall (50). During the course of this work, several different methods were tried. Stepwise fractional precipitation was found to be the most dependable method, although the column methods worked reasonably well and could probably have been made to be entirely satisfactory if enough time could have been spent developing them.

Fractional Precipitation

Stepwise fractional precipitation was used in most of the

fractionations carried out during the course of this study. A large, round-bottom flask was used as a fractionation vessel. It was immersed to the neck in a thermostat maintained at 30° C. A quantity of polymer was weighed, poured into the flask, and dissolved, with gentle stirring, in enough benzene to make the polymer concentration in the initial solution about one percent.

The precipitation was accomplished by slowly adding methanol to the solution with constant stirring. Addition of methanol caused the solution to become cloudy after precipitation had begun. The addition was continued until a mark on the outside of the flask could no longer be seen by looking through the solution.

After sufficient methanol had been added, the temperature of the thermostat was raised until the precipitate had dissolved. The temperature was then allowed to fall slowly back to 30° C., so that phase separation was re-established. This step was taken to ensure that the two phases were in true equilibrium.

After the system had remained at 30° C. for about one hour, the stirrer was turned off and the precipitate allowed to settle. This usually required several hours and normally took place overnight. When the precipitate had settled, the flask was removed from the thermostat, and the large volume of supernatant solution, the polymer-poor phase was decanted into another flask until only a small portion remained, along with the polymer-rich phase. The liquid remaining in the flask was then swirled vigorously to resuspend the relatively immobile polymer-rich phase and minimize its adherence to the walls of the flask. The suspension was poured quickly into a separatory funnel partially

immersed in the thermostat, and allowed to separate. This time separation was complete within a few minutes, and the polymer-rich phase was removed through the bottom of the funnel. The polymer-poor phase remaining in the funnel was recombined with the decanted solution, and a second separation was effected by careful addition of more methanol. This procedure was repeated until all of the polymer had been precipitated.

The polymer-rich solutions thus removed from the original solution were quite viscous. They were diluted with several times their volume of benzene, after which the polystyrene was precipitated by pouring into a large excess of methanol agitated in the Waring blender. Finally the fractions were filtered, washed several times with methanol, and dried as described above.

The viscosity-average molecular weight of each fraction was determined, and those that had appropriate molecular weights were refractionated to provide sharper fractions. (For technique of determining viscosity-average molecular weight, see pages 64-79 below.) The fractions designated B and F used in this study were refractionated by repetition of the fractional precipitation procedure. Those designated J and L were refractionated by column methods described below.

Column Fractionation Methods

In an effort to develop a fractionation procedure less tedious and time-consuming than the fractional precipitation method, two procedures using columns to effect continuous fractionation were tested. Although the results of these fractionations were less satisfactory than those of the stepwise method, they did bring about considerable

separation, and the fractions obtained were used in adsorption studies.

Elution at Constant Temperature. The column used in constant-temperature elution fractionation is shown in Figure 1. It was five centimeters in diameter and about 1.8 meters long. It was provided with a water jacket and stopcocks and the top and bottom for admitting and withdrawing the elutant. At the top of the column was a 12-liter, three-neck flask, A, connected to the column by a glass tube through the bottom of the flask. A second flask, B, beside the first, was connected to A by means of a siphon tube.

The column was packed with "Superbrite" glass beads, manufactured by the Minnesota Mining and Manufacturing Company. These had an average diameter, according to specifications, of about 0.1 millimeter. Before packing, a plug of glass wool was placed in the bottom of the column. The lower stopcock was closed, and the column was partially filled with a mixture of solvent and non-solvent of the same composition as the initial elutant. The glass beads were poured into the top of the column slowly. Enough solution was used so that the level of the packing remained lower than the top of the liquid. In this way a dense, uniform packing was obtained.

Meanwhile, 4.55 grams of polystyrene were dissolved in 500 milliliters of benzene, and methanol was added until apparently all of the polymer was precipitated. The suspension was heated to redissolve the polymer, and 200 grams of glass beads were added. The solution was then allowed to cool very slowly without stirring so as to precipitate the polymer on the beads. When the solution had reached room temperature and the supernatant liquid had become clear, the latter was decanted; and

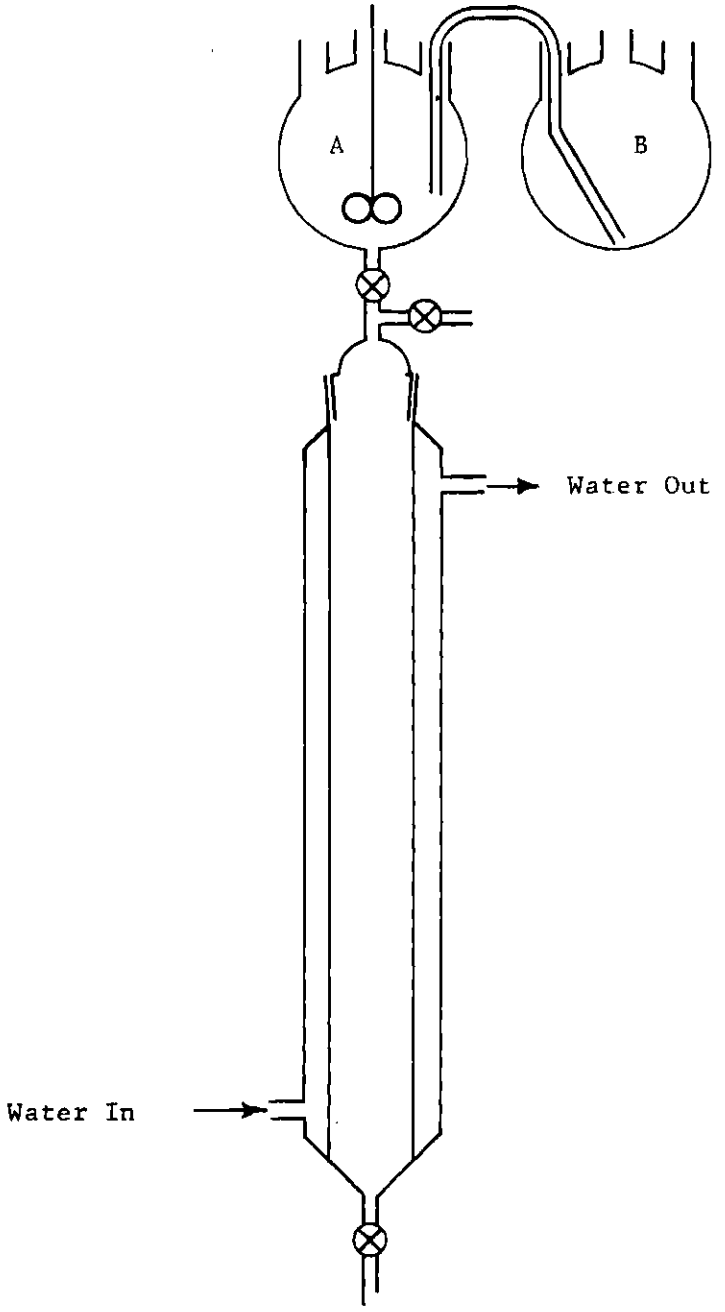

Figure 1. Constant-Temperature Elution Column

the beads and adhering polymer were poured into the top of the column on top of the rest of the packing.

The top of the column was closed, and flask A was half filled with the initial elutant solution, a mixture of 40 percent methanol and 60 percent benzene by volume. Pure benzene was placed in flask B, and the siphon tube was filled with benzene. Water at 25° C. was circulated in the water jacket. Both stopcocks were opened very slightly, and a receiver was provided to catch the effluent solution. The flow rate was kept very low, about one milliliter per minute.

The effluent solution was tested periodically for polymer by adding methanol to it. At the first trace of cloudiness, the receiver was changed, and receivers were changed thereafter whenever 200 milliliters of effluent had been collected.

Phase separation was induced in the effluent solution by addition of methanol, and the heavier phase was allowed to settle in a separatory funnel. Completeness of precipitation was checked by further addition of methanol to the supernatant liquid after settling. If there was no cloudiness, the precipitation was assumed to be complete. The polymer-rich phase was then removed and precipitated as described above. The elution was continued until no more polymer could be detected in the effluent.

The recovered polystyrene was transferred to a tared beaker, dried thoroughly, and weighed. Then a small portion of the polymer was dissolved in benzene, and a one-point determination of the viscosity-average molecular weight was made as described on pages 64-79 below. Results are summarized in Table 1.

Table 1. Results of Column Fractionation at Constant Temperature

Fraction	Weight (Grams)	Intrinsic Viscosity	Molecular Weight
1	0.0803	0.150	16,000
2	0.1711	0.177	20,000
3	0.4637	0.255	32,000
4	0.8771	0.314	43,000
5	1.2132	0.351	49,000
6	0.8610	0.362	51,000
7	0.6658	0.363	51,000
8	0.0116	0.359	50,000

Apparently fractionation was successful until the sixth fraction but failed to distinguish between the last three. It was decided that because of the large size of the available equipment and the consequent necessity for using large quantities of solvents, no further effort would be expended on this column, but that another, smaller column would be built. However, since the fractionation had been partially successful, the fourth through the sixth fractions were combined to make up the fraction designated L. All of these fractions were dissolved in benzene and reprecipitated to ensure uniform composition of the final product.

Thermal-Gradient Elution. The column used for thermal-gradient elution fractionation was similar to that of Baker and Williams (47) but was slightly modified. The apparatus is shown schematically in Figure 2. The column itself was a piece of one-inch copper pipe one meter in length. Copper flanges brazed to the top and bottom had grooves cut in them to fit a one-inch O-ring. At the bottom of the column four turns of quarter-inch copper tubing were tightly wound and soldered securely. At the top of the column was a heater composed of two meters of nichrome wire wound around the column on a thin layer of asbestos. The entire column was insulated with a layer of asbestos about one centimeter thick.

Pyrex fittings were made to be attached at the top and bottom of the column by O-rings. The top fitting had a side arm for the admission of elutant and a vent, closed with a Teflon stopcock. The vent was necessary because air, dissolved in the elutant, was driven off in the high-temperature section of the column and had to be released periodically. The bottom fitting had a medium fritted glass filter to retain the packing and a Teflon stopcock to control the flow.

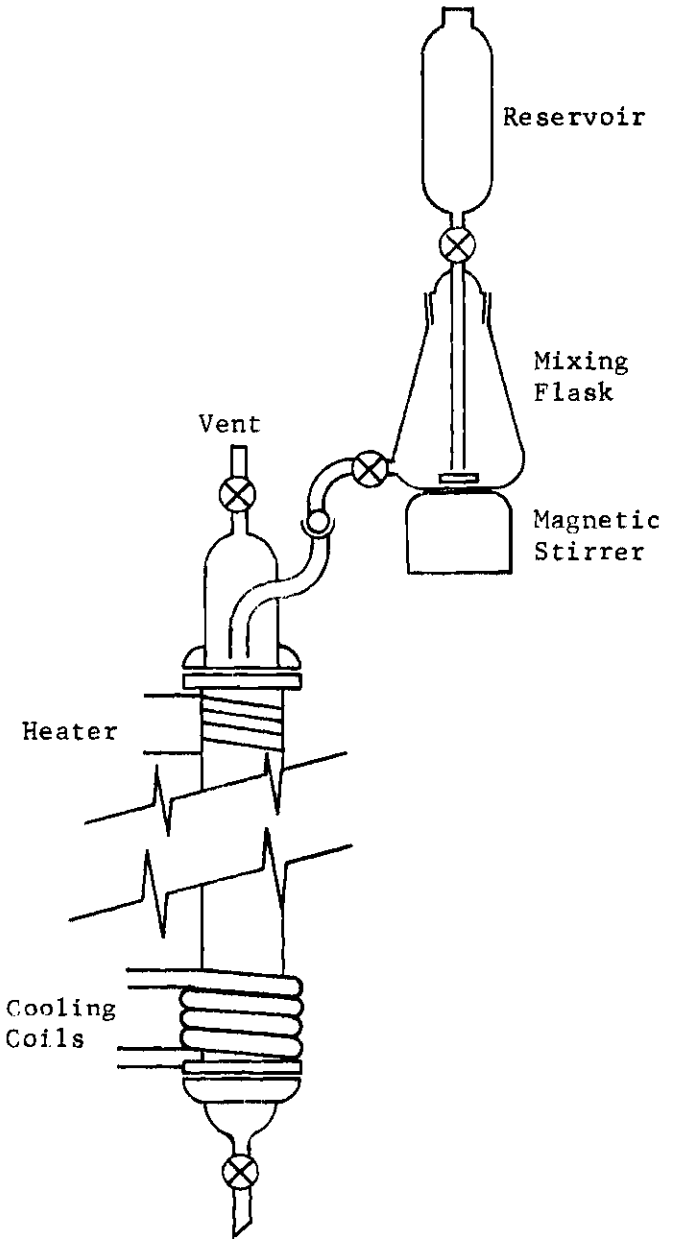

Figure 2. Thermal Gradient Elution Column

A one-liter Erlenmeyer flask was used as a mixing flask. This had a standard-taper joint at the top and was fitted with a discharge tube at the bottom. The latter was closed with a Teflon stopcock and had a ball joint at the end to join it to the side arm at the top of the column.

The solvent reservoir was a 500-milliliter separatory funnel equipped with a standard-taper joint and a stem that reached nearly to the bottom of the mixing flask.

The mixing flask initially contained a mixture of ethanol and methylethyl ketone containing 40 percent ethanol. This solvent-non-solvent pair was chosen because its azeotrope boils at a higher temperature than does that of any other pair considered (53). The reservoir contained pure methylethyl ketone. A magnetic stirrer in the mixing flask provided constant agitation.

Packing the column was accomplished in the manner described above for the constant-temperature column. Before the beads with polymer deposited on them were added, the column was filled with liquid; and, with the tip removed, cooling water was circulated in the coil and electric current was passed at low voltage through the heater. The voltage was adjusted by means of a Variac autotransformer until the temperature at the top of the column remained constant at 60° C.

Then the polymer-bearing beads were added to the column, the top was put on and filled with elutant up to the vent, and the vent was closed. The lower stopcock was opened and adjusted to deliver about ten milliliters of liquid per hour. This adjustment had to be changed frequently because of changes in the viscosity of the effluent solution.

An automatic fraction collector was used to change receivers every two hours.

The liquid in the receivers was tested for polymer by adding methanol. After the first trace of cloudiness appeared when this test was made, the contents of successive receivers were combined to form a total volume of 100 milliliters. The polymer contained in this volume of effluent was arbitrarily defined as a fraction. The receivers were rinsed with methylethyl ketone and the washings were combined with the original solution. The solution was then diluted to a total volume of 300 milliliters and precipitated by pouring into methanol as described above.

One-point viscosity determinations of molecular weight were made and the results are summarized in Table 2. Fractions five through nine were combined to form the fraction designated J.

Molecular Weight Distribution

Any sample of a synthetic polymer contains molecules of many molecular weights, M_i, such that

$$M_i = iM_o \tag{3}$$

where M_o = molecular weight of a monomer unit;

i = an integer.

This relation neglects the fact that the composition of the end groups is slightly different from that of those monomer units not at the chain end, but for high polymers, the difference is usually negligible.

The average molecular weight of a polymer sample may be defined

Table 2. Results of Thermal-Gradient Elution Fractionation

Fraction	Weight (Grams)	Intrinsic Viscosity	Molecular Weight
1	0.0574	0.172	19,000
2	0.0906	0.240	22,000
3	0.1723	0.244	31,000
4	0.3734	0.332	46,000
5	0.5135	0.388	56,000
6	0.6124	0.513	81,000
7	0.7437	0.517	83,000
8	0.7711	0.542	87,000
9	0.7124	0.623	105,000
10	0.6246	0.732	132,000
11	0.0880	0.675	117,000
12	0.1394	0.673	117,000
13	0.0953	0.628	107,000
14	0.0273	0.559	91,000

in various ways. The number-average molecular weight, $\bar{M}_n$, is defined as

$$\bar{M}_n = \sum_i N_i M_i / \sum_i N_i \qquad (4)$$

where N_i = number of molecules having molecular weight M_i. The weight-average weight, $\bar{M}_w$, is defined as

$$\bar{M}_w = \sum_i N_i M_i^2 / \sum_i N_i M_i \qquad (5)$$

These relations are summarized by Tanford (54).

Clearly these two equations can be rewritten

$$\bar{M}_n = W/N \qquad (6)$$

and

$$\bar{M}_w = \sum_i N_i W_i / W_i \qquad (7)$$

where W = weight of sample;

W_i = weight of molecules having molecular weight M_i;

N = total number of molecules in the sample.

For a perfectly homogeneous polymer (all molecules have the same molecular weight) the averages are identical. For non-homogeneous polymers, $\bar{M}_n$ is less than $\bar{M}_w$ (54).

Let a distribution function F_{nj} be defined such that

$$F_{nj} = \sum_{i=0}^{j} N_i/N \tag{8}$$

Then F_{nj} is the fraction of molecules present having molecular weight less than or equal to M_j. Similarly, a function F_{wj} may be defined as

$$F_{wj} = \sum_{i=0}^{j} W_i/W \tag{9}$$

F_{wj} is the weight fraction of polymer present having molecular weight less than or equal to M_j.

Since the number of different molecular weights present in a given polymer sample is usually quite large, the summations may be replaced by integrals to give approximate values for the functions:

$$\bar{M}_n = \int_0^\infty n(M)MdM / \int_0^\infty n(M)\,dM; \tag{10}$$

$$M_w = \int_0^\infty w(M)MdM / \int_0^\infty w(M)\,dM; \tag{11}$$

$$F_n(M) = \int_0^\infty n(M)\,dM/N; \tag{12}$$

$$F_w(M) = \int_0^\infty w(M)\,dM/W. \tag{13}$$

Now it is clear that

$$n(M) = NdF_n(M)/dM \tag{14}$$

and

$$w(M) = WdF_w(M)/dM. \tag{15}$$

Hence

$$\bar{M}_n = \int_0^\infty (dF_n/dM)MdM / \int_0^\infty (dF_n/dM)dM = \int_0^1 MdF_n / \int_0^1 dF_n = \int_0^1 MdF_n \tag{16}$$

and

$$\bar{M}_w = \int_0^\infty (dF_w/dM)MdM / \int_0^\infty (dF_w/dM)dM = \int_0^1 MdF_w / \int_0^1 dF_w = \int_0^1 MdF_w. \tag{17}$$

Only one distribution function need be known since they are related by the equation

$$w(m) = WdF_w/dM = NMdF_n/dM = Mn(M) \tag{18}$$

or

$$\int_0^1 (W/M)\,dF_w/dM = NdF_n/dM. \tag{19}$$

Now

$$\int_0^\infty (1/M)(dF_w/dM)dM = (N/W) \int_0^\infty (dF_n/dM)dM \tag{20}$$

or

$$\int_0^1 (1/M)\,dF_w = (1/\bar{M}_n) \int_0^1 dF_n = 1/\bar{M}_n. \tag{21}$$

Thus, if F_w is known as a function of M (e.g., from a fractionation experiment), both $\bar{M}_n$ and $\bar{M}_w$ are readily determined by graphical integration of Equations 21 and 17 respectively.

Fraction B had a molecular weight too high to permit meaningful osmotic pressure measurements. Hence it was necessary to obtain an approximation to its molecular weight distribution by fractionation. Because of the failure of the column methods to achieve fractionation at high molecular weights, it was decided to use fractional precipitation.

One gram of polymer was dissolved in 500 milliliters of benzene in a one-liter, globe-type separatory funnel. This was immersed to its neck in a thermostat, and the fractionation proceeded as described above. Separation of the polymer-rich phase was simplified by use of the separatory funnel since no decanting of the supernatant liquid was necessary.

After separation, the polymer-rich phase was diluted with benzene and precipitated by pouring into six times its volume of methanol in a beaker agitated by a magnetic stirrer. The precipitate was filtered with a sintered glass filter, washed thoroughly with methanol, and quantitatively transferred to a tared container. The container and its contents were warmed for several hours in a slow stream of air and then dried under vacuum at 80° C. and weighed.

One-point viscosity measurements were made to determine the average molecular weight of each fraction. The molecular-weight distribution curve was constructed by the method of Schulz (55). Booth (56) and Booth and Beeson (57) have compared various methods of constructing

distribution curves from fractionation data and concluded that this procedure is satisfactory for most purposes.

The assumptions in this method are that the distribution in any fraction is symmetrical about the viscosity-average molecular weight, and that the viscosity-average molecular weights of the two fractions adjoining a given fraction represent the outer limits of the overlap between fractions. Thus, if w_i represents the weight of fraction i and W_i is the total weight of polymer having molecular weight less than M_i, then W_i is given by

$$W_i = \sum_{j=1}^{i-1} w_j + \tfrac{1}{2} w_i . \tag{22}$$

Now F_w is given by

$$F_{wi} = W_i / W. \tag{23}$$

Fractionation data are shown in Table 3. The integral and differential distribution functions are shown in Figures 3 and 4. The integral distribution function was determined by drawing a smooth curve through the experimental points. The slope of this curve was measured at several points by placing two glass rods, side by side, over the curve, adjusting the rods until the curve appeared continuous when viewed through the rods, and drawing the normal to the tangent at each point. From the resulting line, the slope of the tangent was readily determined. The differential distribution function (Figure 4) is a

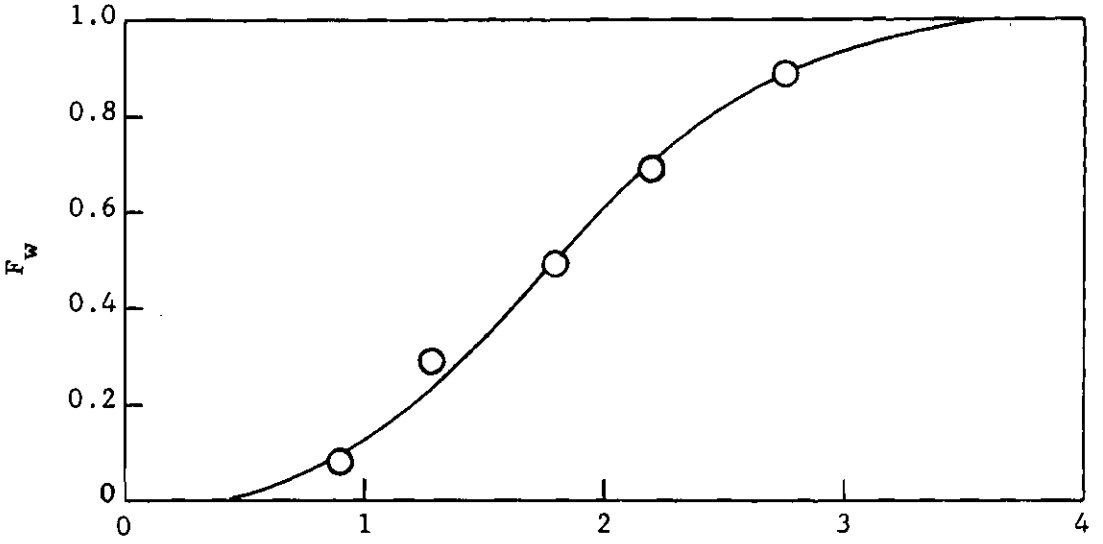

Figure 3. Integral M.W. Distribution - Fraction B

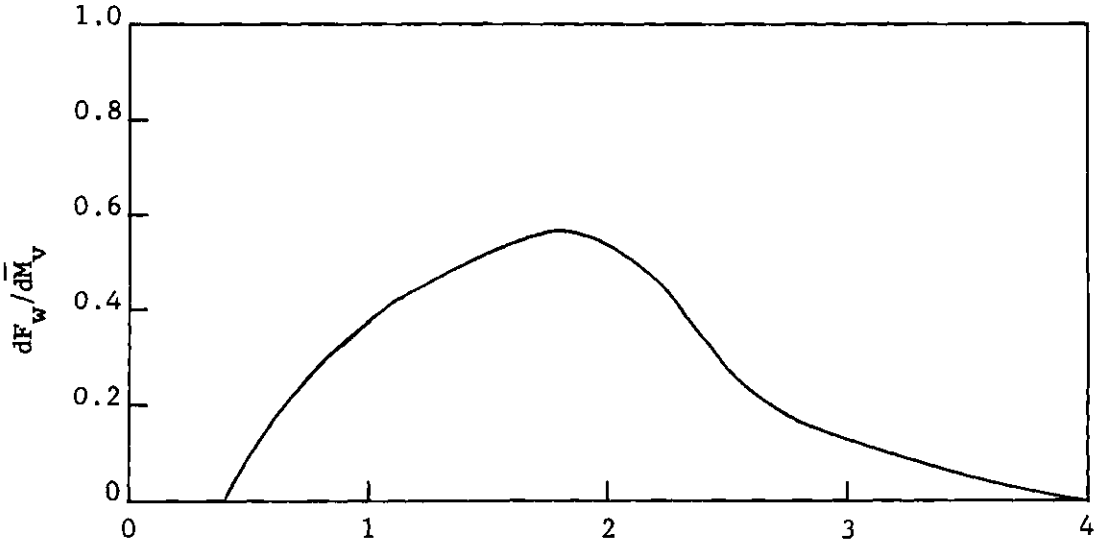

Figure 4. Differential M.W. Distribution - Fraction B

plot of the resulting slopes as a function of M.

The function $F_w(M)$, defined by Equation 23, was plotted against $\bar{M}_v$ (Figure 3). Since $\bar{M}_w$ is given by Equation 17, the weight-average molecular weight is equal to the area between the curve and the ordinate. Also, the reciprocal of $\bar{M}_v$ was plotted against F_{wi} in Figure 5. According to Equation 21, the area under this curve gives the reciprocal of $\bar{M}_n$. The areas were measured by means of a polar planimeter. The value of M_n so calculated was 15.0×10^5; that of $\bar{M}_w$ was 18.4×10^5.

Osmotic Pressure

Number-average molecular weights are most easily measured by osmometry. The relation between osmotic pressure and concentration of polymer in solution is given by

$$\pi/c = RT(1/\bar{M}_n + Bc + Cc^2 + \ldots) \qquad (24)$$

where π = osmotic pressure;

c = concentration of solute;

R = gas constant;

T = absolute temperature;

M_n = number-average molecular weight;

B, C constants in the virial equation.

Equation 24 can also be written

$$\pi/c = (RT/\bar{M}_n)(1 + \Gamma_c + g\Gamma^2c^2 + \ldots) \qquad (25)$$

Table 3. Fractionation Data, Fraction B

Fraction	Weight (Grams)	Concentration (g/100ml.)	Kinematic Viscosity	Relative Viscosity	Intrinsic Viscosity	$M_v \times 10^{-6}$
1	0.2885	0.3475	0.9217	1.930	2.12	2.76
2	0.2201	0.3008	0.7873	1.649	1.81	2.20
3	0.1893	0.2328	0.6900	1.445	1.65	1.80
4	0.2359	0.3730	0.7632	1.597	1.36	1.28
5	0.0746	0.2474	0.5851	1.226	0.89	0.90

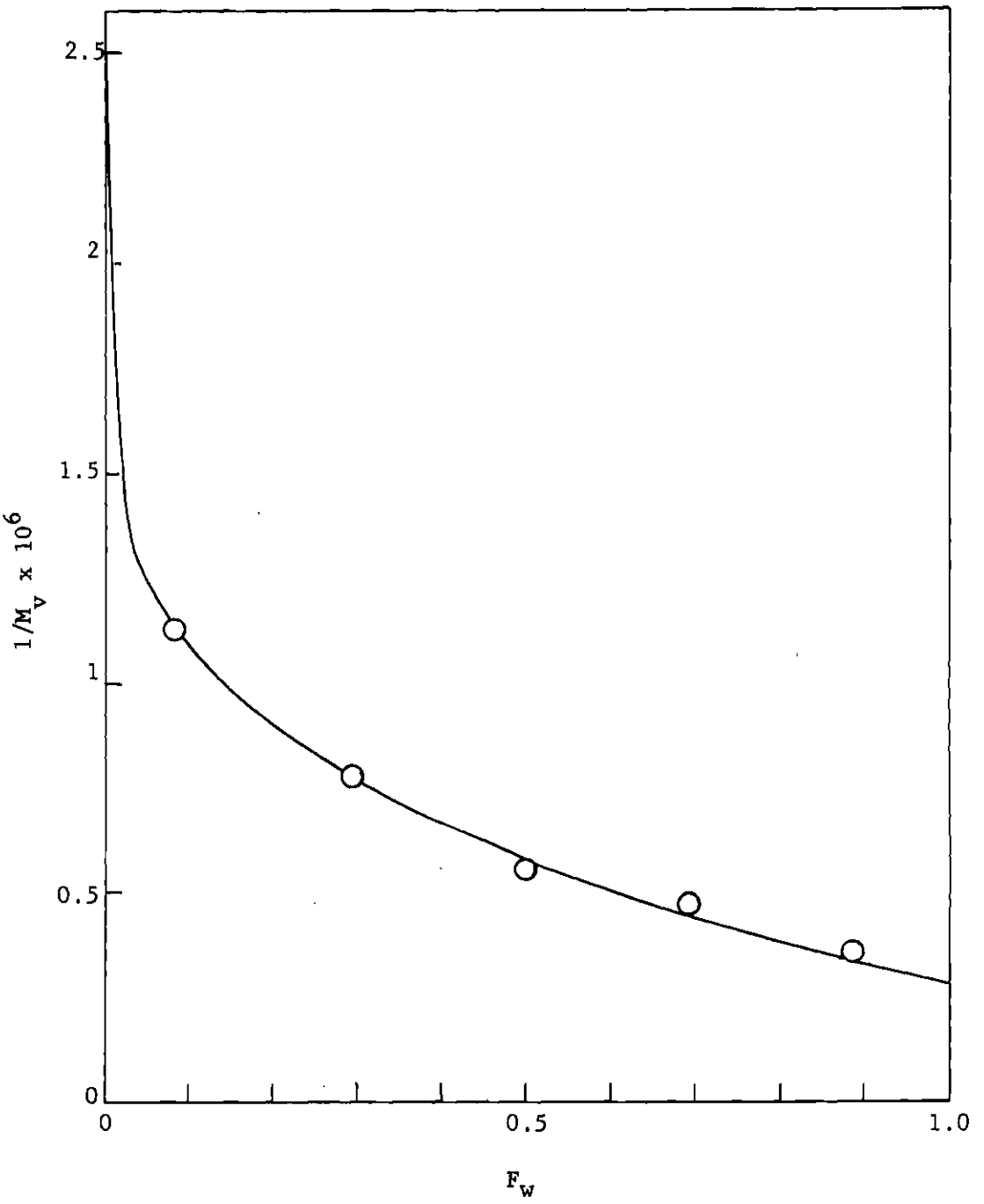

Figure 5. Graphical Integration to Determine $1/\bar{M}_n$

where Γ and g are constants derived from B and C in Equation 24. Experimentally, g turns out to be very near one-fourth in most good solvents, so we can write

$$\pi/c = (RT/M_n)(1 + \Gamma_c/2)^2 \qquad (26)$$

for low concentrations. Thus $(\pi/c)^{1/2}$ is a linear function of concentration having an intercept equal to $(RT/\bar{M}_n)^{1/2}$. The above relations, as well as the experimental procedure for osmometry, are summarized by Hookway (58).

Apparatus

The osmometer used in this work is shown schematically in Figure 6. It is a high temperature modification of the type described by Stabin and Immergut (59) and was supplied by the J. V. Stabin Company. The rate of approach to equilibrium with this type of instrument is very rapid because of the large membrane area (61 square centimeters). Equilibrium measurements could be obtained in a few hours. The membranes used were gel cellophane, No. 450, also supplied by Stabin. The osmotic head was measured by means of a Gaertner cathetometer, which could be read directly to the nearest 0.001 centimeter.

The osmometer was immersed in a large thermostat maintained at 30° C. The variation in the temperature of the thermostat was $\pm$0.015 degrees as measured by a Beckmann thermometer. The osmometer itself was insulated from the thermostat by its jacket and the unstirred benzene in it, so that the temperature variation at the osmometer itself should have been much smaller.

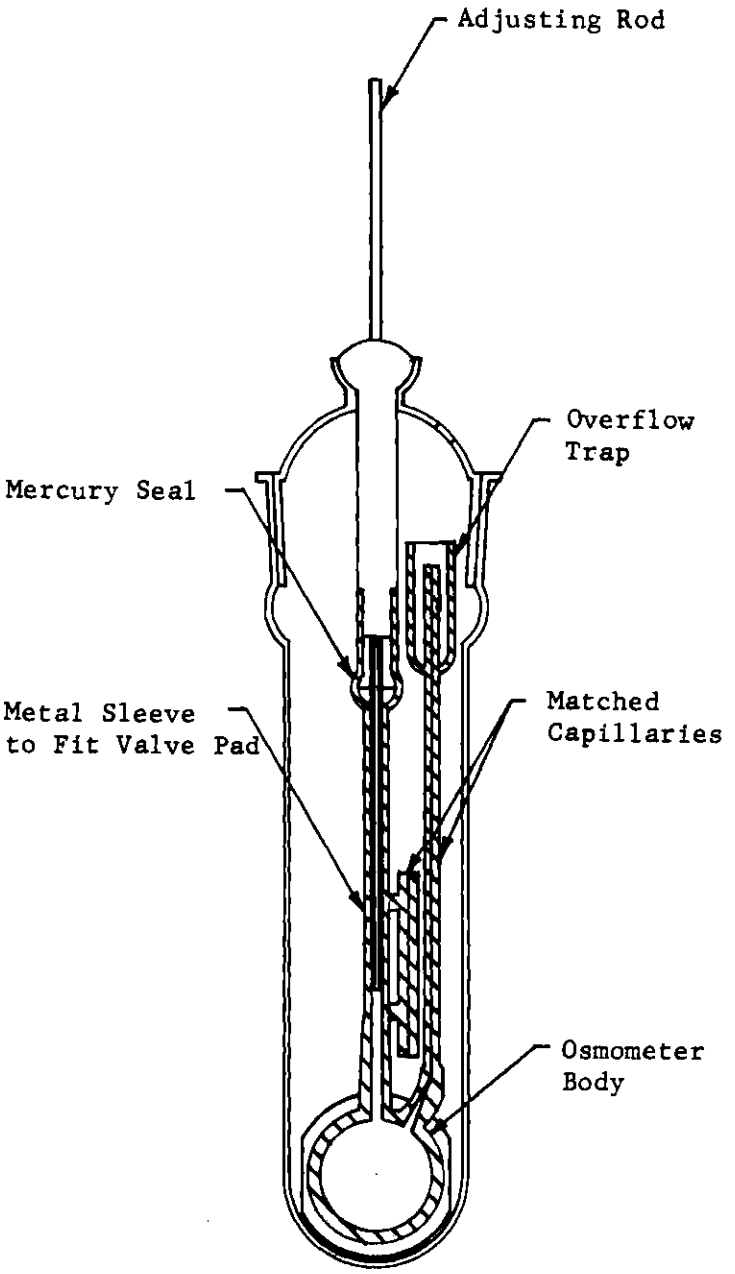

Figure 6. Stabin-Immergut Osmometer

The osmometer could be filled and emptied by means of a long hypodermic syringe, and it was never necessary to remove the osmometer from the thermostat between readings.

Procedure

The membranes were supplied in five percent aqueous ethanol. The first step in preparation of the osmometer was to condition them to pure benzene. Membranes were soaked for several hours each in solutions of 20, 50, and 80 percent aqueous ethanol, two changes of absolute ethanol, 20, 50, and 80 percent benzene in ethanol, and two changes of pure benzene. They were kept in benzene until used.

Fine wire mesh was used to support the membranes in the assembled osmometer. The membranes were removed from the benzene and put between the supporting plates of the osmometer with the wire mesh on the outer side of each membrane. The instrument was assembled and the retaining bolts turned as tight as possible to avoid leakage. The assembled osmometer was placed in its jacket, which contained benzene, and the entire assembly was lowered into the thermostat.

Initially, the osmometer was filled with pure benzene in order to measure membrane asymmetry and test for leaks. The benzene was introduced by means of the hypodermic syringe. Care was taken to remove all bubbles from the instrument. When the filling capillary had run over, the syringe was removed and the steel rod inserted and pushed down until it was visible inside the glass portion of the instrument. Then it was withdrawn carefully to lower the height of the benzene in the measuring capillary.

The head was adjusted to approximately its equilibrium value by

moving the steel rod. Then it was observed through the telescope of the cathetometer for several minutes. If any movement was observed, the head was re-adjusted in the direction of the movement. This procedure was continued until no further motion of the meniscus in the measuring capillary was discernable. Thereafter the height of the column was checked at hourly intervals to determine whether the head was really constant. Usually, no further change in head was observed after two hours.

When the instrument had reached equilibrium, the heights of the columns in the measuring and reference capillaries were measured, and the difference taken as the apparent osmotic head.

The apparent osmotic head for pure benzene was recorded, and the algebraic difference between this value and the apparent head of the polymer solutions was taken as the true osmotic head.

For each fraction the most concentrated solution was prepared by weight, and other solutions were prepared by dilution. Osmotic heads of the polymer solutions were determined in the same way as was the head for pure benzene. After each head had been measured, the solution was removed from the osmometer with the syringe, and a ten-milliliter aliquot was evapoarted in a tared dish and the polymer residue determined as a check on the concentration.

Osmotic pressure is related to the osmotic head by the equation

$$\pi = \rho h \tag{27}$$

where π = osmotic pressure;

h = true osmotic head;

ρ = solution density.

In practice, the quantity $(h/c)^{1/2}$ was plotted against concentration and extrapolated linearly to zero concentration. The intercept was squared and multiplied by the density of pure benzene to give $(\pi/c)_o$. By solving the equation

$$(\pi/c)_o = RT/\bar{M}_n, \tag{28}$$

the number-average molecular weight could be determined. The constant R has the value 848 when pressure is in units of grams per square and temperature in degrees Kelvin (60).

Experimental results are summarized in Figure 7 and Table 4.

Light Scattering

Light scattering provides a convenient measure of the weight-average molecular weight of polymers. If a parallel pencil of monochromatic, unpolarized light is passed through a pure liquid or solution, a portion of the light is scattered. In a pure liquid, this scattering arises from small statistical fluctuations in the density of the liquid in volume elements that are small compared to the wavelength of the light. In solutions, there are additional contributions to the scattering arising from fluctuations in solute concentration in small volume elements.

If the solute molecules have dimensions much smaller than the wavelength of the light used, the light scattered at an angle θ from the direction of the incident beam is related to the molecular weight by the equation

Table 4. Osmotic Pressure Data

Sample	Concentration (c) (g./100 ml.)	Osmotic Head (h) (cm.)	h/c	$(h/c)^{1/2}$
F1	1.213	1.688	1.39	1.18
F2	0.728	0.802	1.10	1.05
F3	0.485	0.446	0.92	0.96
F4	0.243	0.224	0.92	0.96
	0	--	(0.83)	(0.91)
		M_n = 354,000		
J1	0.719	1.773	2.46	1.57
J2	0.431	0.992	2.27	1.50
J3	--	--	--	--
J4	0.145	0.297	2.05	1.43
	0	--	(1.99)	(1.41)
		M_n = 145,000		
L1	0.537	2.696	5.02	2.24
L2	0.323	1.595	4.94	2.22
L3	--	--	--	--
L4	0.107	0.510	4.76	2.18
	0		(4.75)	(2.18)
		M_n = 58,000		

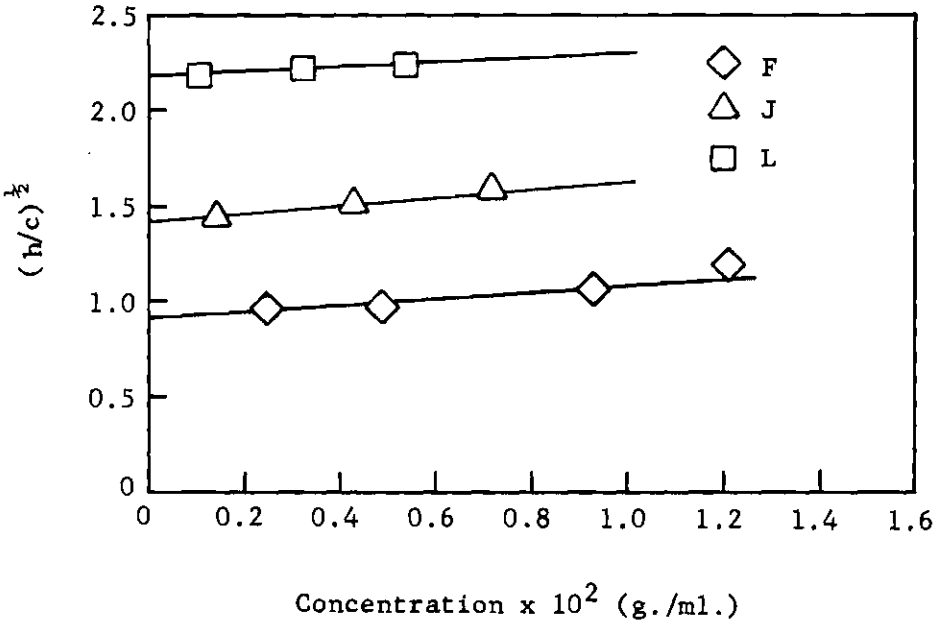

Figure 7. Osmotic Pressure Data

$$\frac{i_\theta}{I_o} = \frac{2\pi^2 n_o^2 (\partial n/\partial c)_T^2 (1 + \cos^2\theta) c}{N_A \lambda^4 r^2 (1/\bar{M}_w + 2Bc + 3Cc^2 + \ldots)} \tag{29}$$

where i_θ = intensity of the scattered light at angle ;

I_o = intensity of the incident beam;

n = refractive index of the solution;

n_o = refractive index of the solvent;

c = concentration of the solute;

N_A = Avogadro's number;

λ = wavelength of light used;

r = distance from the center of the scattering cell to the photocell;

$\bar{M}_w$ = weight-average molecular weight of the solute;

B,C = coefficients in the virial equation (61).

Commonly the optical constants in Equation 29 are combined to form a constant, K, and the factors that depend on the geometry of the photometer are combined with the intensities into a single function of angle, $R(\theta)$:

$$K = 2\pi^2 n_o^2 (\partial n/\partial c)_T^2 / N_A \lambda^4; \tag{30}$$

$$R(\theta) = r^2 i_\theta / I_o (1 + \cos^2\theta) \tag{31}$$

Using these definitions, Equation 29 can now be rearranged in the form

$$Kc/R(\theta) = 1/\bar{M}_w + 2B_c + 3Cc^2 \ldots \tag{32}$$

The quantity $R(\theta)$, known as the reduced scattering intensity, is constant for solute molecules that do not have any dimension greater than one-twentieth of the wavelength of the incident light. In the determination of the molecular weight of such molecules, the ratio i_θ/I_o is measured at an angle of 90 degrees from the incident beam for solutions of several different concentrations. The quantity $Kc/R(\theta)$ is plotted as a function of c and the resulting curve extrapolated to zero concentration. The intercept is equal to the reciprocal of the molecular weight.

When any dimension in the solute molecule is greater than one-twentieth of the wavelength of the incident light, $R(\theta)$ is no longer constant but varies with angle. At high scattering angles the intensity of scattered light is reduced because light scattered from one point of a molecule interferes destructively with light scattered from another point on the same molecule. The effect diminishes as the angle decreases and theoretically vanishes at zero angle. For such large molecules Equation 32 must be written

$$Kc/R(\theta) = 1/\bar{M}_w P(\theta) + 2Bc + 3Cc^2 + \ldots \qquad (33)$$

where $P(\theta) = \text{Lim}_{c\to 0} R(\theta)/R_o(\theta)$;

$R_o(\theta)$ = reduced scattering intensity at zero angle. The function $P(\theta)$ is much less than unity for high scattering angles. At low angles it can be shown (61) that

$$1/P(\theta) = 1 + (16\pi^2/3\lambda^2)R_G^2 \sin^2(\theta/2) \qquad (34)$$

where R_G is the root mean square radius of gyration of the solute molecules. Since $P(\theta)$ is meaningless in all but very dilute solutions, it is necessary to obtain data at several concentrations and extrapolate the plot of $Kc/R(\theta)$ to zero concentration at each angle, θ, and then extrapolate the zero-concentration values so obtained to zero on a plot of $Kc/R(\theta)$ versus $\sin^2(\theta/2)$.

This can be done on a single graph using the method of Zimm (62). In this procedure $Kc/R(\theta)$ is plotted against $\sin^2(\theta/2) + kc$, where k is an arbitrary constant chosen to give a convenient spread in the data. Data for all concentrations and all angles are plotted on the same graph. The curve for each angle is extrapolated to zero concentration, i.e. $\sin^2(\theta/2)$; and the curve for each concentration is extrapolated to zero angle, i.e., kc. Finally the curves through the two sets of points obtained by extrapolation are themselves extrapolated to the ordinate. They must have a common intercept, and the intercept is equal to the reciprocal of the weight-average molecular weight.

Experimental Procedure

The apparatus used was a Brice-Phoenix Universal Light-Scattering Photometer, Model 1000. A cylindrical scattering cell 30 millimeters in diameter was used in scattering measurements on polystyrene solutions. Preliminary scattering measurements on pure benzene were made using a 20-millimeter square cell.

Solution Clarification. All solutions used in light scattering must be scrupulously free of dust. The two methods most often used for clarification of solutions are centrifugation at very high speed and filtration under nitrogen pressure through an ultrafine sintered

glass filter. In this work filtration was used in all cases except for solutions of fraction B, which clogged the filter. Solutions containing fraction B were clarified by centrifugation.

The solution to be filtered was poured into a filter funnel and forced through the filter under pressure of dry nitrogen. When filtration was complete, the cell was immediately covered with a clean glass plate and placed in the photometer. With the room darkened, a beam of white light was passed through the cell with the top of the photometer open. By looking through the cell at a low angle, it was possible to see any particles of dust remaining in the solution as bright specks in the beam. A further test of clarification was to measure scattering at 30 degrees with the sensitivity turned as high as possible. A very unstable galvanometer reading indicated the presence of dust.

When it was necessary to use centrifugation, a Servall Superspeed Centrifuge was used. The instrument was brought up to full speed slowly, allowed to run for one to two hours, then turned off and allowed to coast to a stop. Completeness of clarification was tested in the same way as in the case of filtration.

The cell was freed of dust before each measurement by condensing benzene vapor in the inverted cell and allowing the liquid to run out. A special cell cleaner, shown in Figure 8, was used.

Preliminary Measurements. The turbidity of a solution may be calculated from scattering measurements made at 90 degrees with the Brice-Phoenix instrument using the formula

$$\tau = [16TD/3h(1.045)]\,[n^2R_w/R_c]\,aFG(90)/G(0) \qquad (35)$$

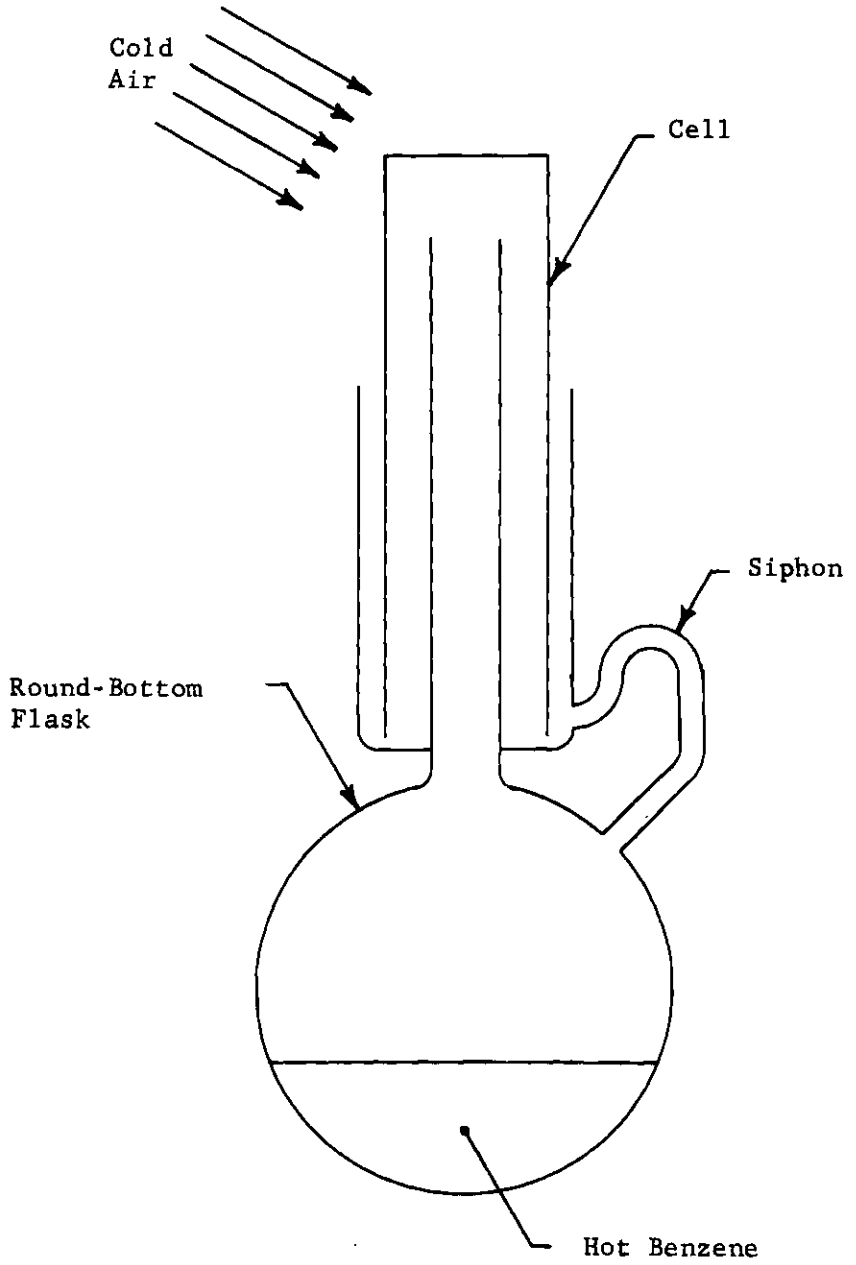

Figure 8. Cell Cleaner

where τ = turbidity;

TD = a constant which is a property of the reference standard supplied with the instrument;

h = beam width;

R_w/R_c = correction for incomplete refraction effects;

a = constant which is a property of the working standard supplied with the instrument and the geometry of the instrument;

F = transimittance of the filter combination used;

G(90) = galvanometer deflection for intensity of scattered light at 90 degrees;

G(0) = galvonometer deflection for intensity of incident light;

1.045 = correction for internal reflections (62). The reduced scattering intensity at 90 degrees is related to the turbidity by the equation

$$\tau = 16\pi R(90)/3 \qquad (36)$$

so that Equation 35 may be written (64)

$$R(90) = [TD/\pi h(1.045)]\,[n^2 R_w/R_c]\,aFG(90)/G(0). \qquad (37)$$

The values of TD, h, R_w/R_c, and individual filter transmittances are given in the Operation Manual (62). It is necessary to determine the constant a experimentally at frequent intervals since it may be strongly affected by small changes in the alignment of the instrument caused by changing lamps or phototubes. This was done according to the

procedure described in the Operation Manual (62) by measuring the galvanometer reading G_{rs} at zero degrees with the reference standard and all four filters in the beam, and the reading G_{ws} with the working standard and filters F_1, F_2, and F_3 in the beam. The constant a is given by

$$a = F_4 G_{ws}/G_{rs} \tag{38}$$

After the value of a had been determined, the reduced scattering intensity of benzene was measured using a square cell. This was necessary because the constant TD, and hence the constant a, are defined only for the wide-beam geometry. In order to make measurements with a cylindrical cell and narrow beam, it is necessary to obtain a correlation factor, k. This is done by measuring G(90)/G(0) using the square cell and wide beam and again using the square cell and narrow beam. The correlation factor is given by

$$k = [FG(90)/G(0)]/[F'G'(90)/G'(0)] \tag{39}$$

where F = transmittance of the filter combination used. Primed quantities are those measured with the cylindrical cell.

Another difference in the form of Equation 37 to be used with the cylindrical cell is in the correction for internal reflection. If x is the fraction of light reflected at the cell window and $G'(\theta)$ is the measured galvanometer reading at angle θ, the value $G(\theta)$ to be used is given by

$$G(\theta) = G'(\theta) - xG'(\pi - \theta). \tag{40}$$

The value of x may be determined from the refractive index of the glass used in the cell by the relation (65)

$$x = (1 - n)^2/(1 + n)^2 \tag{41}$$

Values of n for all cells supplied for use with the Brice-Phoenix Photometer are given in the Operation Manual (62).

Equation 37 may now be written for the cylindrical cell as

$$R(\theta) = [TD/\pi][n^2R_w/R_c]\ kaF[G(\theta) - xG(\pi - \theta)]/G(0). \tag{42}$$

Cell Alignment. Before any measurements could be made, the cylindrical cell had to be aligned and permanently attached to its square base. Redistilled Fisher Reagent Grade benzene was filtered into the dust-free cell, and the cell was placed in the photometer. The cell was aligned visually and then adjusted until scattering measurements at 45 and 135 degrees were the same. A further check on alignment was provided by the equation

$$G(\theta)/G(90) = \sin\theta/[1 + (1 - \rho)\cos^2\theta/(1 + \rho)] \tag{43}$$

where ρ = depolarization of benzene (66).

When the cell had been satisfactorily aligned, it was affixed to the base by means of a small quantity of household cement, carefully applied around the bottom of the cell. After the cement had dried for 24 hours, the cell was ready for use.

Refractive Index Measurements. Both the index of refraction of the solvent and the partial derivative of the refractive index with respect to solute concentration must be known in order to compute the constant (see Equation 30). Refractive indices of benzene at various wavelengths are given in the American Institute of Physics Handbook (67). These have been plotted and are shown in Figure 9. The refractive index at 436 milimicrons, the wavelength of the blue line of mercury, was determined from this plot.

The rate of change of refractive index with respect to solute concentration was measured by means of a Brice-Phoenix Differential Refractometer. This instrument is capable of measuring changes in refractive index with a precision of $\pm 3 \times 10^{-6}$.

In making the measurement of a change in refractive index, pure solvent is placed in one side of a cell and dilute solution in the other side. The two compartments are separated by a transparent partition set at an angle to a beam of light passing through the cell. The beam of light is deflected because of the difference in refractive index between the two compartments, and the deflection, d, can be measured by means of a filar micrometer.

The instrument was calibrated by measuring the micrometer readings using a series of sucrose solutions of known refractive index. This was done using solutions containing two, four, five, and six percent sucrose. The difference, Δd, was taken as the instrument reading for a given concentration. This reading was determined by the relation

$$\Delta d = (d_1 - d_2)_s - (d_1 - d_2)_o \qquad (44)$$

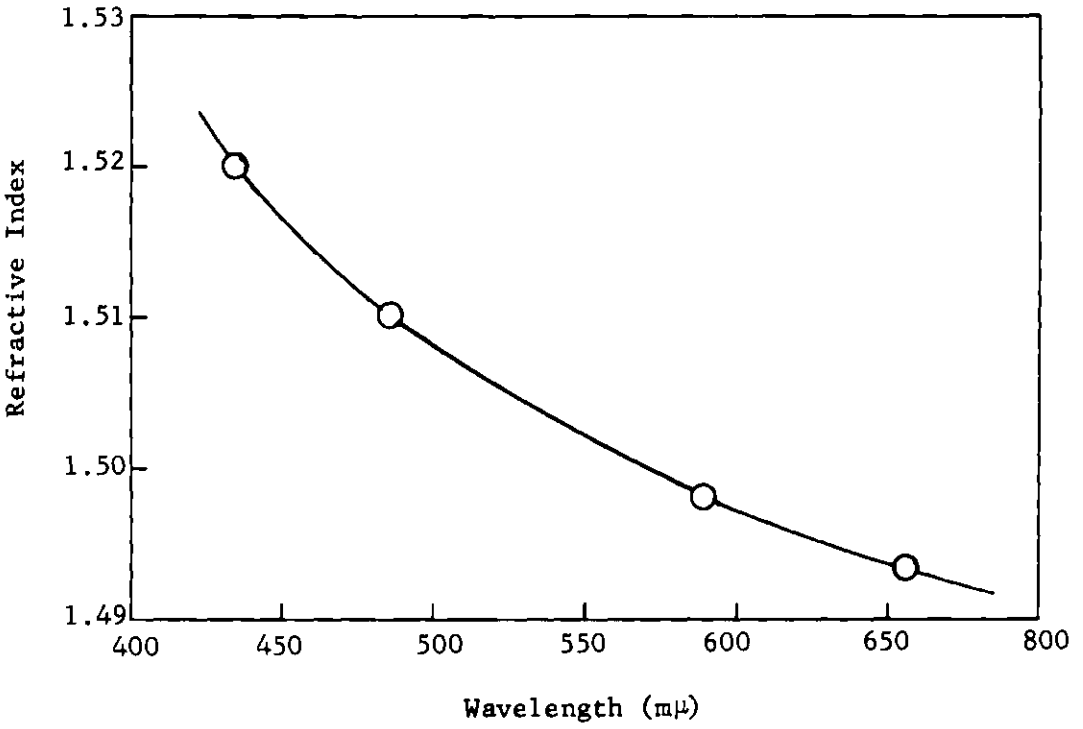

Figure 9. Refractive Index of Benzene as a Function of Wavelength

where the subscripts 1 and 2 refer to readings taken with the cell in two positions 180 degrees apart, and the subscripts s and o refer to readings for solution and pure solvent respectively. It is important that algebraic sums be used, as the signs of the terms in Equation 44 may be like or unlike.

To determine the calibration constant C for the instrument, Δd was plotted as a function of the difference in refractive index between the solutions and pure water, and the slope of the resulting straight line was determined.

Another series of measurements was made in the same manner as those used for calibration, except that the solvent used was benzene and the solute was polystyrene. Each value of Δd determined was multiplied by C to give the change in refractive index, Δn. Finally, the measured values of Δn were plotted against solute concentration, and the slope of this line, $(\partial n/\partial c)_T$, was determined. All measurements were made at 25° C. Results of all these measurements are given in Tables 5 and 6 and in Figures 10 and 11.

Scattering Measurements. After the solution had been clarified and tested, the sensitivity was adjusted so that the minimum galvanometer deflection was about one-half of the scale with the blue filter and no neutral filters in the beam.

The phototube was then moved to zero angle to measure the galvanometer reading for the incident beam. A combination of neutral filters was found by trial and error that gave between 50 and 100 percent of a full scale deflection. The reading and filters used were recorded. Then measurements were made in a similar fashion for

Table 5. Refractometer Calibration Data

Percent Sucrose	$\Delta n \times 10^3$ (Ref. 68)	d_1	d_2	$d_1 - d_2 - \Delta d_o$
0	0.00	5.043	5.070	-0.027
2	2.89	6.488	3.578	2.937
4	5.76	7.933	2.022	5.938
5	7.22	8.655	1.237	7.445
6	8.70	0.382	0.422	8.987

Table 6. Determination of $(\partial n/\partial c)_T$ for Polystyrene in Benzene

Concentration (g./100 ml.)	Δd	$\Delta n \times 10^3$
1.0208	1.182	1.145
0.8168	0.972	0.941
0.6136	0.718	0.695
0.4044	0.490	0.474
0.2032	0.249	0.241

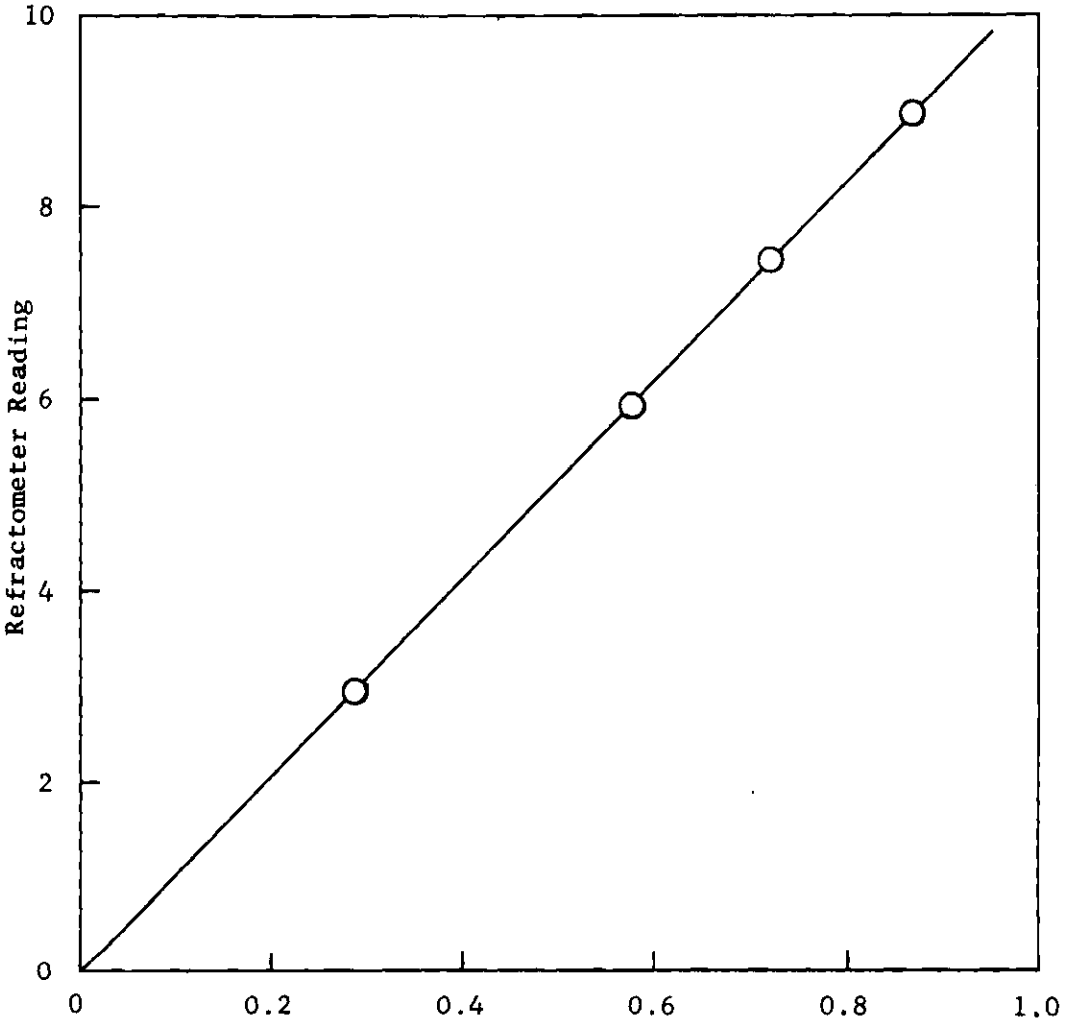

Figure 12. Calibration of Differential Refractomoter

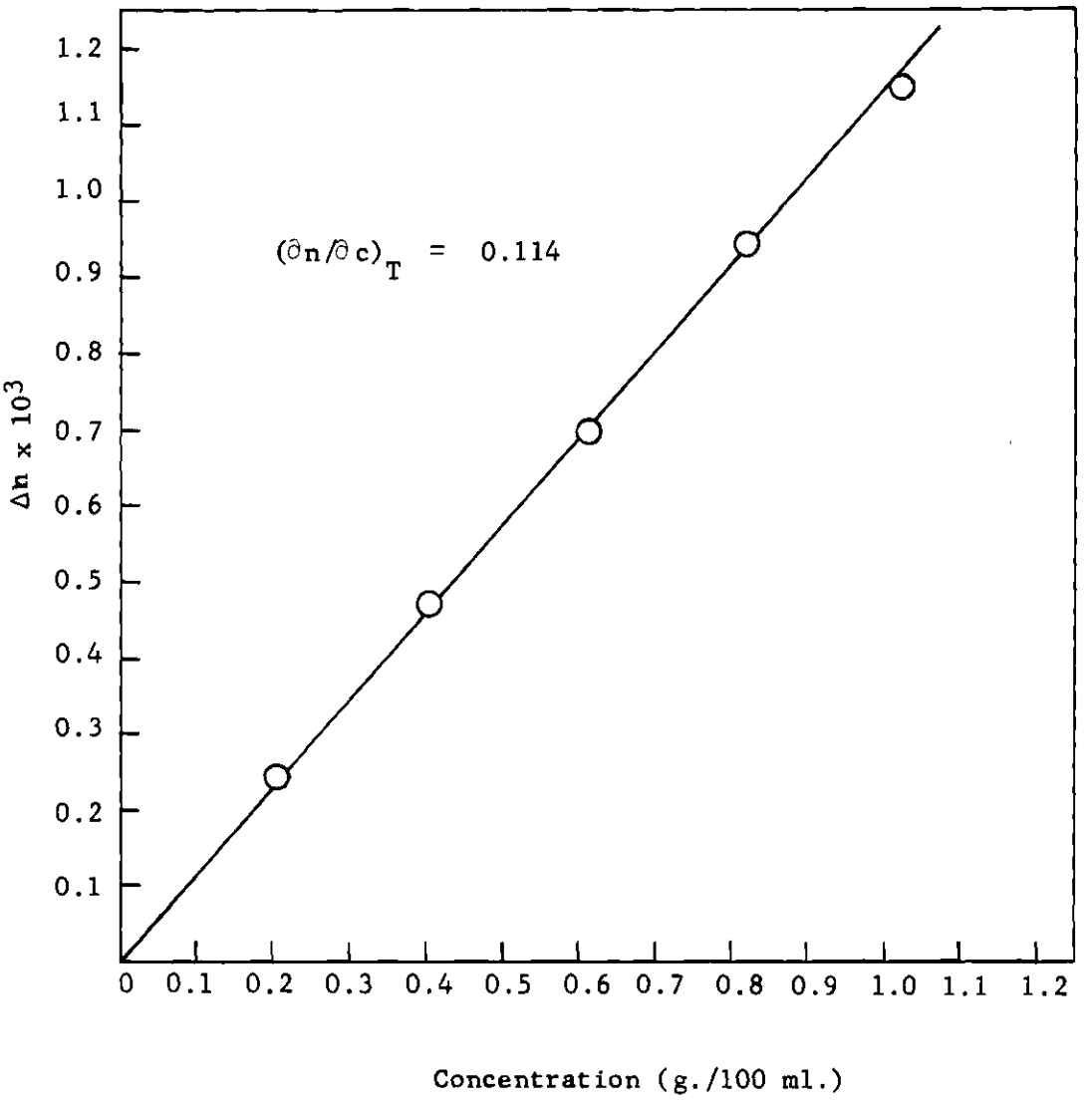

Figure 11. Determination of $(\partial n/\partial c)_T$ for Polystyrene in Benzene

a series of angles from 30 to 135 degrees. Both galvanometer readings and filters used were recorded for each angle.

Solutions were prepared by weighing a quantity of polystyrene into a 100-milliliter volumetric flask, dissolving in benzene, and filling to the mark to make up the most concentrated solution used. Other solutions were prepared by dilution. After scattering measurements were completed, a ten-milliliter aliquot of each solution was evaporated in a tared aluminum dish and weighed to check the concentration. Changes in concentration were negligible in almost all cases.

Treatment of Data

The data were treated according to the procedure of Zimm (64). Four measured galvanometer readings at each angle were averaged and divided by the transmission coefficient of the filter combination used. A correction was made for internal reflection in the cell, and $R(\theta)$ was calculated from Equation 42. Since the scattering due to fluctuation in liquid density should be very nearly the same in pure solvent and all solutions, the value of $R(\theta)$ for pure solvent was subtracted from that for the solution to give the excess scattering, $R(\theta)_{ex}$, which was the quantity used in subsequent molecular weight calculations. A plot was made of $c/R(\theta)_{ex}$ versus $kc + \sin^2(\theta/2)$ and extrapolations were made as described above. For all fractions except B, k was 100; for B, k was 1000.

The constant K was calculated from the known optical constants. The intercept of the Zimm plot was multiplied by K, and the weight-average molecular weight was determined by taking the reciprocal of this product. The Zimm plots for all four fractions are shown in

Figures 12, 13, 14, and 15. The values of the weight average molecular weights are collected in Table 8.

Viscometry

The simplest method of determining the molecular weights of polymers is the measurement of the intrinsic viscosity, $[\eta]$, defined by the relation

$$[\eta] = \mathrm{Lim}_{c \to o}(1/c)(\eta - \eta_o)/\eta_o \qquad (45)$$

where c = concentration of polymer in solution;

η = viscosity of the polymer solution;

η_o = viscosity of the pure solvent.

The intrinsic viscosity is empirically related to the molecular weight by the equation of Mark (69) and Houwink (70),

$$[\eta] = K'M^a \qquad (46)$$

where K' and a are constants which must be determined experimentally for each polymer-solvent system. They are determined by measurement of the intrinsic viscosities of a number of fractions of low polydispersity and known molecular weight. Molecular weights of the fractions can be measured by light scattering or osmometry. A plot of $\log[\eta]$ versus log M gives a straight line with slope a and intercept log K'. Values of K' and a for many polymer-solvent combinations are available in the literature. Table 7 shows values of these

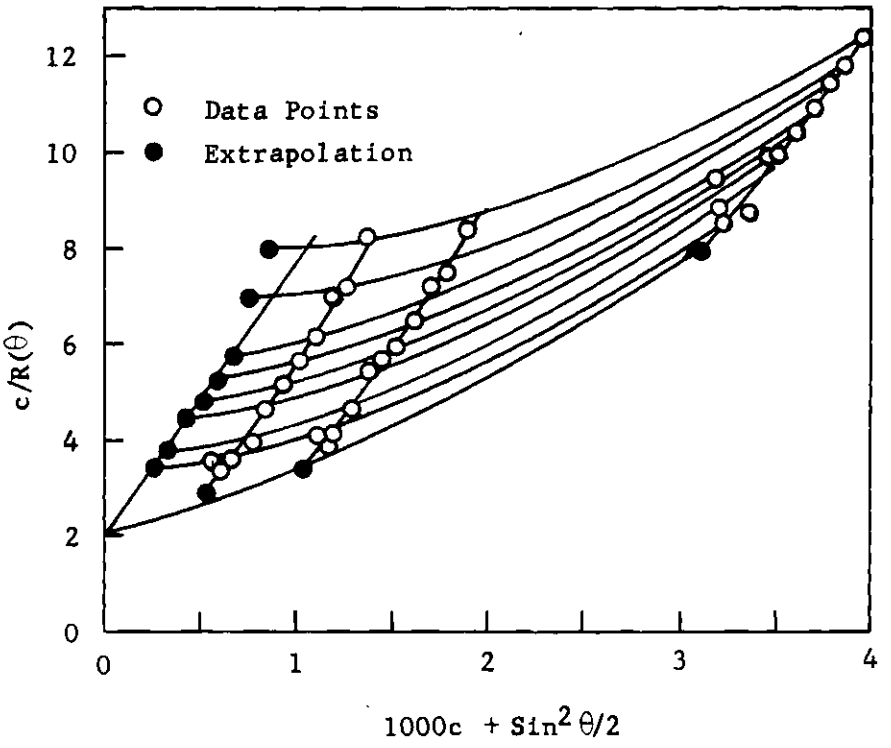

Figure 12. Zimm Plot for Fraction B

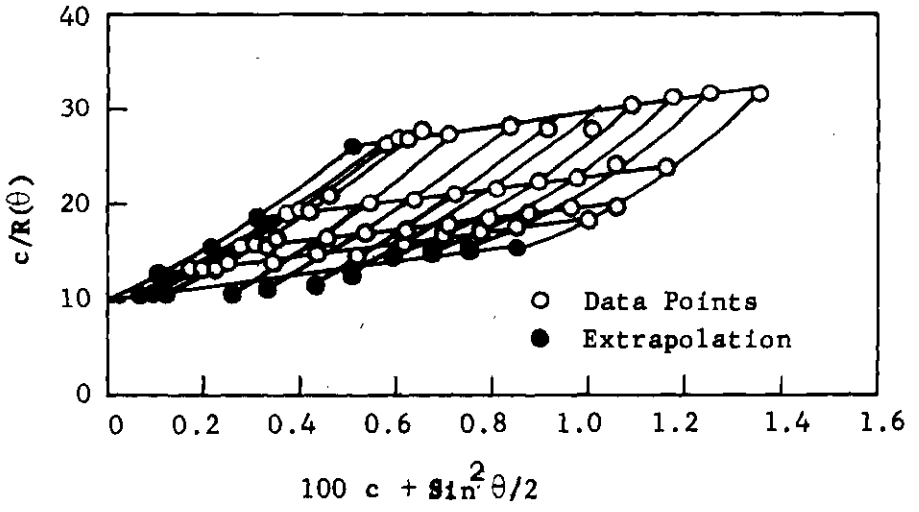

Figure 13. Zimm Plot for Fraction F

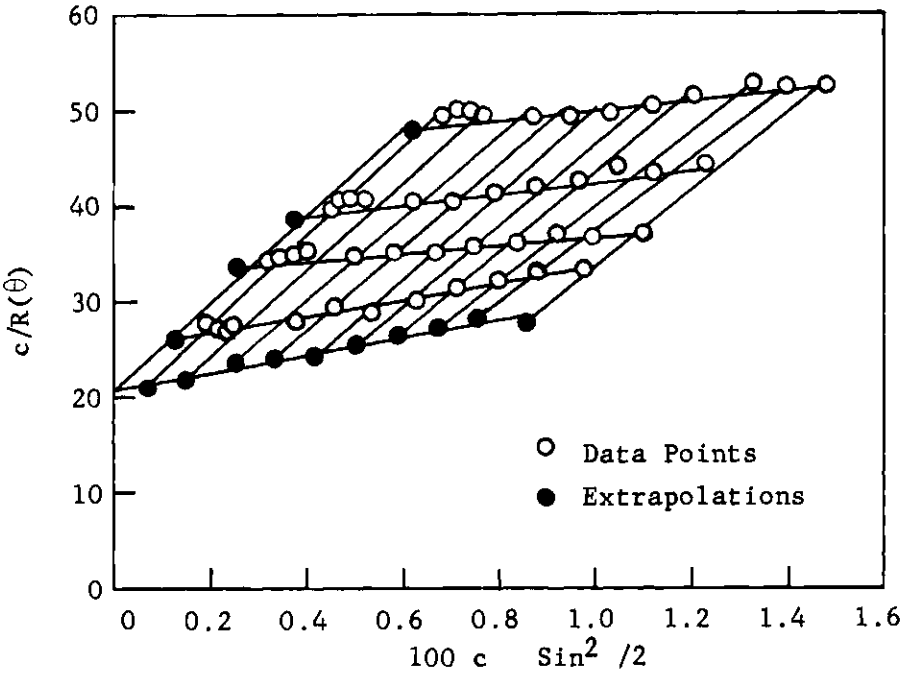

Figure 14. Zimm Plot for Fraction J

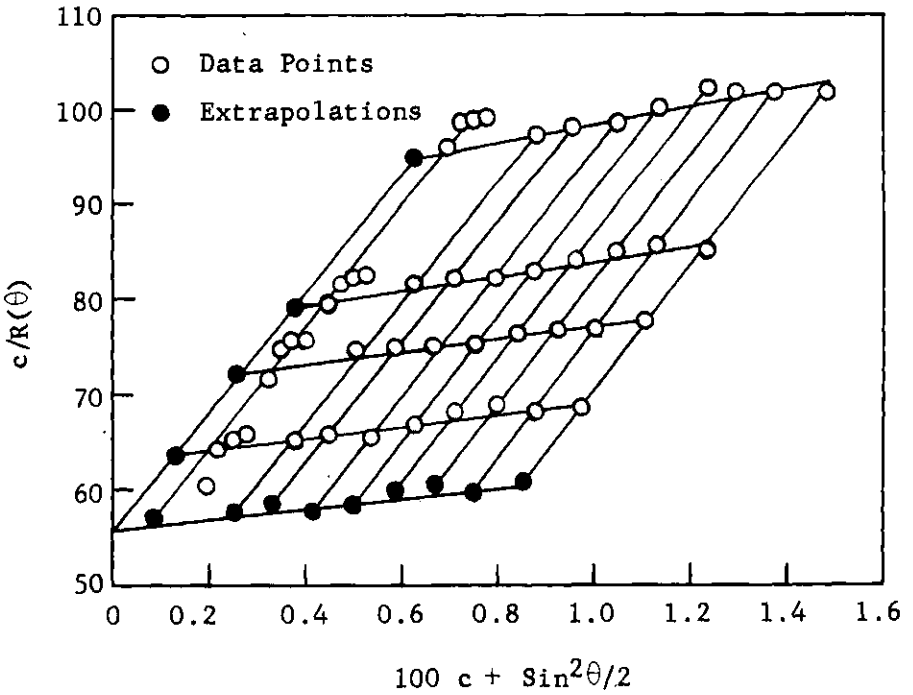

Figure 15. Zimm Plot for Fraction L

Table 7. Mark-Houwink Parameters

System	$K' \times 10^4$	a	Ref.
Polystyrene, benzene, 25° C.	0.95	0.74	71
Polystyrene, Methylethyl ketone, 25° C.	3.9	0.58	72
Polyisobutylene, cyclohexane 30° C.	2.6	0.70	73

Table 8. Molecular Weights of Polystyrene Determined by Various Means

Fraction	$\bar{M}_w \times 10^{-5}$	$\bar{M}_n \times 10^{-5}$	$\bar{M}_v \times 10^{-5}$	$\bar{M}_w/\bar{M}_n$
B	18.2, 18.4*	15.0	15.0	1.22
F	3.70	3.54	2.1	1.05
J	1.77	1.45	0.77	1.22
L	0.67	0.58	0.33	1.15

parameters for the polymer-solvent combinations used in this study.

The procedure for determining the intrinsic viscosity of a polymer is to measure the viscosities of several dilute solutions of varying polymer concentration. The specific viscosity, defined as

$$\eta_{sp} = (\eta - \eta_o)/\eta_o \tag{47}$$

is related to the concentration in solutions sufficiently dilute by the Huggins equation (74)

$$\eta_{sp}/c = [\eta] + k[\eta]^2 c. \tag{48}$$

where k is an empirical constant. A plot of η_{sp}/c versus c gives a straight line whose intercept is $[\eta]$.

A check on the correctness of the extrapolation is provided by another relation that can be derived from Equation 48. The Maclaurin's series expansion for the natural logarithm of a number between one and two may be written

$$\ln(1 + x) = x - x^2/2 + x^3/3 - \ldots \tag{49}$$

For small values of x, terms higher than the square can be neglected. Substituting η_{sp} for x we obtain

$$\ln(1 + \eta_{sp}) = \eta_{sp} - \eta_{sp}^2/2 \tag{50}$$

Solving Equation 48 for η_{sp} and substituting in Equation 50, we obtain

$$\ln(1 + \eta_{sp}) = [\eta]c + k[\eta]^2c^2 - \tfrac{1}{2}([\eta]^2c^2 + 2k[\eta]^3c^3 + k^2[\eta]^4c^4) \qquad (51)$$

which may be written, ignoring terms higher than the square, as

$$\ln(1 + \eta_{sp}) = [\eta]c - (1/2)(1 - 2k)[\eta]^2c^2 \qquad (52)$$

or

$$(1/c)\ln(1 + \eta_{sp}) = [\eta] - (1/2 - k)[\eta]^2c \qquad (53)$$

Hence, a plot of $(1/c)\ln(1 + \eta_{sp})$ versus c gives a straight line of slope $-(\frac{1}{2} - k)[\eta]^2$ and intercept $[\eta]$.

Commonly, both η_{sp}/c and $(1/c)\ln(1 + \eta_{sp})$ are plotted against c on the same graph. The two straight lines are extrapolated to a common intercept (75). Furthermore, the difference in the slopes of the two lines so obtained should be one-half the intrinsic viscosity, thus giving yet another check on the correctness of the value determined.

Equations 48 and 53 can be solved simultaneously to obtain an expression for the intrinsic viscosity determined by a viscosity measurement at only one concentration:

$$[\eta] = [(2/c)^2\{\eta_{sp} - \ln(1 + \eta_{sp})\}]^{1/2} \qquad (54)$$

The determination of intrinsic viscosity in this way does not depend on knowledge of the Huggins constant.

The value of the molecular weight of a polydisperse polymer obtained by viscosity measurements is neither a weight-average nor a number-average. It can be shown to be always less than or equal to the former and greater than the latter (76).

Procedure

The viscometer used in this work was of the Ubbelohde, suspended-level type and is shown schematically in Figure 16. It was suspended in a thermostat, the temperature of which was controlled to 0.03 degrees. A Meylan stopwatch, type 200A, with a precision of ±0.05 seconds was used to measure efflux times.

Calibration. The viscometer was calibrated by measuring the efflux times for distilled water at various temperatures. The viscosity of water has been determined precisely as a function of temperature (77).

The Poisuille equation, relating viscosity and efflux time in a capillary-tube viscometer, may be written

$$\eta/\rho = \pi r^4 ht/8Vl \qquad (55)$$

where η = viscosity;

ρ = density of liquid;

r = radius of the measuring capillary;

h = vertical distance between upper and lower liquid surfaces in the viscometer;

t = efflux time;

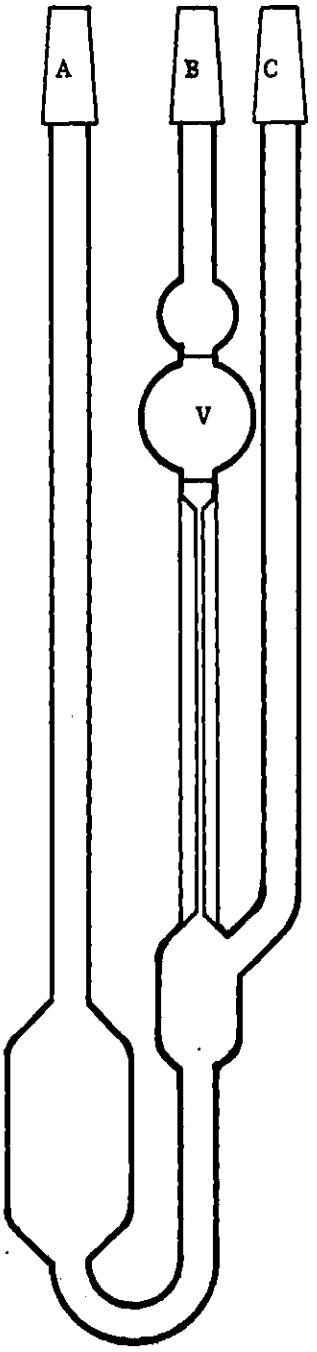

Figure 16. Ubbelohde Viscometer

V = effluent volume;

l = length of the measuring capillary.

Equation 55 neglects the effect of the acquisition of a finite kinetic energy by the fluid in flowing through the capillary, and is strictly valid only for an infinitely slow process. A kinetic energy correction of the form -B/t must be made, where B is an empirical parameter (78). It is usual to treat Equation 55, corrected for kinetic energy effects, as an empirical equation

$$\eta/\rho = At - B/t \qquad (56)$$

where A and B are constants to be determined by calibration. If $\eta/\rho t$ is plotted as a function of $1/t^2$, a straight line is obtained having a slope of -B and an intercept of A.

The data obtained for the calibration of the viscometer with water (77) were fitted to Equation 10 by the method of least squares, and A and B were evaluated. The calibration curve is shown in Figure 17.

Preparation of Solutions. When a considerable amount of polymer was available, as in the case of the samples used for adsorption studies, a series of measurements was made on solutions of varying concentration and the data extrapolated to zero concentration. Solutions were prepared by dilution in the same manner as for osmometry or light scattering. The most concentrated solution was prepared first, and aliquots of this were taken for dilution to prepare more dilute solutions.

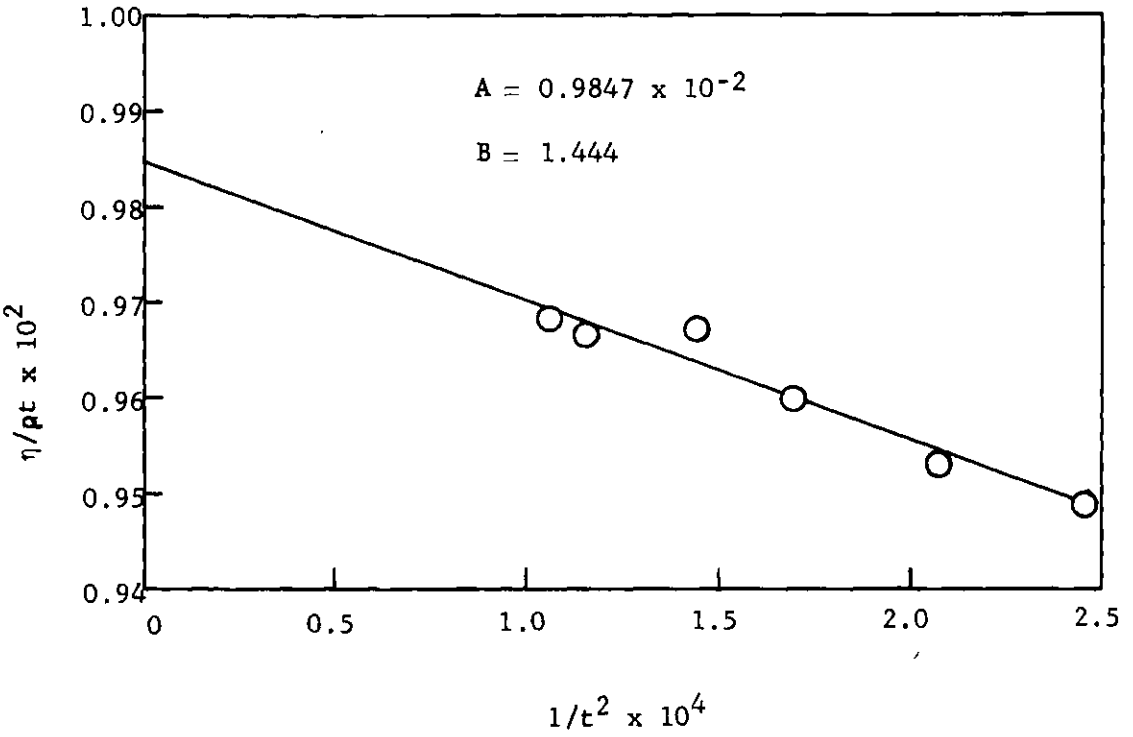

Figure 17. Viscometer Calibration Curve

In the determination of the molecular weight distribution of sample B, the amounts of polymer available were somewhat limited. In this case, a measurement of the viscosity was made at only one concentration, and the intrinsic viscosity was calculated from Equation 54.

Reagent grade benzene was used as the solvent in viscosity measurements on fractions F, J, and L. Measurements on polyisobutylene were made in cyclohexane at 30° C. In the case of fraction B, possible rate-of-shear effects made use of benzene as a solvent undesirable, i.e., the measured value of the viscosity is a function of the rate of shear in the viscometer. However, the effect of the rate of shear on the intrinsic viscosity becomes important only when the intrinsic viscosity is greater than about four (79). In methylethyl ketone the intrinsic viscosity of fraction B was about 1.6. The intrinsic viscosities of the other polystyrene fractions in methylethyl ketone were too low to be measured accurately.

Viscosity Measurements. The viscometer was suspended in the thermostat, which was maintained at 25° C. (except for the polyisobutylene measurements). The solution to be measured was introduced into it through a coarse sintered glass filter, using very gentle suction where necessary.

The arm of the viscometer marked C in Figure 16 was capped, and gentle pressure was applied to the arm marked A by means of a rubber bulb, forcing the solution through the measuring capillary into the bulb V. Enough solution was forced up to fill V and partially fill the small bulb above V. The pressure was then released, and the cap and rubber bulb were removed quickly from their respective arms.

The stop watch was started when the meniscus passed the upper fiducial mark and stopped when it passed the lower one. The time was recorded and the process repeated several times. The average of several determinations was used to calculate the viscosity of the solution.

The specific viscosity was determined for each solution, and intrinsic viscosities were calculated or determined graphically as described above. Graphical determinations of intrinsic viscosities of the polystyrene fractions and the polyisobutylene sample are shown in Figures 18, 19, and 20.

Viscosity-average molecular weights were calculated from Equation 46 using the values of K' and $\underline{a}$ given in Table 7. A comparison of molecular weights measured by different methods is given in Table 8.

No explanation has been found for the large discrepancy between the viscosity-average molecular weights of fractions F, J, and L, measured in benzene, and the other values for the molecular weights of these fractions. The viscosity-average molecular weight of fraction B was measured in methylethyl ketone and is in good agreement with the values determined by light scattering and fractionation. The discrepancy is not serious since the only use made of viscosity-average molecular weights was in the determination of the molecular weight distribution of fraction B. These measurements were made in methylethyl ketone and are presumably reliable.

The "sharpness" of the fractions as indicated by the values of $\overline{M}_w/\overline{M}_n$ in Table 8 is quite variable and reflects the variations in procedure used to obtain the various fractions. Fractionation of very high

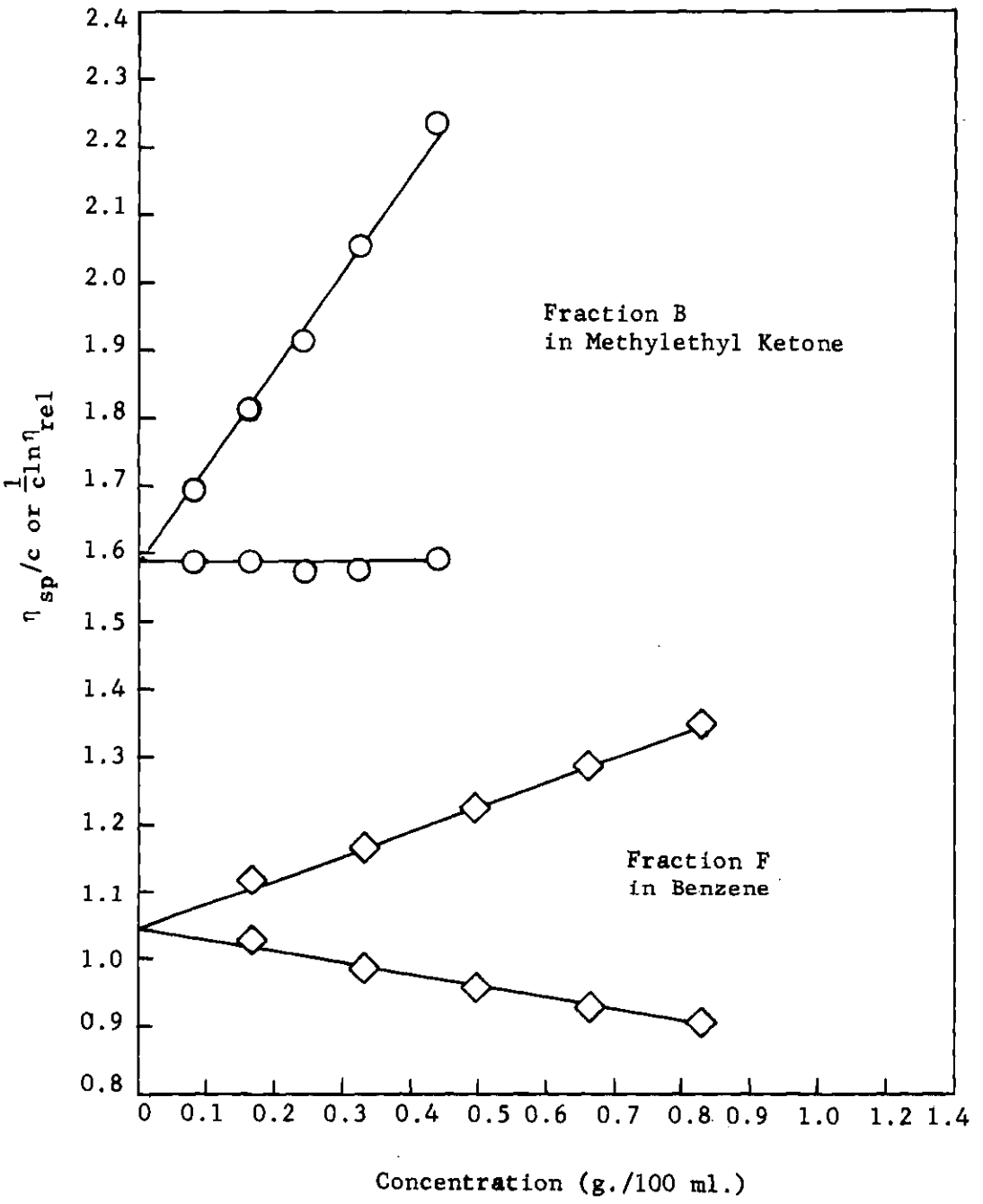

Figure 18. Determination of Intrinsic Viscosity of Fractions B and F

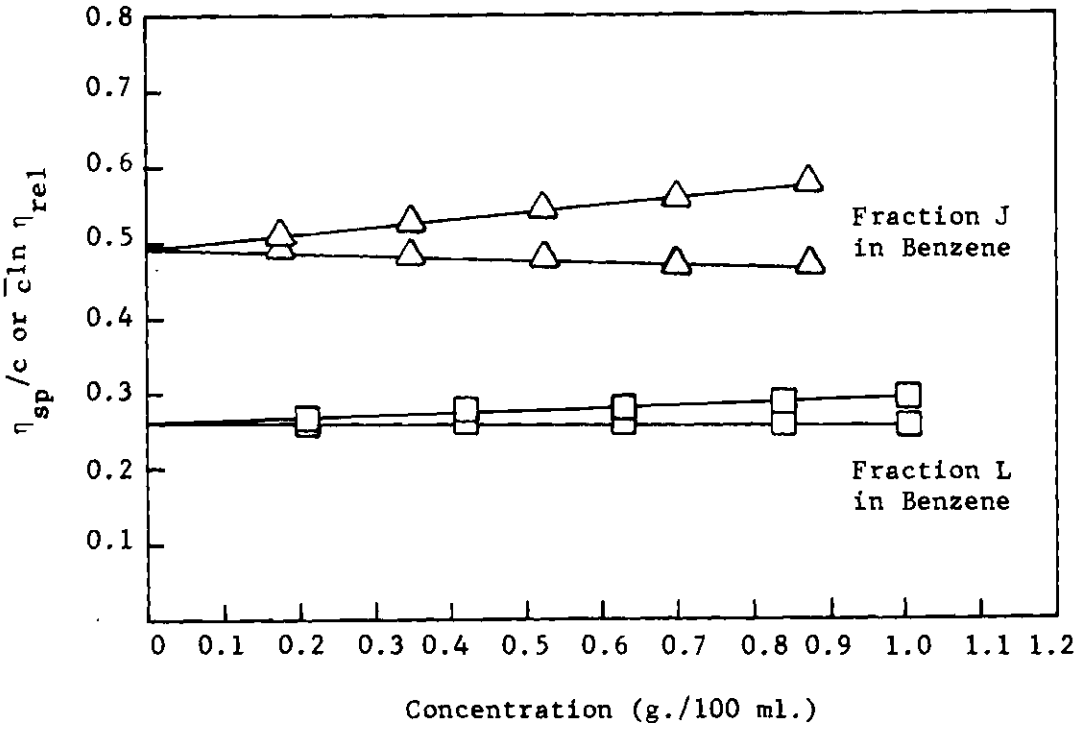

Figure 19. Determination of Intrinsic Viscosities of Polystyrene Fractions J and L

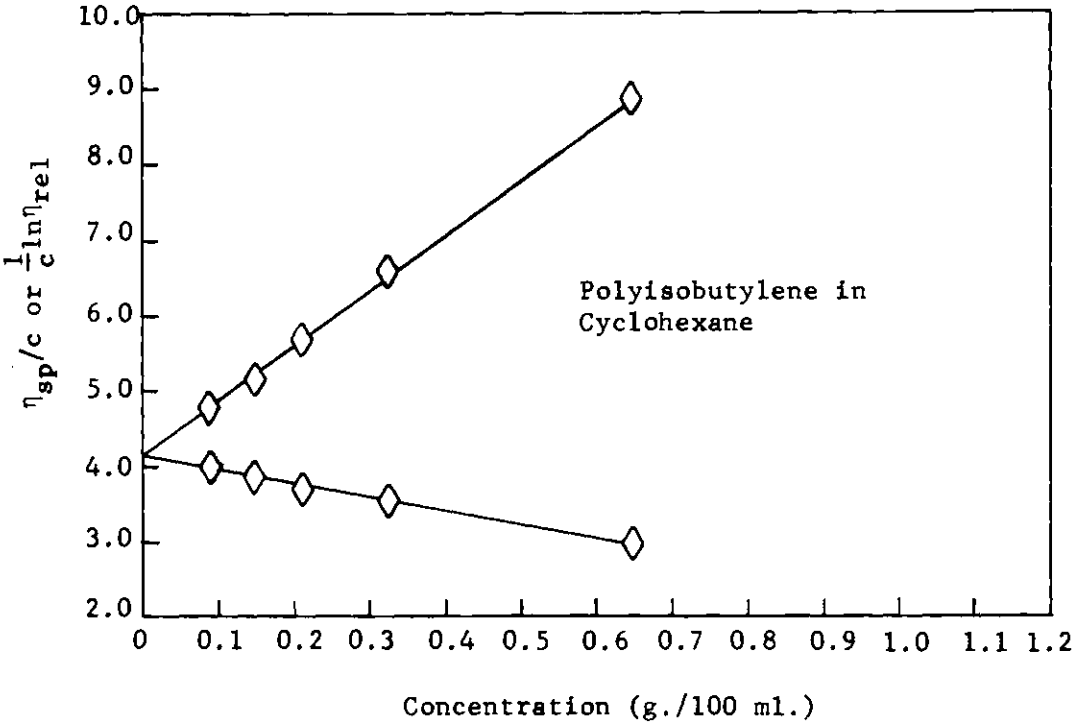

Figure 20. Determination of Intrinsic Viscosity of Polyisobutylene

molecular weight polymers is notoriously difficult (48), which probably accounts for the broad distribution of fraction B. Fraction F is quite sharp, as is to be expected of a fraction obtained in two stages of fractional precipitation. The broadness of the other two indicates a need for further development of the column fractionation techniques.

Adsorbent Characterization

The principal adsorbent characteristics of interest in this study were the specific surface area, the pore-size distribution, and the fraction of the total area contained within pores in each size range. These quantities are conveniently determined from the adsorption isotherm for nitrogen at the temperature of liquid nitrogen.

Surface area may be determined using the theory of Brunauer, Emmett, and Teller (80). According to the BET theory, the isotherm for the adsorption of nitrogen at its normal boiling point onto a solid surface can be written in linear form as

$$p/V(p_s - p) = (1/V_m c) + (p/p_s)(C - 1)/V_m C \qquad (57)$$

where p = pressure;

p_s = saturation pressure of nitrogen;

V = volume adsorbed per gram of adsorbent corrected to standard temperature and pressure;

V_m = volume required to form a monolayer, corrected to standard conditions;

C = a constant.

Thus if $p/V(p_s - p)$ is plotted as a function of p/p_s, a straight line should result. The sum of the slope and the intercept of this line gives the reciprocal of the volume of nitrogen at standard temperature and pressure necessary to cover the surface with one monolayer of adsorbed molecules. By using an appropriate value for the area, a_o, of one nitrogen molecule, one obtains the surface area of the solid from the relation

$$S = (pV_m/RT)N_A a_o \tag{58}$$

where S = surface area;

p = pressure (one atmosphere);

V_m = volume (at STP) corresponding to one monolayer;

R = gas constant;

T = absolute temperature (273.16° Kelvin);

N_A = Avogadro's number.

For determination of pore-size distribution, it is necessary to measure the entire isotherm, from zero pressure to saturation or as near saturation as practicable. For porous adsorbents some hysteresis is observed when adsorption and desorption isotherms are measured. Accordingly, the desorption isotherm is used because it is considered to approximate thermodynamic equilibrium more closely (81). The isotherm is plotted as volume of gas adsorbed (corrected to STP) versus the relative pressure, p/p_s.

The procedure for determining the pore-size distribution from nitrogen adsorption was developed by Barrett, Joyner, and Halenda (82)

and by Pierce (83). The underlying theory is based on the lowering of the vapor pressure of a liquid inside a capillary due to surface tension. The pore is assumed to be a cylinder, inside of which liquid condenses. If all adsorption consisted of capillary condensation, the meniscus of the liquid inside the pore would have a radius equal to the pore radius. However, adsorption takes place on non-porous surfaces; and we must assume that there is an adsorbed film over the entire surface as well as liquid condensed in the pores. Hence, the radius of the meniscus, or "capillary radius," r_k, is given by

$$r_k = R_c - t \tag{59}$$

where R_c = pore radius;

t = thickness of adsorbed film.

The maximum radius of a meniscus in equilibrium with the vapor at a given pressure is given by the Kelvin equation (82):

$$\ln p/p_s = -2\sigma V^*/RTr_k \tag{60}$$

where σ = surface tension of liquid nitrogen;

V^* = molal volume of liquid nitrogen;

R = gas constant in ergs per degree;

T = absolute temperature.

Combining Equations 59 and 60 and solving for R_c, we obtain

$$R_c = -(2\sigma V^*/RT\ln p/p_s) + t. \tag{61}$$

It is assumed that the film thickness is the same at a given pressure inside filled capillaries as it is on the exposed surface. The value of t must be determined either by calculation from the BET theory or by measurement of an isotherm on a non-porous adsorbent. Figure 21 shows values of t and R_c as functions of p/p_s (81). Values of t are those determined by Shull (84) for adsorption of nitrogen on large crystals. R_c is determined from Equation 61.

In making calculations the abscissa of the desorption isotherm is divided into a number of increments of convenient size, in this case 0.05. Each increment represents a reduction in pressure, and therefore the desorption of a volume V of nitrogen. This volume is made up of two parts: that which is evaporated from the menisci of filled pores, V_m, and that which is desorbed from the absorbed film, V_f; that is

$$V = V_m + V_f. \tag{62}$$

The increment of surface area, S_p, exposed by the evaporation of an increment of gas from filled pores is given by

$$S_p = 2\Delta V_p^*/R_c \tag{63}$$

where ΔV_p^* = volume of pores emptied by evaporation from menisci. This volume is given by

$$\Delta V_p^* = (1.558 \times 10^{-3}) V_m R_c^2/(R_c - t)^2 \tag{64}$$

where the factor 1.558×10^{-3} is the ratio of the volume of liquid nitrogen to that of nitrogen gas at STP.

After n desorption increments, the value of V_f may be calculated from

$$V_f = \Delta t \sum_{i=1}^{n} (S_p)i. \tag{65}$$

The number $\sum(S_p)_i$ is the surface area of the unfilled pores.

Equations 63 through 65 have been derived on the assumption that consistent units are used. In practice the dimensions used are: square meters per gram for S_p; cubic centimeters for all volumes; Angstroms for R_c and t. Volumes used for calculation are gas volumes at STP rather than liquid volumes. The following is a catalog of the above equations including the appropriate dimensional corrections:

$$V_f = 0.064 \Delta t \sum_{i=1}^{n} (S_p)i; \tag{66}$$

$$\Delta V_p = V_m R_c^2/(R_c - t)^2; \tag{67}$$

$$S_p = 31.2 \Delta V_p/R_c. \tag{68}$$

The procedure for the computation is as follows: The total volume of gas adsorbed, R_c, and t at a series of values of p/p_s are recorded. The change, V, in the volume adsorbed for each increment is determined by difference, as is the change in film thickness. Then V_f is calculated from Equation 66, V_m from Equation 62, ΔV_p from Equation 67, and S_p from

Equation 68. The total area, $\sum S_p$, is calculated and used in Equation 66 for the next increment. The calculations are continued until $\sum S_p$ is equal to the total area as determined by the BET method. The value of $\sum \Delta V_p$ at this point should be equal to the total volume of nitrogen adsorbed, providing a check on the reliability of the calculation.

Apparatus

The apparatus used in this work is shown schematically in Figure 22. Vacuum was provided by a mechanical pump and an oil diffusion pump. The manometer was attached to a mercury reservoir, so that mercury could be added or removed at will. With the edge of the mercury meniscus at the fiducial mark at the bottom of the high-pressure side of the manometer, the volume of the apparatus, excluding the sample tube, was known from careful calibration. This volume could be adjusted in 50-milliliter increments by changing the level of mercury in the gas burette.

The sample tube was attached to the apparatus by means of a ground glass joint, lubricated with vacuum grease. Either nitrogen or helium could be admitted to the system through a three-way stopcock. An oxygen vapor-pressure thermometer was used to measure the temperature of the liquid nitrogen.

Procedure

The first step in determining an isotherm was to measure the volume of the "dead space" or unoccupied volume of the sample tube. After the sample tube, containing a weighed sample of dry solid, had been attached to the apparatus and outgassed overnight at 200° C. under high vacuum, the sample tube was immersed in liquid nitrogen and closed off from the manifold by means of stopcock A in Figure 22. Mercury was

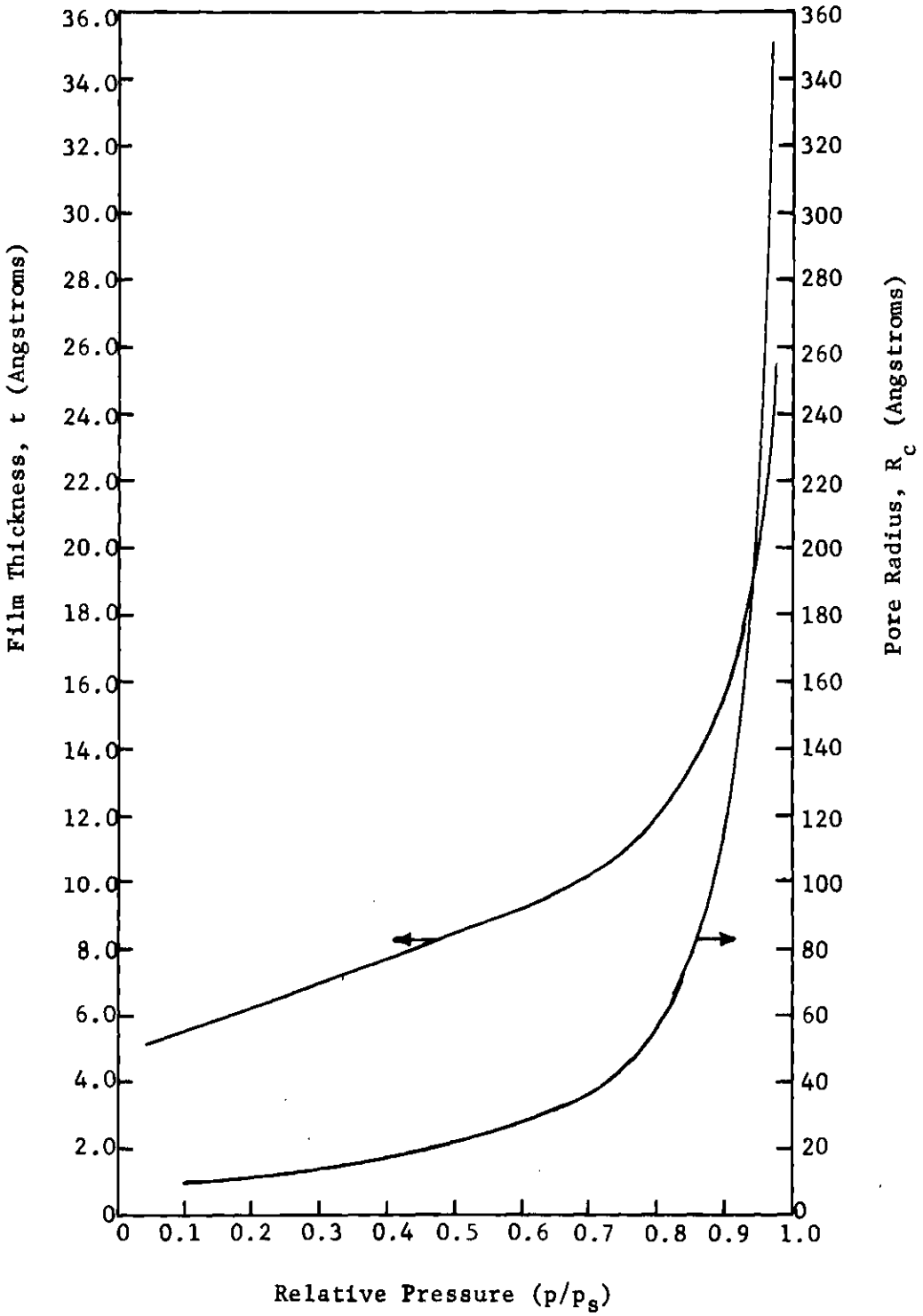

Figure 21. Film Thickness and Pore Radius as Functions of Relative Pressure

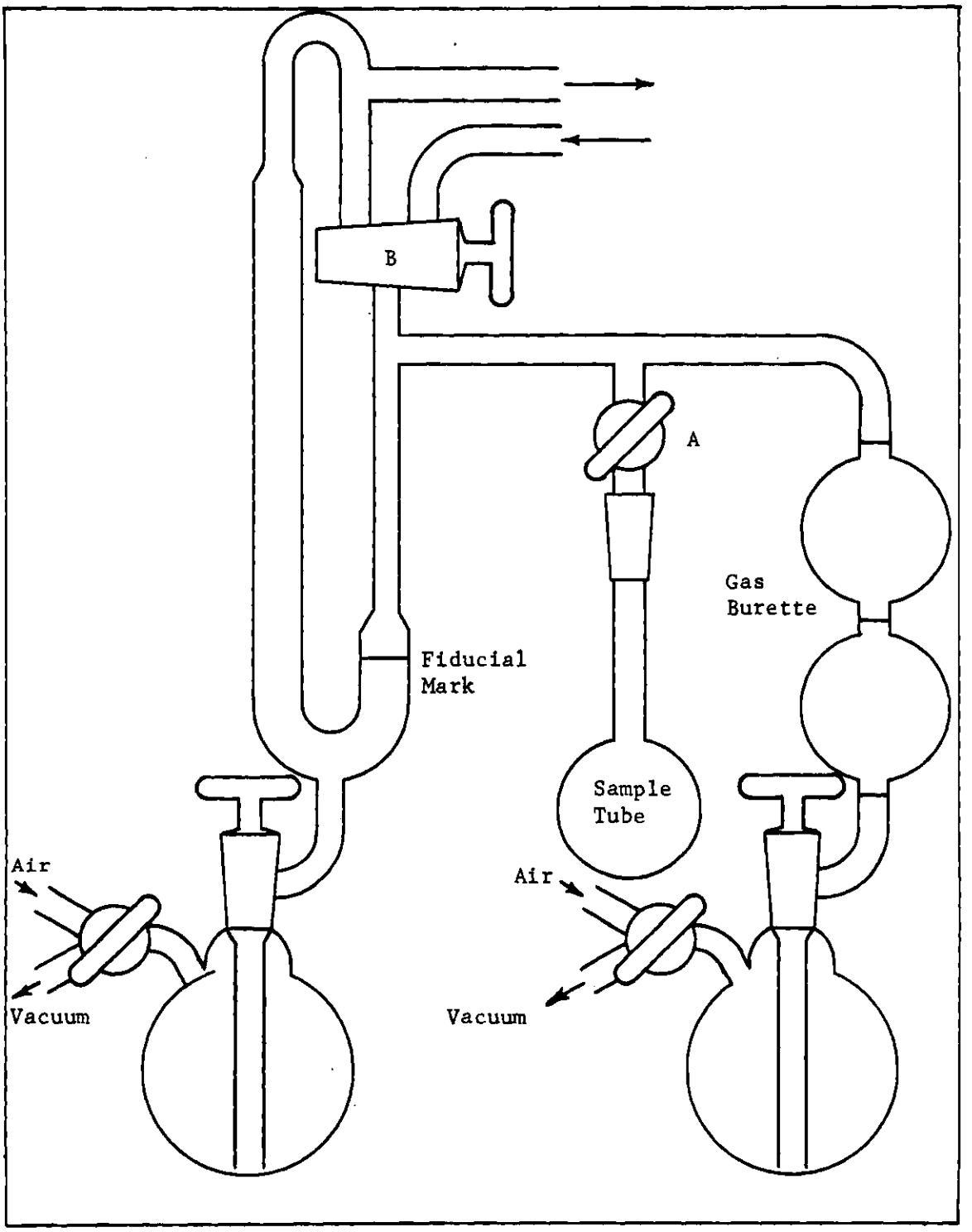

Figure 22. Nitrogen Adsorption Apparatus

admitted to the manometer until the level of mercury was about 15 centimeters above the fiducial mark. The manifold was isolated from the vacuum pumps by stopcock B, and helium was admitted to it carefully until the mercury level on the high-pressure side of the manometer had fallen back just to the fiducial mark. The difference in height of the mercury columns on the two sides of the manometer was measured with a cathetometer and recorded as p_1.

The sample tube was then opened. The level of mercury on the high-pressure side of the manometer rose with the change in pressure, and was again adjusted to coincide with the fiducial mark by drawing some mercury out of the manometer into the reservoir by means of the aspirator. This adjustment had to be repeated several times as the gas in the sample tube came to thermal equilibrium with the liquid nitrogen. After the pressure had remained constant for several minutes, it was measured and recorded as p_2.

The volume, V_s, of the dead space in the sample tube is given by

$$V_s = (p_1 - p_2)V_T T_s / p_2 T_b \qquad (69)$$

where V_T = volume of apparatus excluding sample tube;

T_s = absolute temperature of liquid nitrogen;

T_b = ambient air temperature.

When V_s had been determined, the system was again evacuated and the sample heated to 200° C. in order to drive off all of the helium before beginning nitrogen adsorption experiments.

Nitrogen adsorption measurements were made in much the same manner

as the helium pressure measurements. With the sample tube immersed in liquid nitrogen and shut off from the manifold, the mercury level in the manometer was raised and purified nitrogen admitted to the manifold until the level on the high-pressure side of the manometer coincided with the fiducial mark. The difference in height between the two columns was determined with the cathetometer and recorded as p_1. The sample tube was opened and the mercury level in the manometer readjusted to coincide with the fiducial mark. When equilibrium had been established, the difference in height was again measured and recorded as p_2. The sample tube was again closed off, more nitrogen was admitted, and the process was repeated. At each step the value of p_2 for the previous step was recorded as p_o.

When p_2/p_s was less than 0.3, the amount of nitrogen admitted at each step was adjusted so as to give a change in p_2 of about 40 millimeters. At higher values of p_2, nitrogen was admitted in larger increments, so as to reach saturation in a reasonable number of steps. When the saturation pressure of nitrogen at the temperature of the liquid nitrogen used had been attained, desorption was begun.

In making the desorption measurements, the sample tube was closed off, and the manifold was opened carefully to the vacuum system, drawing a small portion of the nitrogen in the manifold out. The mercury level was adjusted and p_1 measured. Some mercury was let into the manometer, and the sample tube was opened, increasing the pressure in the manifold. The mercury level was readjusted, and, when equilibrium had been established, p_2 was measured and recorded. The process was repeated until p_2 had been reduced to less than one-tenth of the saturation pressure.

Nitrogen does not behave ideally near its saturation temperature, and a correction to the ideal gas law must be applied. The equation for the volume adsorbed per gram at each step is (81)

$$V_a/w = (273.16/760w)\, V_T(p_1 - p_2)/T_b - V_s(p_2 - p_o)/T_s - \alpha V_s(p_2^2 - p_o^2)/T_s \qquad (70)$$

where V_a = volume of nitrogen adsorbed;

w = weight of adsorbent;

V_t = volume of vacuum system;

T_b = ambient air temperature;

V_s = volume of dead space;

T_s = temperature of liquid nitrogen;

α = a constant, assumed to be 6.6×10^{-5}.

The surface areas of both the aluminum and aluminum oxide adsorbents were determined by the BET method. The BET plots are shown in Figures 23 and 24. The surface area measured for aluminum was 1.14 square meters per gram; that for aluminum oxide was 310 square meters per gram. The adsorption and desorption isotherms for aluminum oxide are shown in Figure 25. Figure 26 shows the area within pores of radius greater than R_c as a function of R_c.

The aluminum powder had a surface area too small to permit reproducible measurement of the isotherm; however the isotherms measured were flat over a range of relative pressure from about 0.04 to 0.09, suggesting little porosity. This evidence, together with the appearance

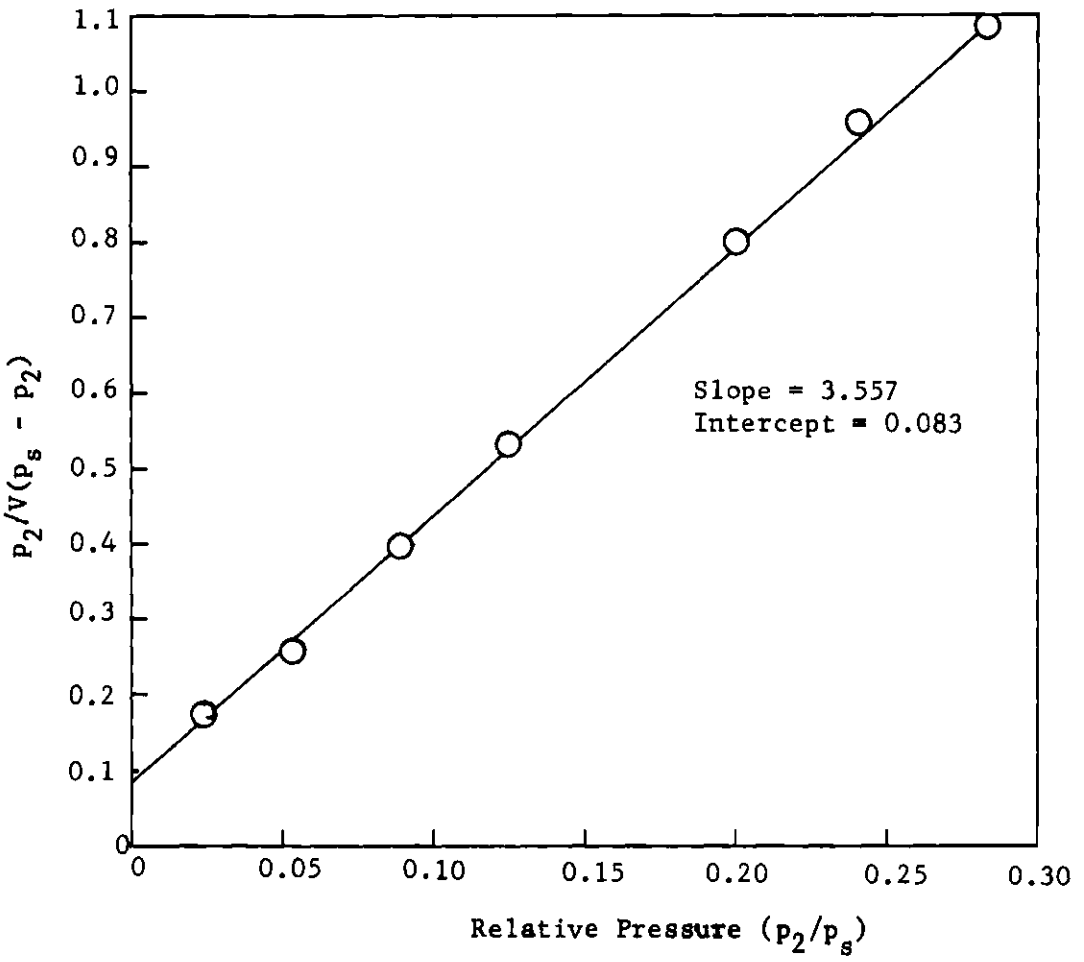

Figure 23. BET plot - Aluminum Powder

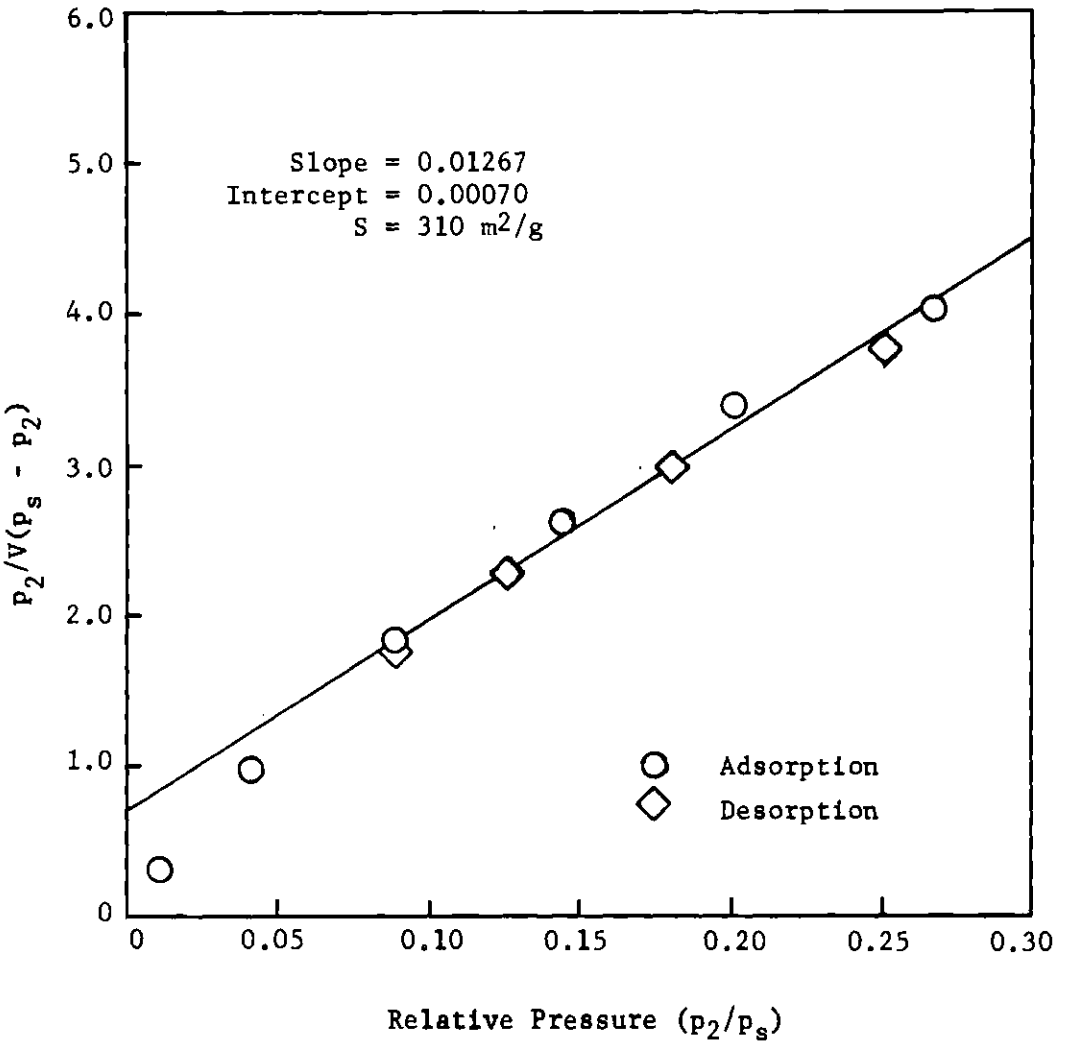

Figure 24. BET Plot - Aluminum Oxide

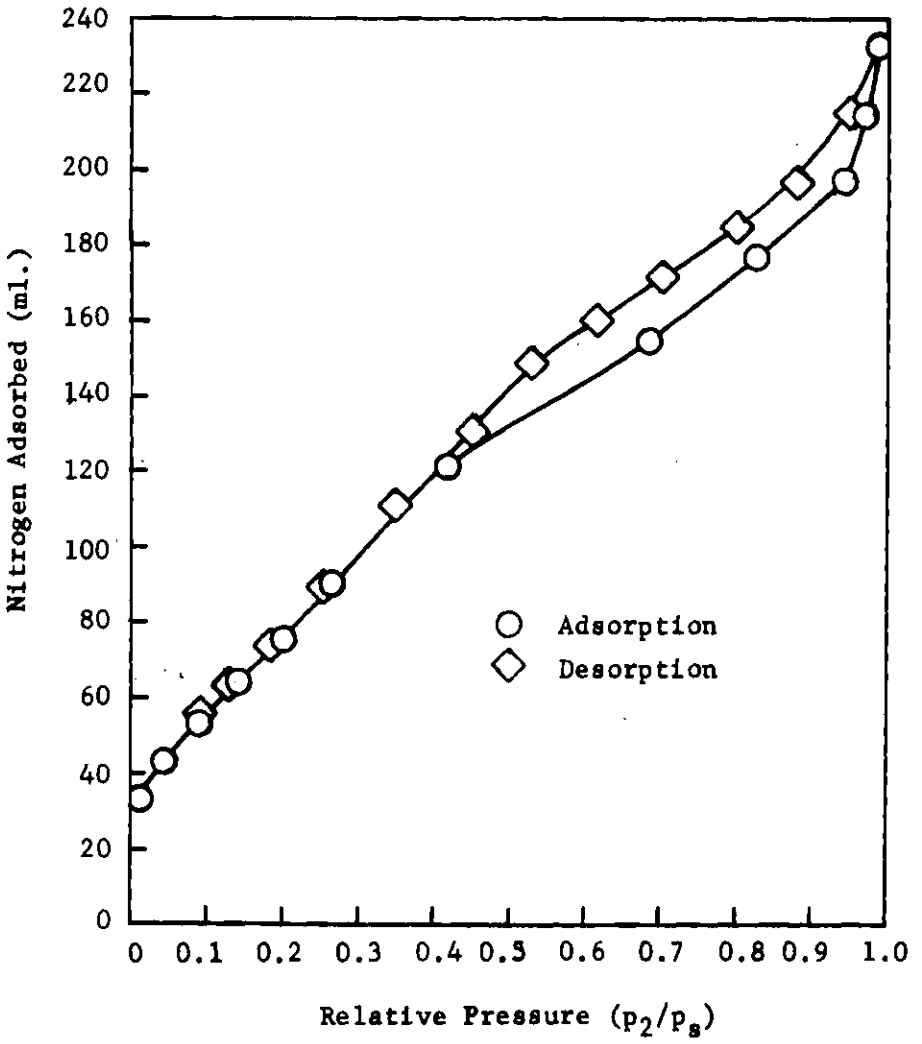

Figure 25. Nitrogen Adsorption Isotherm - Aluminum Oxide

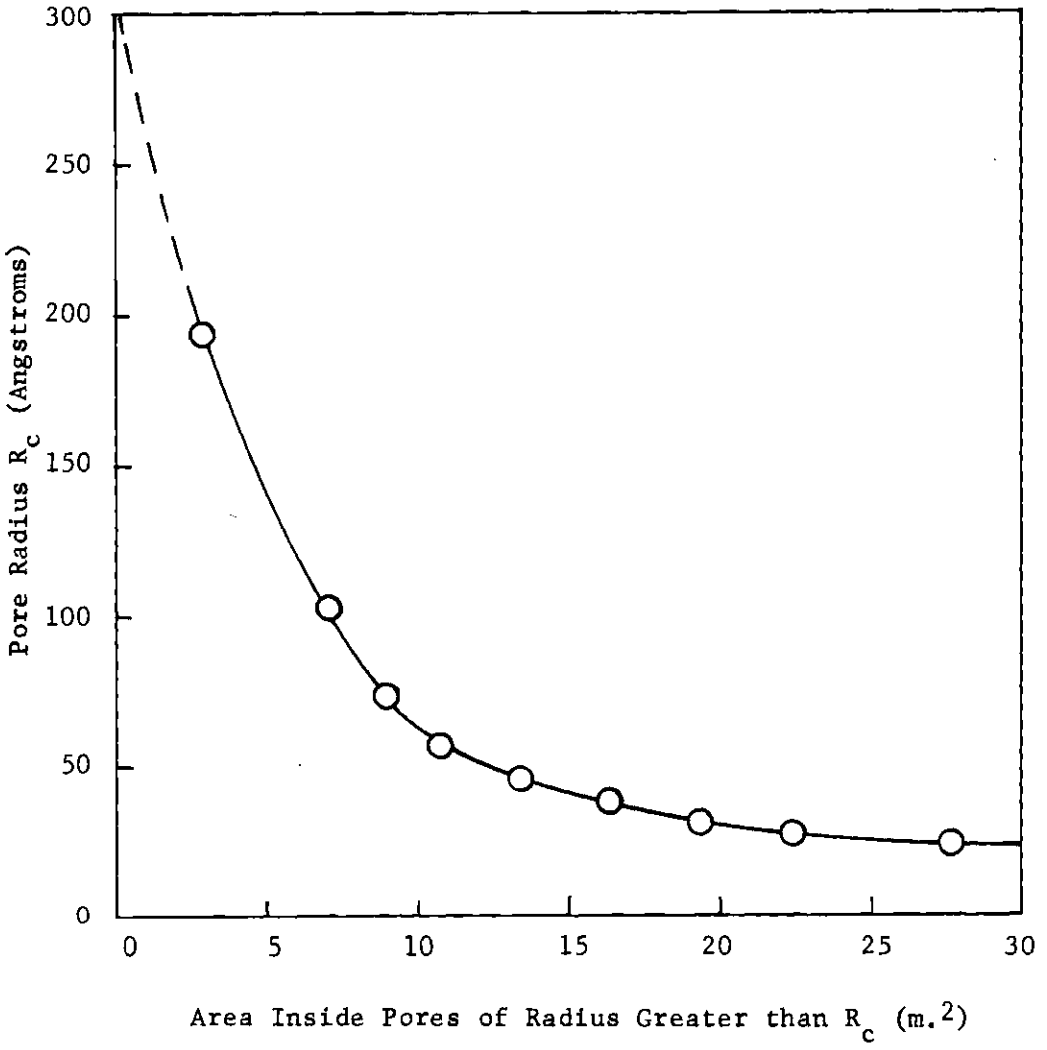

Figure 26. Distribution of Area of Aluminum Oxide Inside Pores

of the powder under the microscope and the results of the particle-size measurements (see below) led to the conclusion that the powder was essentially non-porous.

Particle-Size Measurements

It was assumed in the present work that the aluminum powder provided a non-porous surface. The adsorption isotherm seemed to support this assumption but was not regarded as conclusive because of the difficulty in obtaining reproducible curves. Under the microscope the particles in the aluminum powder appeared to be of irregular shape, somewhat elongated; and the surface seemed smooth and shiny. It was decided that further evidence concerning the nature of the surface might be obtained indirectly by determining the particle-size distribution and calculating a specific surface area from that.

If one assumes all particles to be spherical, it is easy to calculate a specific surface area from a distribution of particle diameters. The specific surface area of a collection of particles of uniform size is giv

$$= \pi D^2/(\rho\pi D^3/6) \qquad (71)$$

area;

r;

olid.

s of various sizes, S is given by

$$N(D)\pi D^3/6\Big]$$

$$= 6\sum_{D=0}^{\infty} N(D)D^2/\rho\sum_{D=0}^{\infty} N(D)D^3 \qquad (72)$$

where N(D) = number of particles having diameter D.

Let $F_n(D)$ be a distribution function defined as the fraction of particles having a diameter less than or equal to D. Then, assuming a continuous rather than a discrete distribution, N(D) is given by

$$N(D) = N dF_n/dD \tag{73}$$

where N = total number of particles present.

The summations in Equation 72 can now be replaced by integrals, and we have

$$S = 6 \int_0^\infty D^2 (dF_n/dD)\, dD / \rho \int_0^\infty D^3 (dF_n/dD)\, dD = 6 \int_0^1 D^2 dF_n / \rho \int_0^1 D^3 dF_n. \tag{74}$$

The data are usually obtained as a weight distribution rather than as a number distribution, so we must define a weight distribution function, $F_w(D)$, as the weight fraction of particles having a diameter less than or equal to D. Now $F_w(D)$ is related to $F_n(D)$ by the equation

$$F_w(D') = (1/W) \sum_{D=0}^{D'} \pi D^3 N(D) \rho /6 \approx (\pi\rho/6W) \int_0^{D'} D^3 N(D)\, dD \tag{75}$$

where W = total weight of the sample.

In differential form, Equation 75 becomes

$$dF_w = (\pi\rho/6W) D^3 N(D)\, dD = (\pi\rho N/6W)\, dF_n \tag{76}$$

or

$$dF_n = (6W/\pi\rho N)(1/D^3)\,dF_w \tag{77}$$

Substituting Equation 77 in Equation 74 we obtain

$$S = 6\int_0^1 (1/D)\,dF_w / \rho\int_0^1 dF_w. \tag{78}$$

Since $\int_0^1 dF_w$ is unity, we have the final result

$$S = (6/\rho)\int_0^1 (1/D)\,dF_w. \tag{79}$$

Equation 79 is readily evaluated by graphical integration if the experimental distribution function $F_w(D)$ is available.

The distribution of particle sizes in the aluminum powder was measured by Mr. John H. Burson of the Georgia Institute of Technology Engineering Experiment Station, using a Coulter Counter. The principles and method of operation of this instrument are summarized by Corbett, Burson, and Young (85). The instrument measures directly the volume of the particle. The volume is then converted into an equivalent spherical diameter. When this diameter is used in Equation 79 to determine the specific surface of a non-spherical sample, the result is necessarily low. Table 9 shows the formulae for the equivalent spherical diameters of some non-spherical shapes and the ratios between calculated and true specific surfaces for these shapes. Figure 27 shows the measured integral

distribution function. Figure 28 shows 1/D as a function of F_w. The area under the curve in Figure 28 was measured with a polar planimeter and substituted for the integral in Equation 29. The value of ρ was taken as 2.70 (86).

The area calculated from the particle-size distribution was 0.56 square meters per gram, and the ratio between this and the BET area was 0.49, comparable in magnitude with the ratios calculated for the square-prism shapes shown in Table 9. Because of the apparent irregularity of the particles, this value seems to support the hypothesis that the surface is non-porous.

Table 9. Variation of Calculated Surface Area with Shape

Shape	Equivalent Spherical Diameter	S(Calc.)/S(True)
Sphere	D	1.00
Cube	1.24w	0.81
Square Prism 1 2w	1.56w	0.77
Square Prism 1 4w	1.97w	0.68

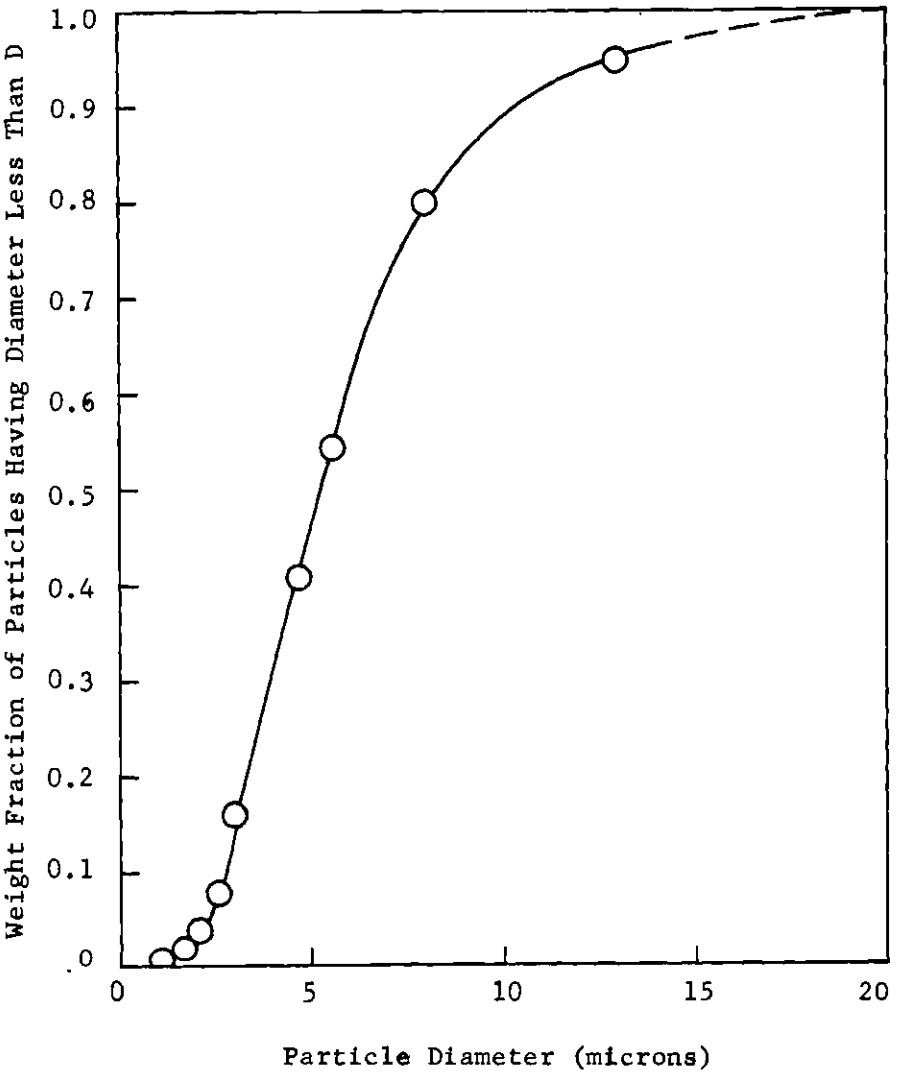

Figure 27. Integral Distribution of Particle Sizes

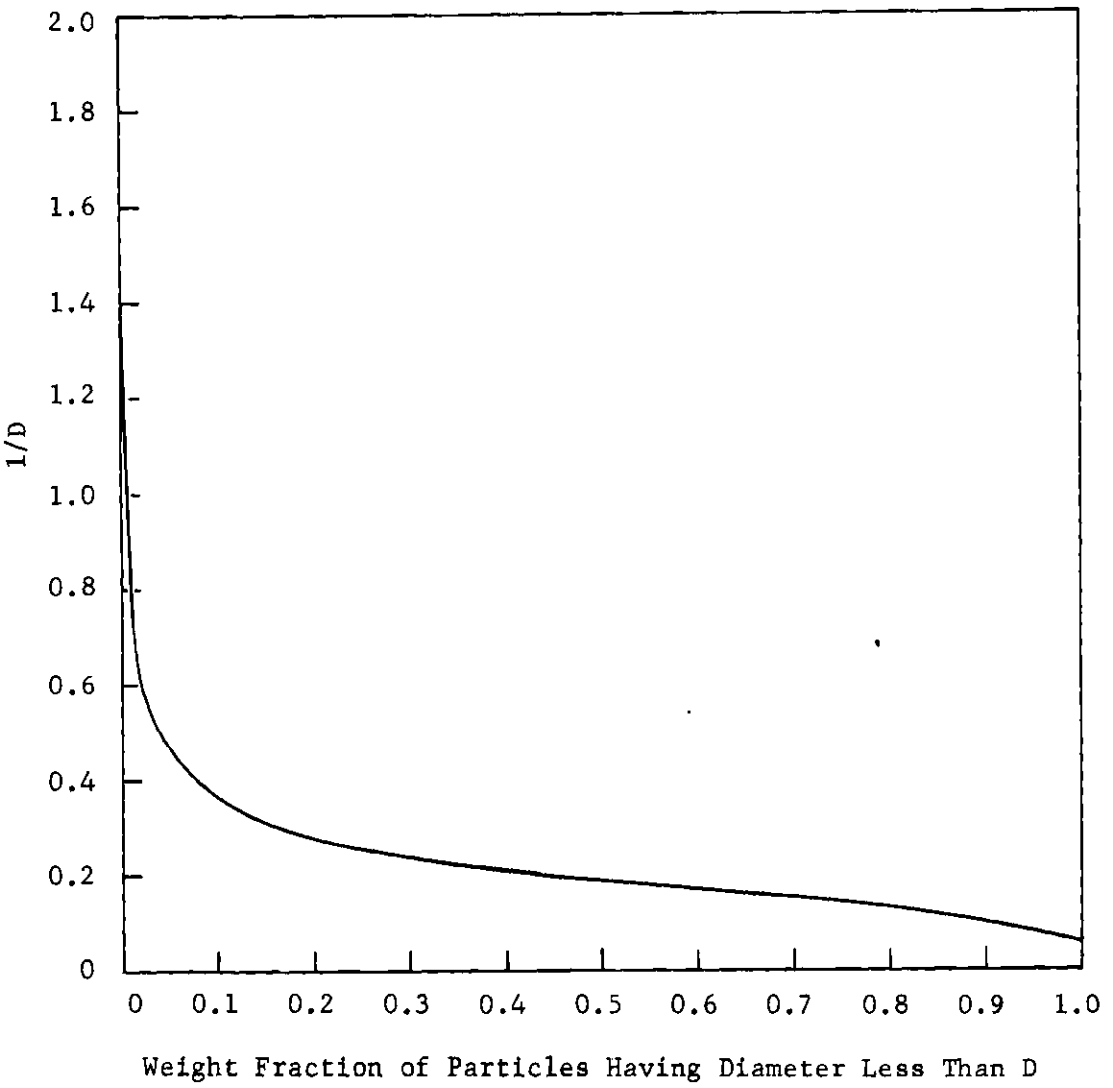

Figure 28. Estimation of Surface of Al from Particle Size Measurements by Graphical Integration

CHAPTER III

ADSORPTION MEASUREMENTS

Measurements of the adsorption of polystyrene from cyclohexane onto aluminum and aluminum oxide made up the bulk of the adsorption measurements in this study. Both kinetic and equilibrium or quasi-equilibrium measurements were made. In addition, brief studies were made of the adsorption of polyisobutylene onto aluminum from benzene, another theta system, and the adsorption of ethylbenzene from cyclohexane onto aluminum oxide as a monomeric analog of the polystyrene system.

Analysis of the polymer solutions presented a problem since it was desired to study the behavior at very low concentrations. Since most of the adsorption studies involved the adsorption of polystyrene, the ultra-violet absorption spectrum of this polymer provided a convenient analytical method, which could also be applied to ethylbenzene. No such convenient spectrophotometric method was available for analysis of polyisobutylene solutions, however, and a less precise gravimetric method was used in these analyses.

Spectrophotometric Analysis

Polystyrene absorbs ultraviolet radiation quite strongly in the neighborhood of 2600 Angstroms. The ultraviolet spectrum of polystyrene, measured with a Cary Model 14 spectrophotometer, is shown in Figure 29. Three very prominent peaks occur at 2595, 2615, and 2690 Angstroms, and

all three were used in determining solution concentrations.

A series of solutions of polystyrene in spectro-quality cyclohexane were prepared, ranging in concentration from 20 to 100 milligrams of polystyrene per 100 grams of solution. The absorbance of these solutions was measured at each of the three wavelengths, and the absorbance was plotted as a function of concentration, giving a straight line passing through the origin in each case. The slopes of these lines were determined by the method of least squares. Thereafter, the concentration of an unknown solution could be determined by dividing the absorbance at a given wavelength by the slope, ε, of the corresponding calibration curve. Typical calibration curves are shown in Figure 30.

A calibration curve was run every time a set of adsorption measurements was made. Variations of about plus or minus three percent in the values of ε were observed from one run to the next, presumably because of fluctuations in the performance of the spectrophotometer. Variations of the order of plus or minus one percent were observed between fractions. These showed no trend with molecular weight and appeared to be entirely random.

Analysis of ethylbenzene solutions was accomplished using the same procedure. Ethylbenzene absorbed somewhat more strongly than did polystyrene, and it was necessary to use a weak band at 2485 Angstroms. The ultraviolet spectrum of ethylbenzene is shown in Figure 31.

Adsorption Measurements on Polystyrene

The adsorption experiments consisted of shaking a quantity V of a polymer solution of initial concentration c_o with w grams of adsorbent.

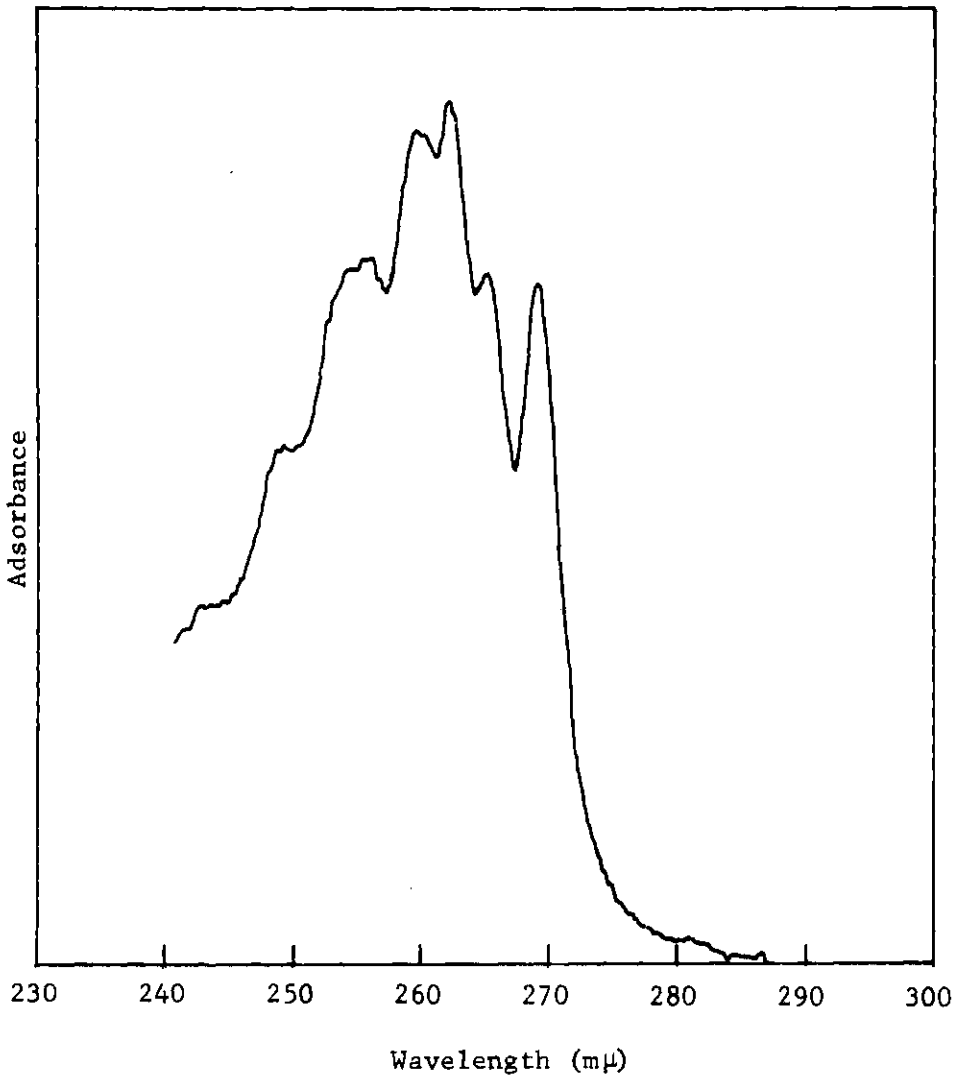

Figure 29. Ultraviolet Spectrum of Polystyrene

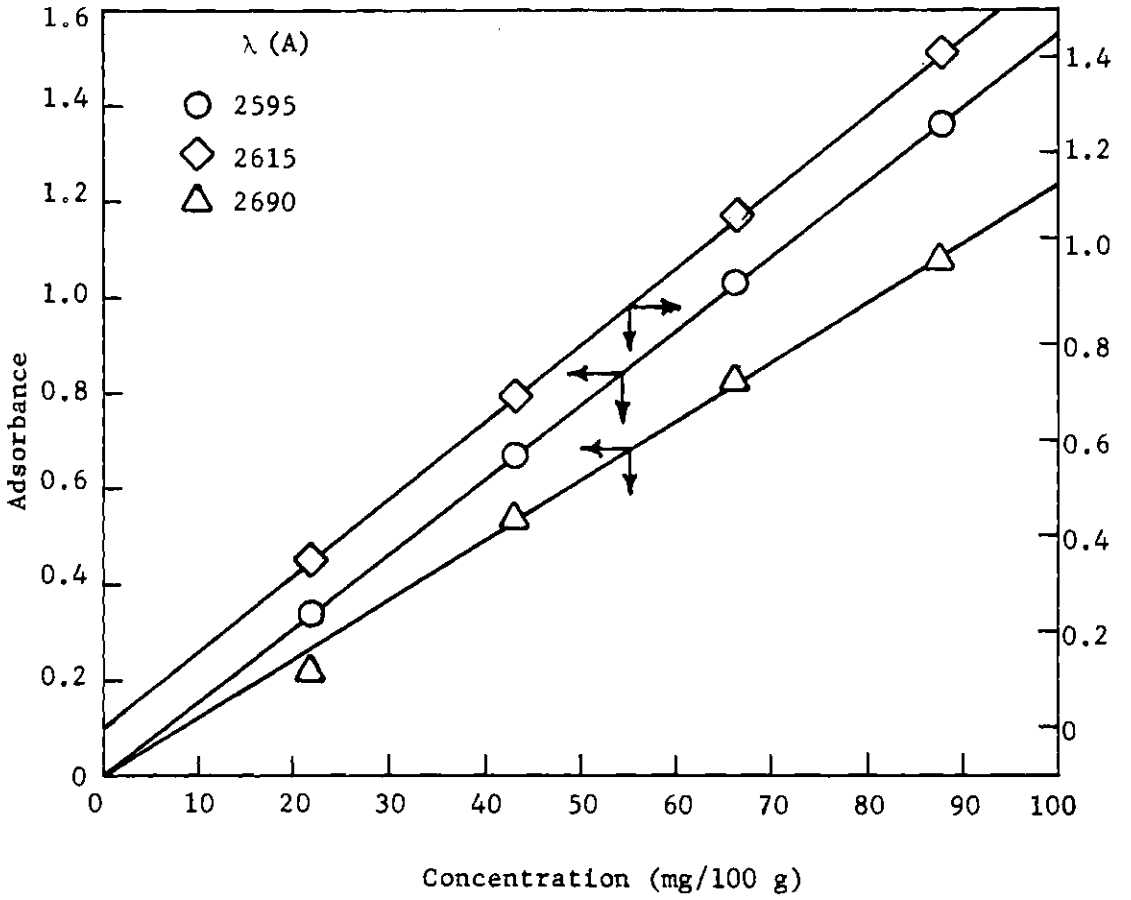

Figure 30. Typical Spectrophotometer Calibration Curves
Polystyrene, Fraction F

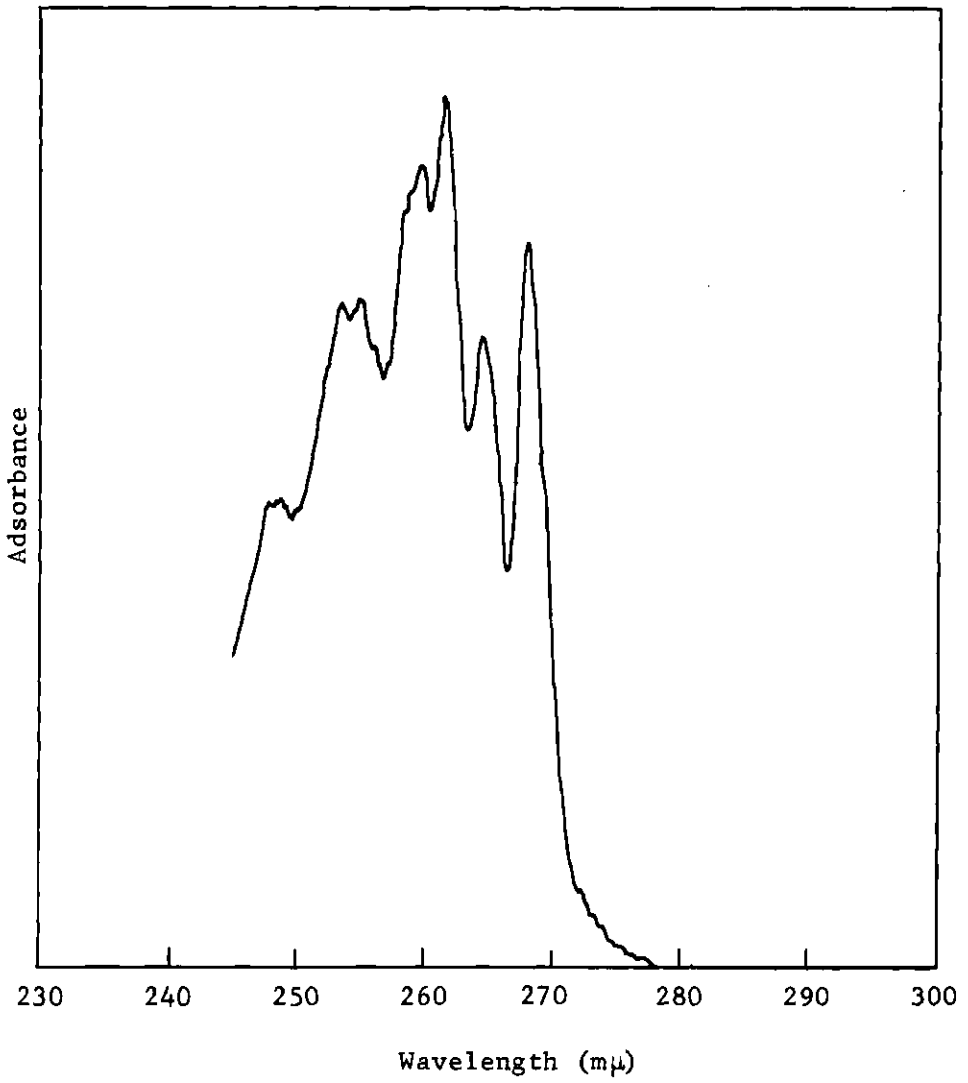

Figure 31. Ultraviolet Spectrum of Ethylbenzene

The final concentration c was measured, and the specific adsorption A was calculated from the equation

$$A = (c_o - c)V/w. \tag{80}$$

In making the "equilibrium" measurements, all solutions were made up by weight, rather than by volume, because it was necessary to keep them somewhat above room temperature in order to avoid precipitation of the fractions of high molecular weight. It was thought that under these circumstances volumetric procedures would be less accurate than purely gravimetric ones. Hence V in these measurements has the dimensions of mass rather than volume, and concentrations are expressed in milligrams per 100 grams.

The solutions were prepared by weighing enough polystyrene into a glass-stoppered erlenmeyer flask to make the desired quantity of solution. The concentration was usually approximately 100 milligrams per 100 grams. The flask was tared on a large analytical balance, and the proper amount of polystyrene was put into it. The flask and its contents were dried overnight at 80° C. under vacuum, cooled, and weighed again to determine the exact quantity of dry polystyrene present. About 25 milliliters of solvent were added, and the flask was put into an air bath at about 50° C. until all polymer appeared to have dissolved. Then, with the flask sitting on a rough balance, solvent was added until the total weight of the solution reached the desired value. The final weight of the solution was determined to within $\pm$ 0.02 grams. Shortly before the solution was placed in the ampules with the adsorbent,

a small piece of sodium wire was added to it to remove traces of moisture.

Adsorption was carried out in 20-milliliter glass ampules. These were numbered and dried for several hours in an oven at 120° C. They were tared on an analytical balance, and some adsorbent was added to each. Then the ampules were heated under vacuum at about 140° C. for 24 hours.

At the end of this time, the ampules were placed in a dessicator charged with Drierite and allowed to cool. They were then weighed on the analytical balance and returned to the dessicator.

Ten-milliliter aliquots of the polymer solution were drawn into a warm hypodermic syringe and introduced into the ampules. Aluminum foil caps were placed over the tops of the ampules to retard evaporation and prevent entrance of moisture. The ampules were weighed again immediately. The caps were removed for only the few seconds necessary to weigh the ampules on the automatic analytical balance. Evaporation from the ampules was negligible during the time they were open.

After weighing, the ampules were partially immersed in a bath of acetone and dry ice to freeze the solution. The tips of the ampules were then sealed using a gas-oxygen flame.

The sealed ampules were placed in a test-tube rack which had been fitted with a wire retainer to hold them in place. The rack was placed on a shaker in a water bath with the ampules in a horizontal position. The ampules were shaken gently for the time allotted for adsorption.

When the adsorption runs were completed, the shaker was stopped and the ampules set in an upright position, still immersed in the constant

temperature bath, to allow the solid to settle. The ampules were then removed from the bath, quickly broken open, and each solution was carefully decanted into a screw-cap vial, which was immediately closed tightly. When all samples had been taken, the spectra of the solutions were measured.

At the same time as the adsorption tubes were prepared, a set of solutions was prepared for calibration of the spectrophotometer. These were made by dilution of the stock solution and were kept in sealed glass ampules.

The polymer concentration of each solution was calculated from the absorbance at each of the three wavelengths used, and the average of the three taken as the true concentration. The specific adsorption was calculated from Equation 80.

Adsorption Kinetics

The kinetics of adsorption of polystyrene were studied using the technique described above as well as a slight modification. Nearly identical quantities of adsorbent and solution were used in each vial, and samples were taken and analyzed at intervals. Thus A or c could be plotted as a function of time.

In the modified technique, the vials used were made of 22-millimeter Pyrex tubing. Each vial was made of a 12-centimeter length of tubing which was sealed at one end. A thin glass bulb with a diameter slightly smaller than the inside diameter of the tube held a weighed quantity of dry adsorbent sealed inside. This was placed inside the tube, and a narrow neck was drawn at the open end. The tube and bulb were weighed, ten milliliters of polymer solution were put

inside with a hypodermic syringe, and the tube and its contents were weighed again. After weighing, the tube was immersed in a dry-ice-acetone bath, and its neck was sealed.

When all tubes had been sealed, they were put into the thermostat and allowed to come to thermal equilibrium. Then each tube was removed, shaken violently to break the bulb containing the adsorbent, and replaced in the thermostat. The tubes were agitated gently, and were broken and their solutions analyzed at regular intervals.

Several efforts were made to obtain kinetic data in this way. The experimental difficulties involved were considerable, and the results were fragmentary and generally unsatisfactory. One set of curves was obtained for adsorption on aluminum oxide, and these are shown in Figure 32.

The other method, which did not involve the use of an inner bulb to hold the adsorbent, was much less difficult and gave better results. It was subject to criticism, however, on the grounds that the solution and adsorbent were in contact for a considerable period during which the temperature was different from that of the thermostat; and the effect of suddenly freezing and then melting the solution is unknown.

The procedure was essentially that described in the preceding section. A volumetric technique was used. The solution was introduced into the ampules with a ten-milliliter volumetric pipette, and the ampules were not weighed after the introduction of the solution. They were frozen immediately in an effort to minimize adsorption prior to equilibration with the thermostat. Fractions F and L were used in these studies. These fractions remained in solution at room temperature,

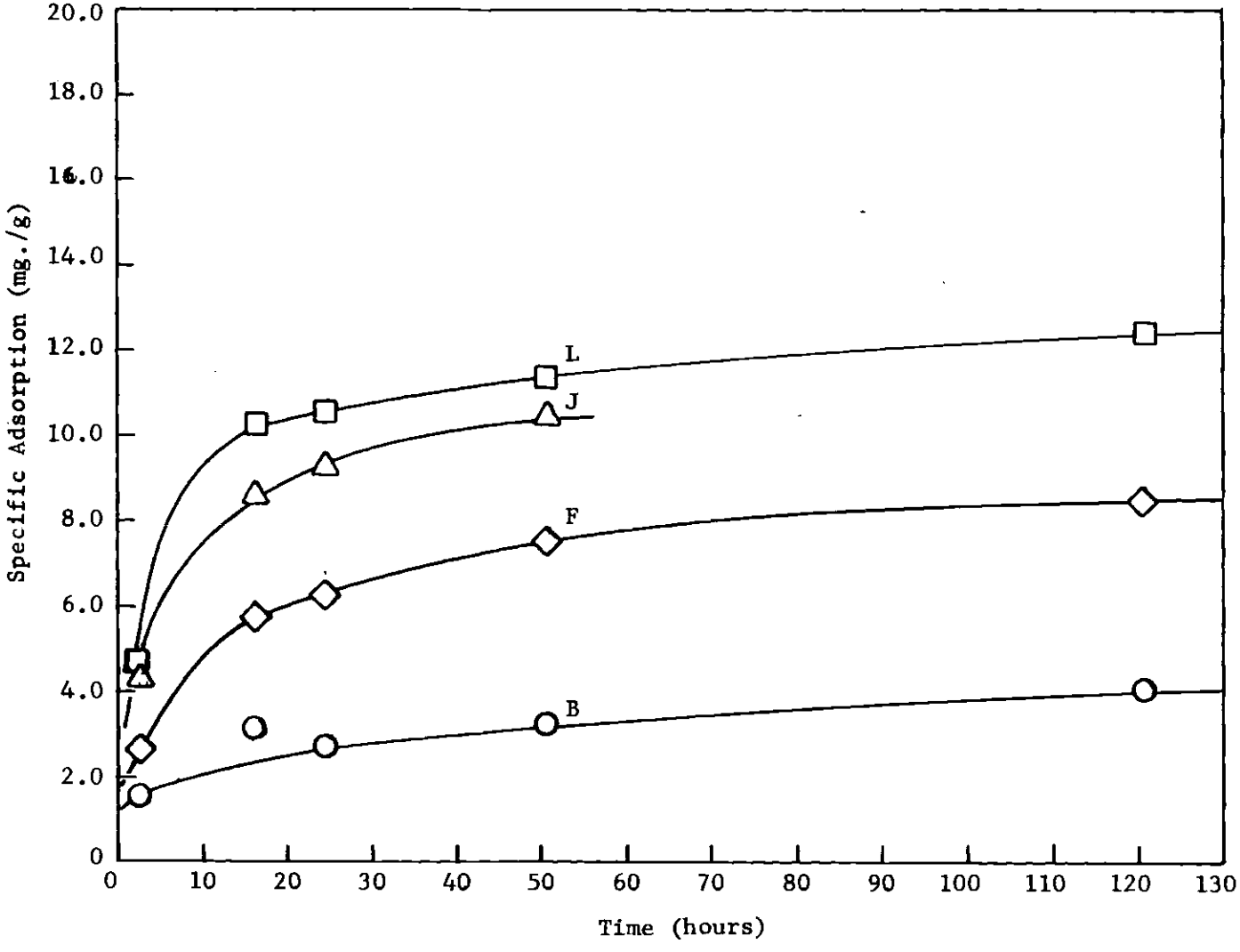

Figure 32. Rate Curves for Adsorption of Polystyrene on Aluminum Oxide

so no problems with precipitation were encountered during filling.

After sealing, the ampules were kept in a dry-ice-acetone mixture, so that their contents remained frozen until they were put into the thermostat, they were allowed to remain there for a few minutes until they had come to equilibrium with it; then the first vials were taken for analysis. The solutions were decanted into screw-cap vials, which were sealed and kept in the freezing compartment of a refrigerator until all samples were ready for analysis. Thereafter, samples were taken at intervals over a period of 11 days. When all samples had been taken, the vials of frozen solution were placed in a warm air bath and brought quickly to a temperature of 35° C. before being analyzed spectrophotometrically.

Results are shown in Figures 33 and 34.

Determination of Isotherms

The isotherms for the adsorption of all four fractions of polystyrene on aluminum and aluminum oxide were determined over a concentration range from zero to about 100 milligrams per 100 grams of solution. The variation in concentration was obtained by using varying amounts of adsorbent. The initial concentration of each solution in a given run was the same. Appropriate amounts of adsorbent to be used were determined by trial and error.

Initially the solutions were left in contact with the adsorbents for six days. Later, however, some runs were made for 25 days when it was discovered that equilibrium was definitely not established in the shorter period. Isotherms were obtained at 34.8° C. (the theta temperature) and at 50° C.

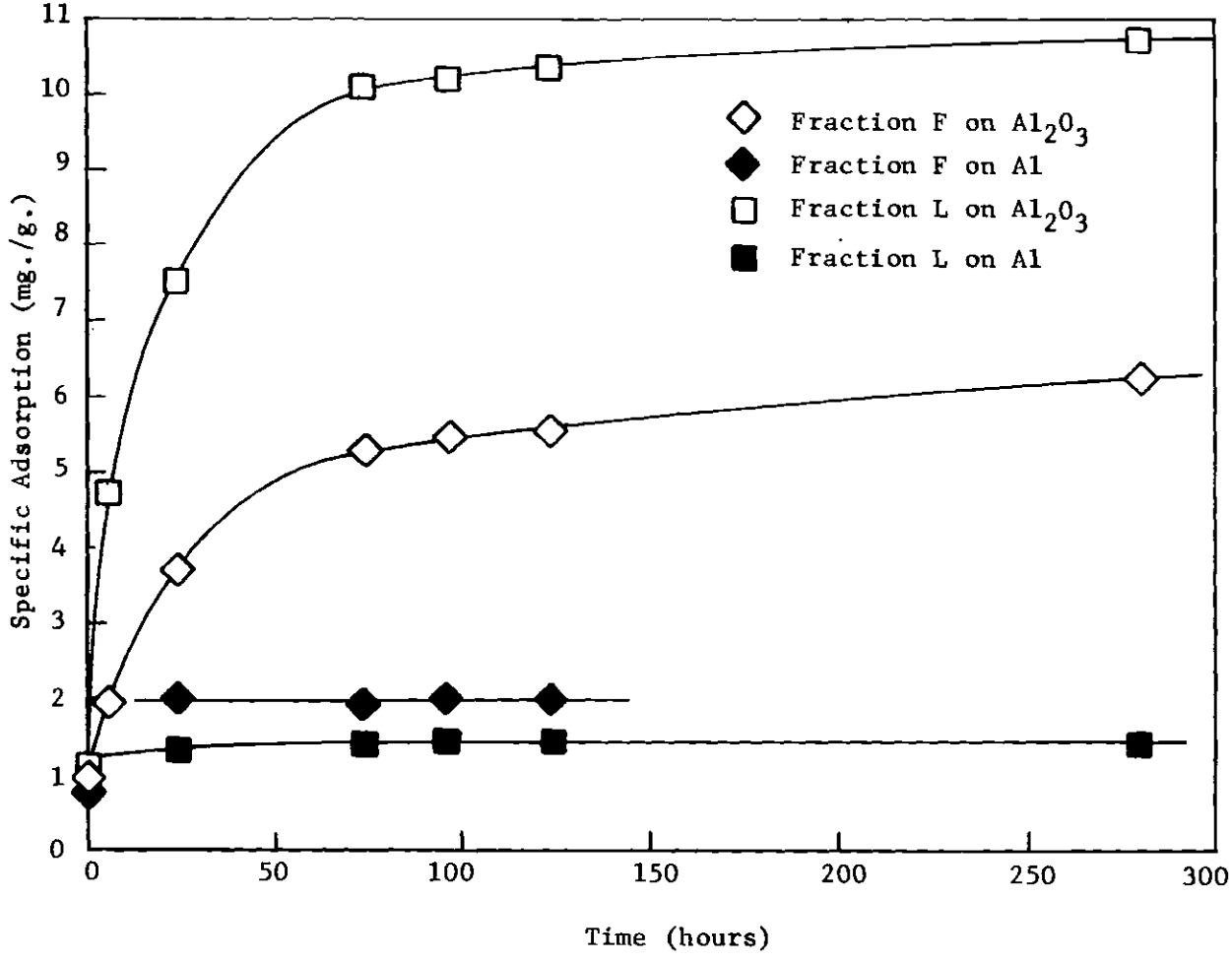

Figure 33. Rate Curves for Adsorption of Polystyrene on Aluminum Oxide and Aluminum

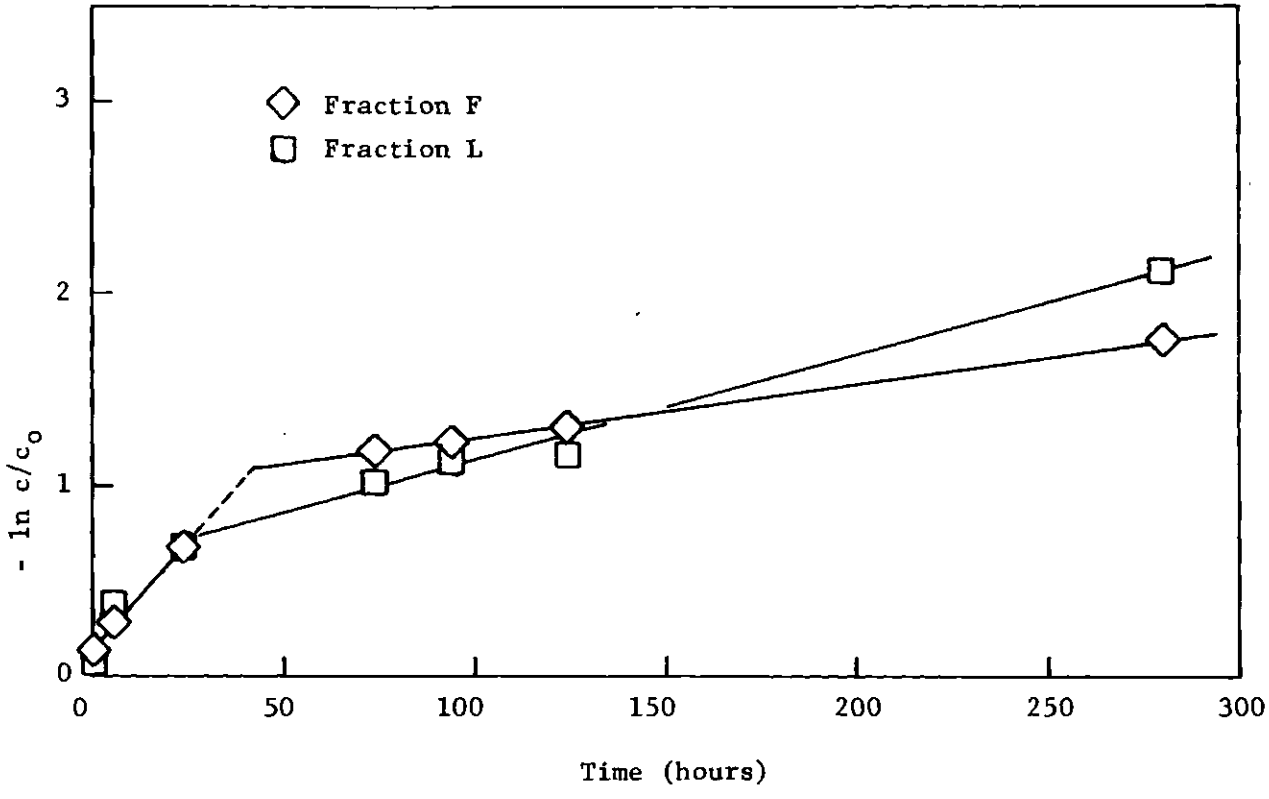

Figure 34. Rate Curves for Adsorption of Polystyrene on Aluminum Oxide - First-Order Plot

The specific adsorption was plotted as a function of concentration. Results are shown in Figures 35 through 40.

Desorption Studies

A brief study of the desorption of polystyrene from aluminum was carried out using cyclohexane and benzene as solvents. Polystyrene (fraction F) was adsorbed onto three grams of aluminum for six days at 34.8° C., in each of four vials. Two of the vials were opened and analyzed, after which the temperature was increased to 50° C. After six days at this temperature, the other two were opened and analyzed. Within experimental error no desorption was observed to take place after the increase in temperature.

In another experiment, five grams of aluminum were shaken with 25 milliliters of polystyrene solution for six days at 34.8° C. The solution was then removed by filtration and analyzed. The aluminum on the filter was washed once with cold cyclohexane to remove any polymer solution adhering to the surface. It was then removed from the filter and put into a weighed vial. After the solid had been dried under vacuum at room temperature for several hours, it was weighed, ten milliliters of benzene were added to it, and it was capped tightly. Then it was allowed to remain in an air bath at 50° C. with occasional shaking for four days. After this time the benzene was removed by filtration, poured into a weighing pan that had been tared on a microbalance, and the solvent was evaporated. The residue was dried for 24 hours under vacuum at 80° C. and the weight of the residue determined. The benzene removed about 94 percent of the adsorbed polystyrene. Results are summarized in Table 10.

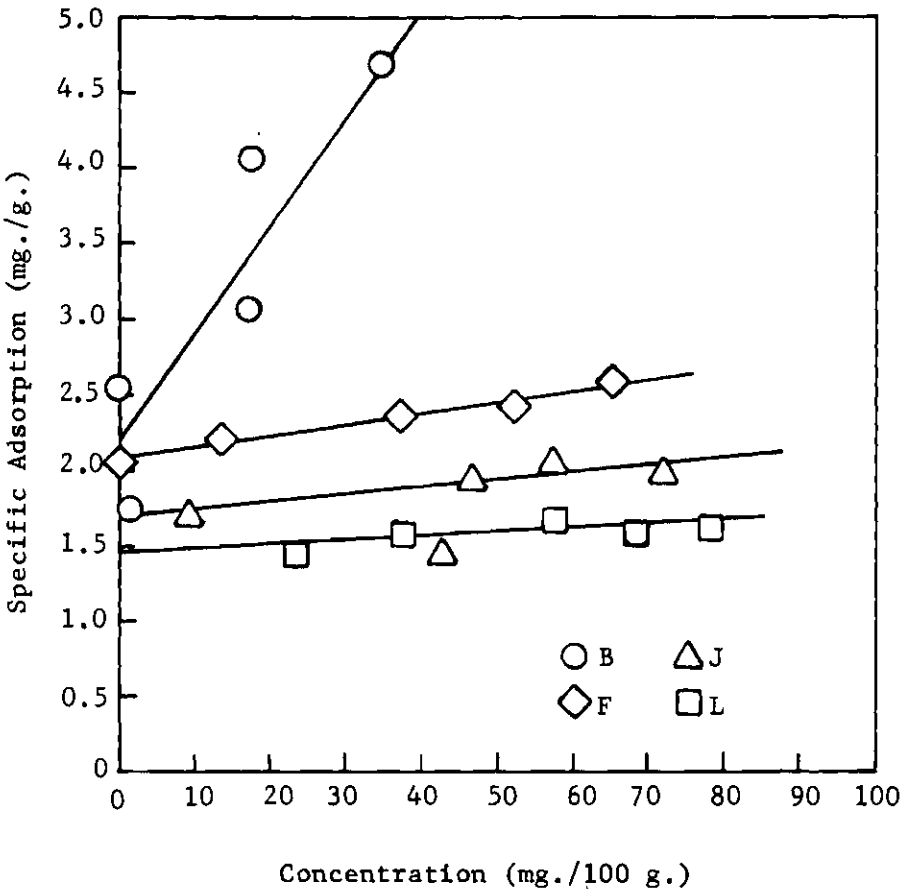

Figure 35. Adsorption of Polystyrene Fractions on Aluminum at 34.8° C. after Six Days

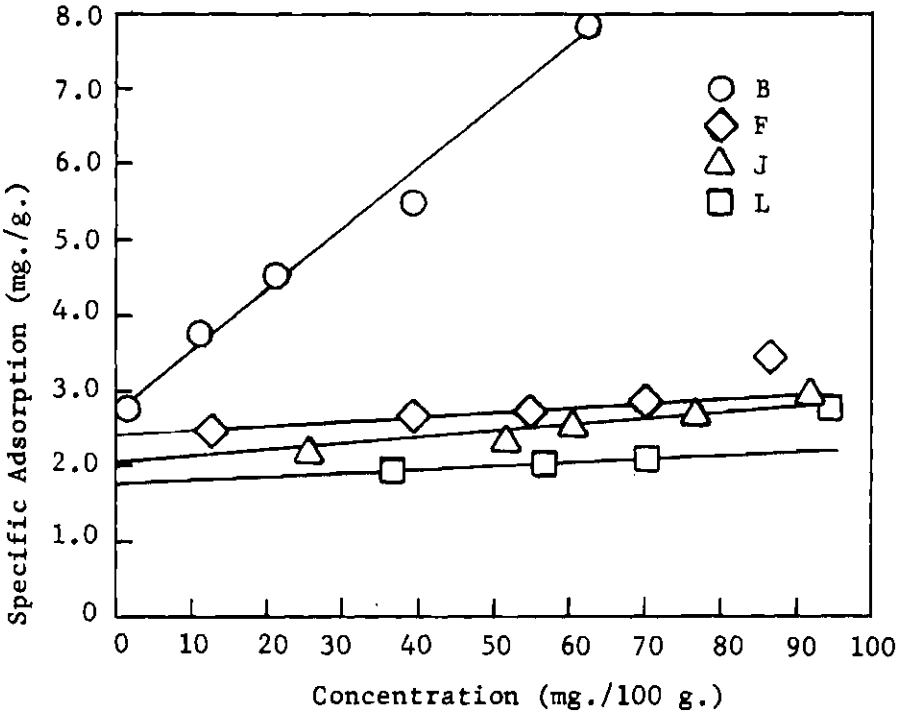

Figure 36. Adsorption of Polystyrene Fractions on Aluminum at 34.8° C. after 25 Days

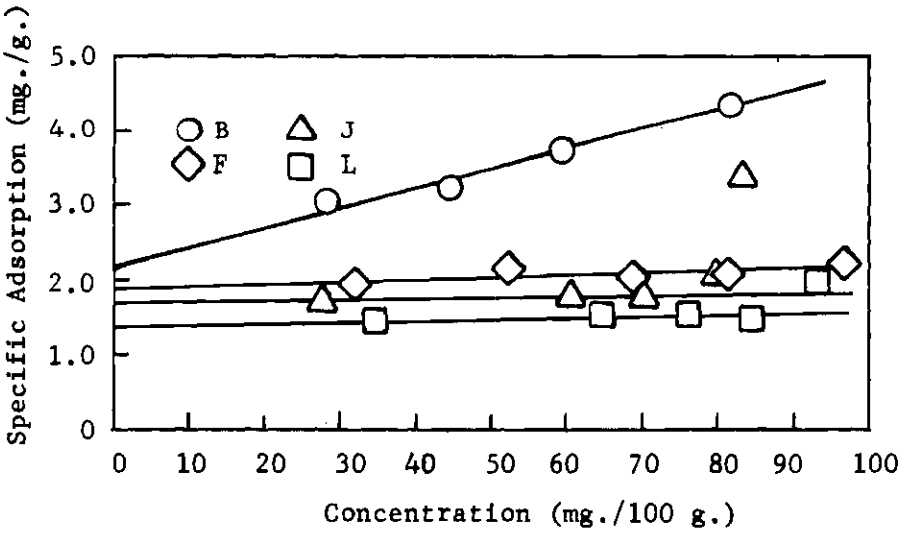

Figure 37. Adsorption of Polystyrene Fractions on Aluminum at 50° C after 25 Days

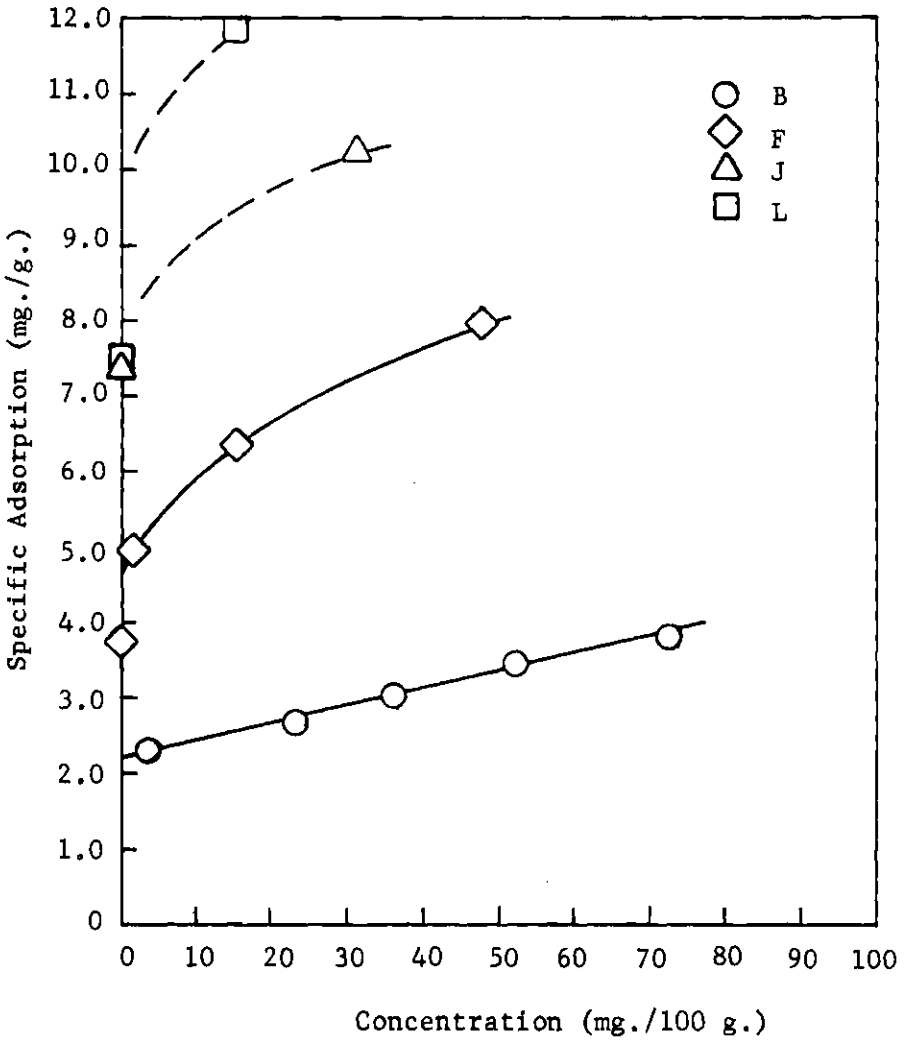

Figure 38. Adsorption of Polystyrene Fractions by Aluminum Oxide at 34.8° C. after Six Days

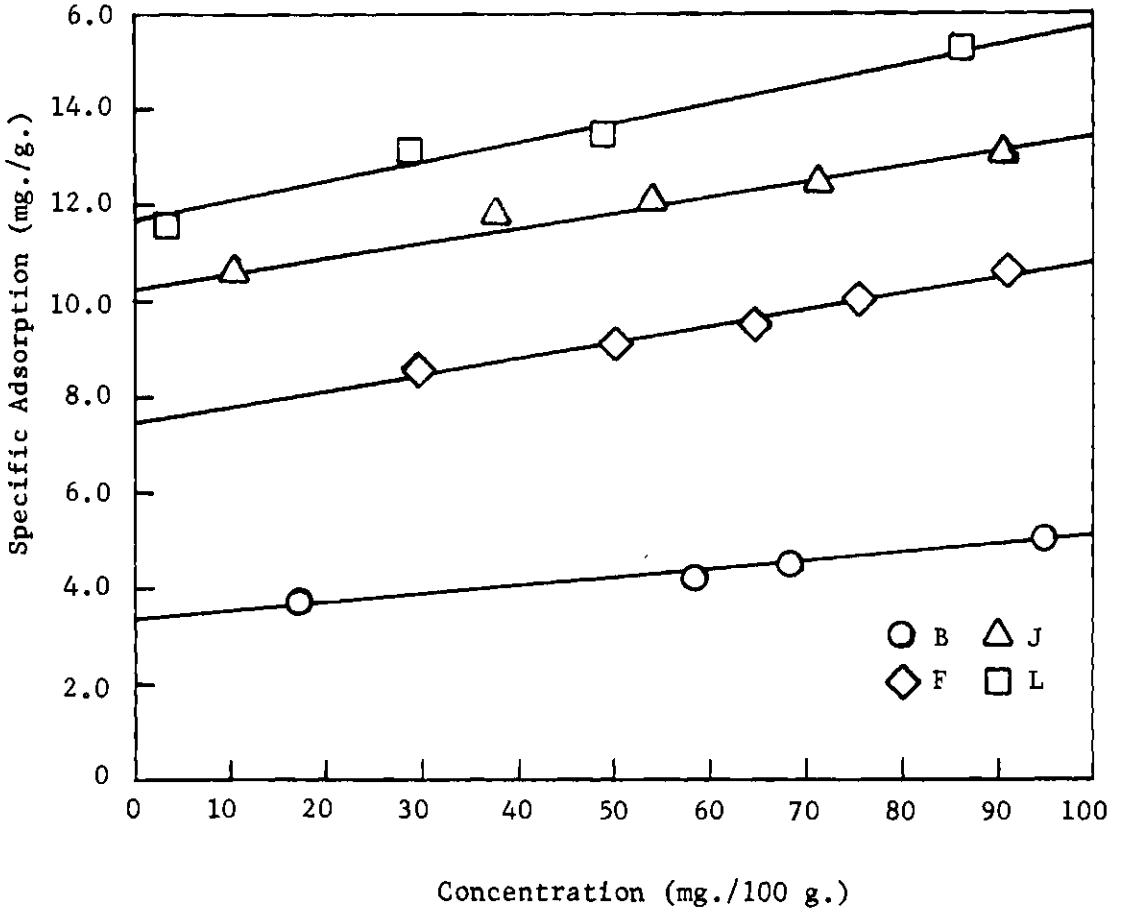

Figure 38. Adsorption of Polystyrene Fractions by Aluminum Oxide at 34.8° C. after 25 Days.

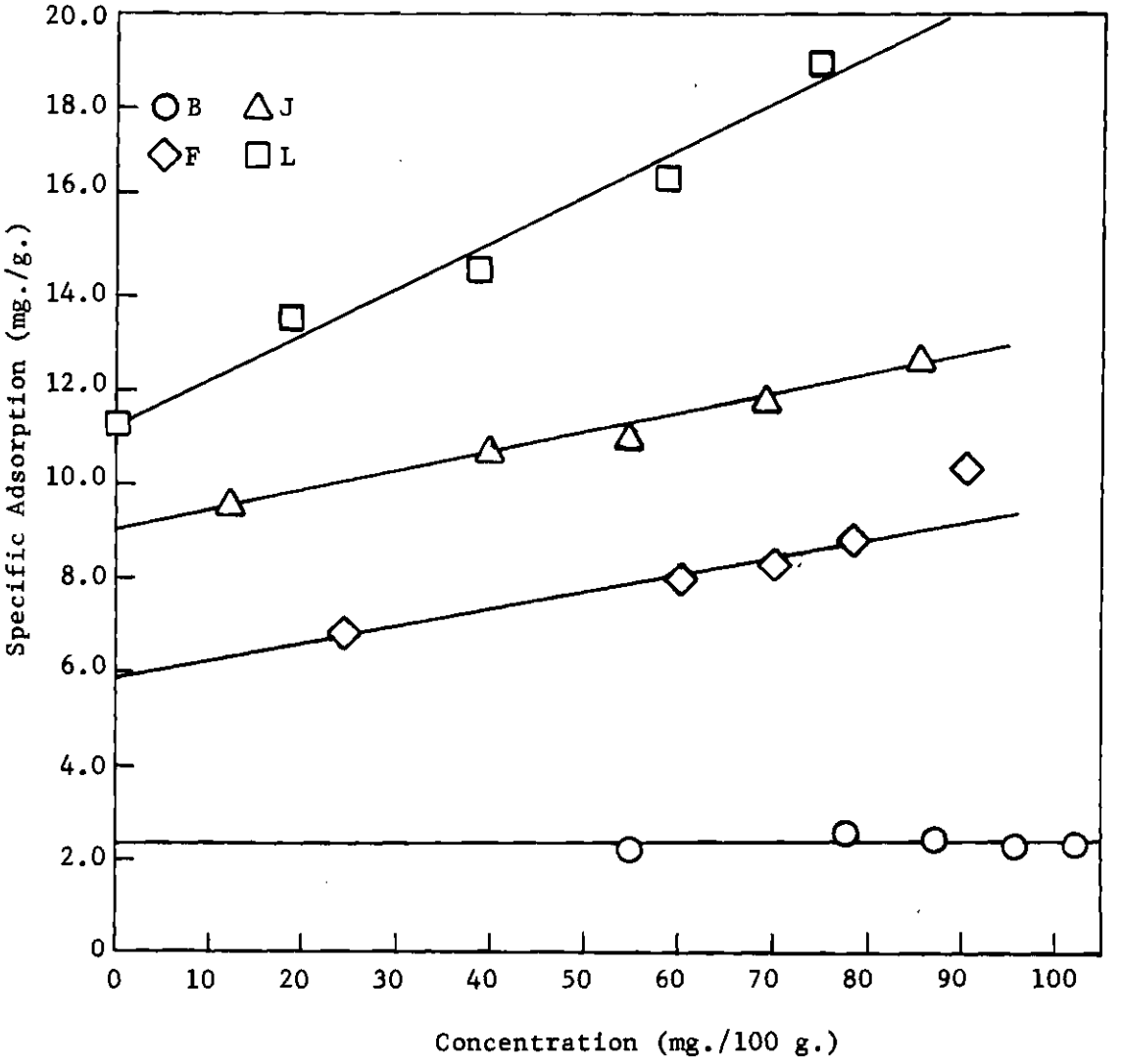

Figure 40. Adsorption of Polystyrene Fractions on Aluminum Oxide at 50° C. after 25 Days

Table 10. Desorption of Polystyrene by Benzene

Adsorption Data	
Weight of Aluminum	5.0122 grams
Volume of Solution	25 milliliters
Initial Concentration	40.1 mg./100 ml.
Final Concentration	0.8 mg./100 ml.
Concentration Change	39.3 mg./100 ml.
Specific Adsorption	1.96 mg./g.
Desorption Data	
Weight of Aluminum	4.7560 grams
Total Polystyrene	9.35 milligrams
Polystyrene Recovered	8.729 milligrams
Percent Desorbed	93.6

Adsorption of Polyisobutylene

An effort was made to determine the adsorption isotherm of polyisobutylene from benzene onto aluminum powder at 25° C. No convenient spectrophotometric method of analysis was available, so a gravimetric technique was used instead.

The solution was made up by weighing 60 milligrams of polyisobutylene into a tared 100-milliliter volumetric flask. The polymer was dissolved in a small quantity of reagent grade benzene, after which the flask was filled to the mark with benzene. A second solution was prepared by diluting a 25-milliliter aliquot of this solution to 50 milliliters. Two sets of four ampules each were prepared, containing from one to three grams of aluminum powder. The original stock solution was put into one set of ampules; the dilute solution was put in the other. Ten milliliters of solution were introduced into each ampule by means of a volumetric pipette.

Aluminum weighing pans were marked to correspond with the numbers on the ampules and were tared on a microbalance. Pans were also prepared for the two stock solutions. A five-milliliter aliquot of each stock solution was put into a pan and the solvent allowed to evaporate.

The ampules were sealed and shaken at 25° C. for four days. Before being opened, they were shaken vigorously to suspend the adsorbent. Then they were opened quickly, and the entire contents of each ampule were poured into a steel centrifuge cup, which was capped immediately to retard evaporation. The solutions were centrifuged at high speed for about ten minutes, leaving them entirely free of suspended aluminum. Five-milliliter aliquots were taken of all

solutions and placed in the appropriate weighing pans. The pipette used to take these aliquots had a rubber stopper attached to it so as to prevent its going far enough into the centrifuge cup to pick up any adsorbent. Great care was taken to avoid agitating the solution and so stirring up the aluminum while taking samples.

The solvent was allowed to evaporate, after which all pans were dried for 24 hours under vacuum at 60° C. They were weighed on the analytical balance, and the change in concentration, if any, determined and A calculated from Equation 80. Results are tabulated in Table 11.

Ethylbenzene Adsorption

The adsorption of ethtylbenzene was studied at 350° C. and 50° C. as a means of estimating the heat of adsorption per segment of polystyrene. In these studies a different technique was practicable since equilibration times were expected to be much shorter. Ten grams of aluminum oxide were weighed into a 100-milliliter volumetric flask. Fifty milliliters of spectroquality cyclohexane in equilibrium with the thermostat were added to the flask by means of a pipette, and ten milliliters of a dilute solution of ehtylbenzene in cyclohexane. A magnetic stirring bar was placed in the flask, and the weight of the flask and its contents was determined to plus or minus 0.02 gram. The solution was stirred vigorously, then immersed in the bath and left for fifteen minutes. An ten milliliter aliquot of the solution was removed and placed in a screw-cap vial. The solution was replaced with ten milliliters of the stock ethtylbenzene solution, stirred again, and again immersed in the thermostat. This procedure was continued until twelve samples had been taken. The samples were analyzed

Table 11. Adsorption of Polyisobutylene from Benzene

Vial Number	Weight of Aluminum (Grams)	Initial Concentration (g./100 ml.)	Final Concentration (g./100 ml.)	Specific Adsorption (g./g.)
1	1.0153	0.0610	0.0672	----
2	1.5269	0.0610	0.0628	----
3	1.9964	0.0610	0.0626	----
4	2.9979	0.0610	0.0628	----
5	1.0089	0.0319	0.0450	----
6	1.4986	0.0319	0.0311	0.00005
7	1.8689	0.0319	0.0314	0.00003
8	2.9948	0.0319	0.0317	0.00001

spectrophtometrically.

If the concentration of the solution at the nth step is c_n, the concentration of the stock solution is C, the total volume is V, and the volume of the qliquot removed is v, the amount, Δ, of ethylbenzene adsorbed per gram of adsorbent at a given step is

$$\Delta A = [c_{n-1}(V - v) + Cv - c_n V /w] \tag{81}$$

or

$$\Delta A = [v(c - c_{n-1}) - V(c_n - c_{n-1})]/w \tag{82}$$

where w is the weight of adsorbent. However, the amount of solution taken is greater than the amount put back because a pipette does not deliver all of the solution that it contains. Hence, a correction must be made to obtain a more accurate result. If δ is the difference between the amount of solution removed and the amount added, we have

$$\Delta A = [(V_{n-1} - v - \delta)c_{n-1} + Cv - v_n c_n] /w \tag{83}$$

or

$$\Delta A = [v(C - c_{n-1}) + (V_{n-1} - \delta)c_{n-1} - v_n c_n]/w. \tag{84}$$

But

$$V_n = V_o - (n - 1)\delta \tag{85}$$

where V_o = original volume, and

$$V_n = V_{n-1} - \delta. \tag{86}$$

Equation 84 may be written

$$\Delta A = [v(C - c_{n-1}) - V_n(c_n - c_{n-1})]/w. \tag{87}$$

The quantity δ and hence V_n, can be determined, neglecting evaporation losses, by weighing the flask before and after sampling, and dividing the difference by the product of the number of samples taken and the density of the liquid at the temperature of the thermostat.

The specific adsorption, A, is obtained by taking the sum of values of ΔA for all steps. Figure 41 shows A as a function of c for the two temperatures.

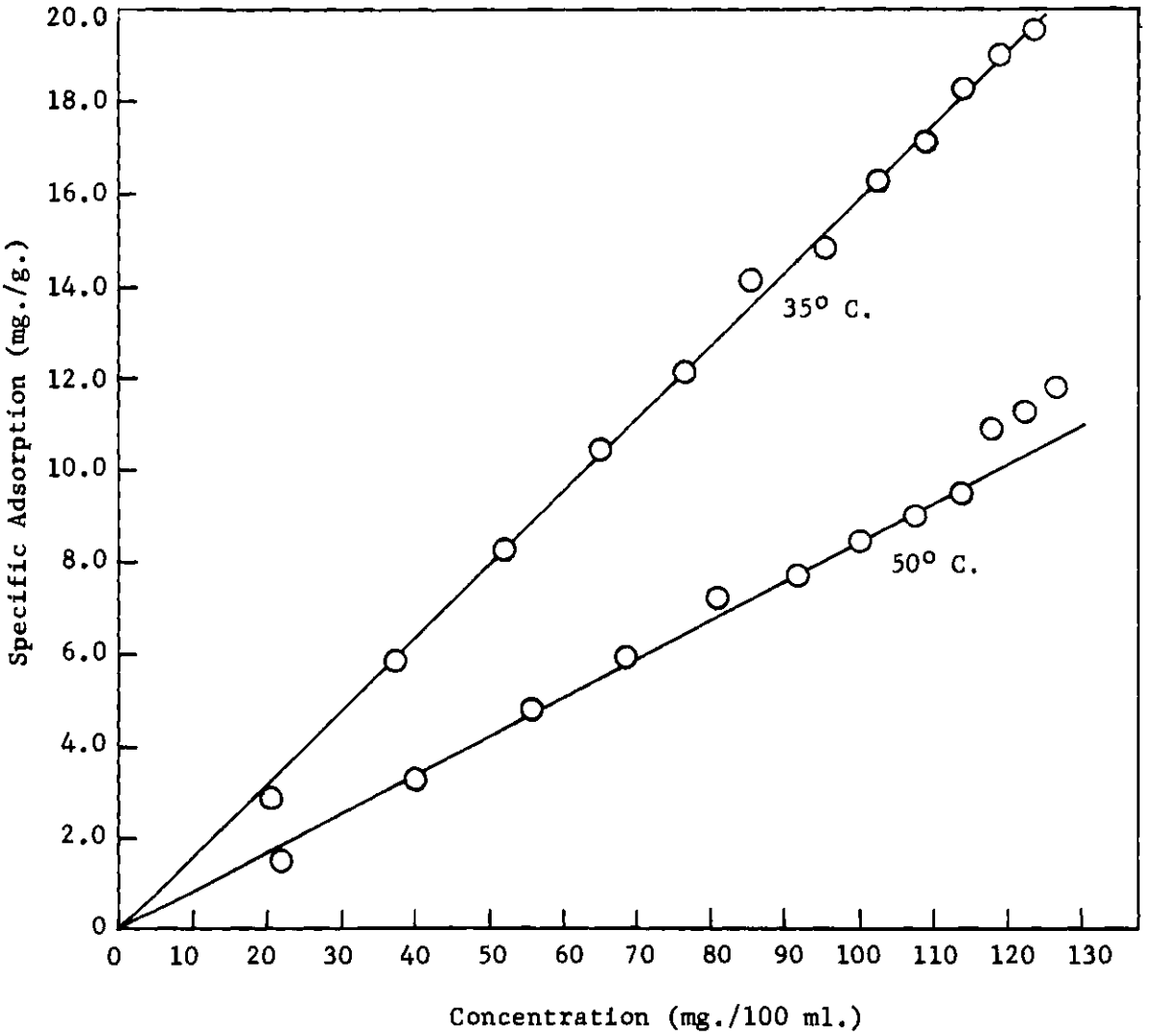

Figure 41. Adsorption Isotherms for Ethylbenzene on Al_2O_3

CHAPTER IV

DISCUSSION OF RESULTS

Experimental Error

It is difficult in a study of this kind to make a quantitative estimate of the experimental error because there are many sources of error whose effect cannot be reliable gauged. In the following discussion, errors in measurement and analytical technique will be discussed as quantitatively as possible; errors arising from causes unrelated to the measurements themselves, such as temperature fluctuations, moisture, evaporation, etc. will be mentioned and an effort made to indicate the direction and approximate magnitude of their effect.

Analysis of Solutions

Table 12 shows a typical set of spectrophotometer calibration data. The concentration of polystyrene and the absorbance at each of three wavelengths are given. From these data values of ε were calculated by the method of least squares and used to calculate the concentration from the absorbance at each wavelength. The average of these three calculations was taken as the calculated value of concentration in the analyses. The standard deviation, σ, assuming the experimental concentration to be correct, expressed as a magnitude and a percentage, is given for each concentration in Table 13. Data for the lowest concentration for fraction F have been discarded because one absorbance

Table 12. Spectrophotometer Calibration Data

Concentration* (Prep.)	Absorbance (2595)	Concentration* (Calc.)	Absorbance (2615)	Concentration* (Calc.)	Absorbance (2690)	Concentration* (Calc.)
- - - - - - - - - - - - - - - - Fraction F - - - - - - - - - - - - - - - -						
87.6	1.360	88.2	1.404	87.5	1.074	87.0
66.2	1.030	66.8	1.065	66.5	0.820	67.1
43.1	0.667	43.2	0.688	42.9	0.554	(43.7)
21.6	0.338	21.8	0.346	21.6	0.219	(17.9)
	ε = 0.0154		ε = 0.0160		ε = 0.0122	
- - - - - - - - - - - - - - - - Fraction L - - - - - - - - - - - - - - - -						
84.3	1.325	84.2	1.351	84.3	1.038	83.2
63.0	0.996	63.2	1.009	62.9	0.797	63.9
41.6	0.660	41.8	0.678	42.2	0.528	42.3
20.3	0.325	20.6	0.330	20.5	0.255	20.4
	ε = 0.0158		ε = 0.0161		ε = 0.0125	

*All concentrations in units of g./100 g.

Table 13. Errors in Polystyrene Analysis Based on Calibration Data

Concentration (Prep.)	Average Concentration	σ	100 /Conc.
- - - - - - - - - - - - - - - - - - Fraction F - - - - - - - - - - - - - - - - - -			
87.7	87.6	0.5	0.6
66.2	66.8	0.2	0.3
43.1	43.3	0.3	0.7
21.6	(20.5)	(1.8)	(8.8)
- - - - - - - - - - - - - - - - - - Fraction L - - - - - - - - - - - - - - - - - -			
83.9	83.9	0.5	0.6
63.0	63.4	0.4	0.6
41.6	42.1	0.2	0.5
20.3	20.5	0.1	0.5
Average Standard Deviation		0.3	0.5

is obviously grossly in error. (In practice, such readings were discarded and the concentration determined from the other two.) The average standard deviation is about 0.5 percent, and seems to be independent of concentration.

Table 14 shows actual analytical data obtained using the values of ε determined above. Since there are no experimental concentrations with which to compare the calculated concentrations, the standard deviations are determined based on the average calculated concentration of each sample. Table 15 shows the results. The values of σ are noticeably larger in this case than in the previous one, possibly due to low-level contamination of the solutions by materials in the adsorbents, though no such contamination was observed independently. The solutions having zero concentration appeared to be spectroscopically pure.

The conclusion drawn from this analysis is that the analytical technique is reliable within one to two percent with errors greater than one percent being relatively uncommon.

The error in the analysis of polyisobutylene solutions cannot be determined as precisely, but is almost certainly greater than that for polystyrene. Analyses of two polyisobutylene solutions of known concentration were made at the same time as the adsorption measurements. Errors in these were 0.3 and 4.2 percent respectively. Analysis of some polystyrene solutions of comparable concentration made by the same technique had errors ranging from zero to two percent, though in the latter case there is reason to believe the error was in preparation rather than analysis.

Table 14. Typical Data from Spectrophotometric Analysis

Sample	Absorbance (2595)	Concentration	Absorbance (2615)	Concentration	Absorsance (2690)	Concentration
- - - - - - - - - - - - - - - - - -			Fraction F		- - - - - - - - - - - - - - - - - -	
1	1.399	90.1	1.435	89.5	1.112	91.1
2	1.217	78.4	1.247	77.8	0.966	79.1
3	1.085	69.9	1.111	69.3	0.859	70.3
4	0.932	60.0	0.961	59.9	0.740	60.6
5	0.379	24.4	0.387	23.5	0.300	24.5
6	1.506	97.0	1.547	96.5	1.188	97.2
7	1.266	81.5	1.298	81.0	1.000	81.8
8	1.067	68.7	1.090	68.0	0.842	68.9
9	0.816	52.6	0.839	52.3	0.549	53.1
10	0.497	32.0	0.511	31.8	0.393	32.1
- - - - - - - - - - - - - - - - - -			Fraction L		- - - - - - - - - - - - - - - - - -	
1	1.169	74.3	1.208	76.7	0.929	74.6
2	0.923	58.6	0.949	60.3	0.729	58.5
3	0.610	38.7	0.621	39.4	0.483	38.7
4	0.293	18.6	0.301	19.1	0.233	18.7
5	0	0	0	0	0	0
6	1.469	95.0	1.499	95.2	1.158	93.0
7	1.330	84.5	1.357	86.2	1.061	85.3
8	1.201	76.3	1.222	77.7	0.946	76.0
9	1.026	65.2	1.038	65.9	0.803	64.5
10	0.546	34.6	0.559	35.4	0.431	34.6

Table 15. Deviations in Spectrophotometric Analysis

Sample	Average Concentration	σ	100 /Conc.
- - - - - - - - - - - - - - - - - -	Fraction F	- - - - - - - - - - - - - - - - - -	
1	90.2	0.7	0.8
2	78.4	0.5	0.6
3	69.8	0.4	0.6
4	60.2	0.3	0.5
5	24.1	0.4	0.7
6	96.9	0.3	0.3
7	81.4	0.3	0.4
8	68.5	0.4	0.6
9	52.7	0.3	0.6
10	32.0	0.1	0.3
- - - - - - - - - - - - - - - - - -	Fraction L	- - - - - - - - - - - - - - - - - -	
1	75.2	1.1	1.5
2	59.1	0.8	1.4
3	38.9	0.3	0.8
4	18.8	0.2	1.1
5	0	--	--
6	94.1	1.0	1.1
7	85.3	0.6	0.7
8	76.7	0.6	0.8
9	65.2	0.6	0.9
10	34.9	0.4	1.1
Average Standard Deviation		0.5	0.8

Unfortunately the analyses of these polyisobutylene solutions could not be carried out under conditions identical to those of the adsorption studies. Because the solutions used in the adsorption studies. Because the solutions used in the adsorption studies had to be handled rather extensively after the vials were opened, loss of solvent by evaporation was possible. In addition, contamination of the samples by adsorbent was possible, despite the fact that efforts were made to avoid it. Some early experiments on polystyrene solutions using a similar technique showed that such contamination, even in very small amounts, can usually be detected by careful inspection of the dried residue. None was observed in the polyisobutylene residues, but the possibility cannot be ruled out. Either contamination or evaporation would give rise to high values for the concentration. The observed values were obviously high in most cases. However, the error necessary to account for the results if adsorption were as high as one milligram per gram is improbably great, of the order of 25 to 50 percent. The result that the adsorption of polyisobutylene is much less than that of polystyrene from a theta solvent appears to be correct.

Other Sources of Error

Other sources of error in measurements of polystyrene adsorption include temperature fluctuation, variation in moisture content, evaporation losses in handling, and errors in weighing and volume measurement.

Temperature fluctuations in the thermostat were generally of the order of plus or minus 0.3 degree of less. Such fluctuations should not have caused large errors in view of the small thermal effect, and,

in any case, should have had the same effect on all samples.

Frisch, Hellman, and Lundberg (15) reported less adsorption and greater scatter of data when solutions and adsorbents were very wet or very dry than when a trace of moisture was present. In some preliminary work in this study, adsorption was much diminished when large amounts of water were present. In this work the solutions were dried with sodium wire, and the adsorbents were dried at 120° C. for 24 hours or more. However, moisture was not rigorously excluded during filling and handling of tubes prior to sealing. A small amount of moisture was almost certainly present, and the quantity may have varied slightly from tube to tube. The magnitude of the error so introduced cannot be estimated accurately, but it should have been small.

On several occasions ampules containing polymer solution were allowed to stand open on a balance for as long as ten minutes. The change in weight in each case was less than 0.2 milligram. This indicates that evaporation losses prior to sealing were negligible. Losses during sampling may have been greater, especially when ampules were opened at 50° C. The error so introduced would have increased the apparent concentration and decreased the value of A. The magnitude of the error is unknown.

Errors in weighing and volume measurement are believed to have been generally negligible. One possible exception to this is in the weighing of aluminum oxide. This adsorbent underwent a weight loss of up to 15 percent on drying. In the event of insufficient or uneven drying, substantial errors might have been introduced by residual moisture. However, in view of the procedure used for drying, the

chance of important errors from this source is considered small.

Errors in Polymer Characterization

It is more difficult to evaluate the error in the polymer characterization experiments. There are numerous sources of error in both osmotic pressure and light scattering measurements. Partial permeability of the membrane to solute molecules is a source of error in osmometry. The magnitude of the error depends upon the nature of the membrane itself, the time necessary for equilibration, and the amount of low molecular weight material in the sample. Since any membrane is more permeable to small molecules than to large ones, the low molecular weight molecules are lost, and the osmotic molecular weight tends to be too high.

Dust and stray light are sources of error in light scattering measurements, as are even small uncertainties in wavelength, refractive index, and the rate of change of refractive index with concentration, all of which appear in Equation 29 to powers greater than one. Extrapolations are not exactly linear in either light scattering or osmometry, and extrapolation errors may be appreciable.

A comparison of values of the second virial coefficients and radii of gyration obtained from these measurements with each other and with independent results should give an idea of the reliability of the measurements. Table 16 shows experimental values of $\overline{R}_G$ and B. $\overline{R}_G$ was calculated from Equation 34. The value of B calculated from light scattering data was given by Equation 33; that from osmotic pressure data by Equation 24. For comparison, values of B determined for polystyrene in toluene by osmometry by Danusso and Moraglio (87) are shown. Since

Table 16. Radii of Gyration and Second Virial Coefficients of Polystyrene Fractions

Fraction	$\bar{M}_w \times 10^{-5}$	R_G L. S. (A.)	R_G Calc. (A.)	B x 10^4 L. S.	B x 10^4 Osm.	M x 10^{-5} (87)	B x 10^4 (87)
B	18.2	998	888	0.43	----	8.50	2.95
F	3.70	469	399	1.21	0.96	3.36	3.40
J	1.77	369	277	2.27	2.84	1.63	4.35
L	0.67	190	170	3.12	3.22	0.76	5.00

toluene is a better solvent than benzene for polystyrene (88), the higher values of B in toluene should be expected.

Experimental values of R_G for polystyrene in a good solvent over a wide range of molecular weights could not be found in the literature. Accordingly, an estimated value was calculated at each molecular weight. If R_{Go} is the radius of gyration of a polymer molecule in an ideal solvent, the radius of gyration of the same molecule in a good solvent is given by

$$\overline{R}_G = \alpha \overline{R}_{Go} \tag{88}$$

where α = an expansion factor (89).

The expansion factor is related to the intrinsic viscosity by the equation

$$\alpha^3 = [\eta] M_o^{3/2} / \Phi \beta^3 \, M^{1/2} \tag{89}$$

where M_o = Molecular weight of a monomer unit;

Φ = a constant;

β = effective bond length;

M = molecular weight of the polymer molecule.

But $[\eta]$ can be replaced by its equivalent in Equation 48 giving

$$\alpha^3 = K' M^{(a - 0.5)} M_o^{3/2} / \Phi \beta^3 \tag{90}$$

The value of β is 5.02 A., and Φ has a value in good solvents of about

2.0×10^{21} (89). M_o is 105. K' and a are 0.95×10^{-4} and 0.74 respectively (71). Substituting these values in Equation 90, we obtain

$$\alpha^3 = 0.407\ M^{0.24} \tag{91}$$

or

$$\alpha = 0.741\ M^{0.08} \tag{92}$$

Thus α is readily estimated. R_{Go} can be estimated by the equation

$$K = (L_o^2/M)^{3+2} \tag{93}$$

where L_o^2 = mean square distance between chain ends for the unperturbed random coil; K = a constant whose value for polystyrene is 8.3×10^{-4} at 25^o C. (90).

R_{Go} is readily obtained from a knowledge of L_o since

$$L_o^2 = 6R_{Go}^2 \tag{94}$$

Combining Equations 88, 92, 93, and 94, we obtain the radius of gyration of polystyrene in benzene at 25^o C.:

$$R_G = 0.225\ M^{0.58}. \tag{95}$$

This estimate indicates the range in which R_G may reasonably be expected

to fall. Agreement with experiment is satisfactory.

The distribution function determined for fraction B cannot be regarded as more than a crude indication of the actual distribution because too few fractions were taken for an accurate determination (57). Thus, the remarkable agreement between the weight-average molecular weight calculated from the measured distribution and that determined from light scattering is probably fortuitous.

Adsorption on Aluminum

Results of the kinetic studies of the adsorption of polystyrene on aluminum (see Figure 33) show very rapid attainment of saturation of the aluminum surface. Apparently a slow increase in adsorption does occur since adsorption after 25 days was greater than after six, but the increase in adsorption is clearly less pronounced than in the case of adsorption on aluminum oxide (see next section).

The isotherm for the adsorption of polystyrene onto aluminum powder are qualitatively similar to those of other polymers studied in previous investigations when adsorbed on metal and glass powders (14, 16). The adsorption isotherms for three of the four fractions are nearly horizontal straight lines over the entire concentration range studied, with no apparent decrease in amount of polymer adsorbed per gram of adsorbent, even at the lowest concentration. The amount adsorbed increases with molecular weight and decreases with temperature. This behavior is predicted by both the Simha-Frisch-Eirich (32, 34, 35) and Silberberg (42, 43) theories.

Perhaps the simplest method of treating the data is to assume that

the molecules are adsorbed as somewhat distorted random coils and calculate a molecular radius based on the area, S_m, occupied by a single molecule. The value of S_m is given by

$$S_m = SM/6.023A \tag{96}$$

where S = specific surface area of the adsorbent ($m.^2/g.$);

M = molecular weight of the adsorbate;

A = specific adsorption (mg./g.).

The dimensions of S_m in Equation 96 as written are square Angstroms per molecule.

An equivalent molecular radius, R_e, is readily computed from the equation

$$R_e = (S_m/\pi)^{1/2}. \tag{97}$$

A comparison between R_e and R_G should indicate the degree of molecular distortion or interpenetration in the adsorbed film.

The mean square radius of gyration in cyclohexane at 34° C. may be estimated from the empirical equation (91).

$$L_o^2/M = 0.49 \times 10^{-16} \tag{98}$$

where L is expressed in centimeters. Another empirical equation, proposed by Notley and Debye (92) is

$$L = k'M^a$$

where k' and a are parameters. Table 17 shows values of k' and a at three different temperatures. R_G is readily calculated from L via Equation 94.

Equation 98 is applicable only to ideal solutions (91). Accordingly, it is necessary to make use of Equation 99 for estimating the radius of gyration at 50° C. However, the parameters in Equation 99 were calculated using fractions whose molecular weights were greater than 600,000 (92), so that their application to fractions of relatively low molecular weight involves a considerable extrapolation. Table 18 shows calculated values of R_G at 34° C. based on Equation 98 and at 34°, 43°, and 57° C. based on Equation 99 for the fractions used in this work. Values of R_G at 50° C. are estimated from those calculated at other temperatures. At 34° C. agreement between the two calculations is satisfactory. The decrease in R_G from 43° to 57° in the case of fractions J and L indicates that these fractions are beyond the range in which Equation 99 is valid. However, since no other method for estimating R_G at 50° was avilable, the mean of the calculated values of R_G for each fraction was taken as an approximation to the value of R_G at 50°.

Table 19 shows values of S_m, R_e, and R_e/R_G calculated from the experimental data. The correct value of A to be used in calculating S_m is the saturation or plateau value. However, the experimental isotherms have a small, finite slope throughout the concentration range studied, so that no plateau was observed. Therefore, the isotherms were extrapolated to zero concentration and, the value, A_o, of the specific adsorption at zero concentration was used in the calculations. This

Table 17. Notley-Debye Parameters for Polystyrene in Cyclohexane

T° C.	k'	a
34	0.687	0.500
43	0.751	0.502
57	0.494	0.535

Table 18. Radii of Gyration of Polystyrene in Cyclohexane

Fraction	34° Eq. 98	34° Eq. 99	43° Eq. 99	57° Eq. 99	50° Est.
B	387 A.	379 A.	426 A.	451 A.	440 A.
F	174	171	191	193	192
J	113	118	132	130	131
L	74	73	81	77	79

Table 19. Apparent Dimensions of Adsorbed Polymer Molecules

Fraction	$S_m \times 10^{-4}$ (A^2) 34°	50°	R_e (A.) 34°	50°	R_e/R_G 34°	50°
B	12.8	15.8	202	225	0.516	0.511
F	2.92	3.71	96.4	107	0.564	0.560
J	1.63	1.97	72.1	79.2	0.611	0.605
L	0.72	0.93	47.9	54.5	0.666	0.682

Table 20. Γ as a Function of a_o

Fraction	a_o = 50 A.^{2} 34°	50°	a_o = 20 A.^{2} 34°	50°	a_o = 10 A.^{2} 34°	50°
B	6.8	5.5	2.7	2.2	1.4	1.1
F	6.0	4.8	2.4	1.9	1.2	1.0
J	5.2	4.3	2.1	1.7	1.0	0.9
L	4.5	3.4	1.8	1.4	0.9	0.7

procedure can be justified on the grounds that virtual saturation seems to be attained at concentrations too low to measure spectrophotometrically. Thus, the extrapolation to infinite dilution amounts to studying adsorption at saturation with concentration effects eliminated. This point will be discussed further below.

The fact the R_e/R_G is considerably less than unity in all cases indicates either that the molecules at the surface are laterally compressed or they interpenetrate one another to a considerable extent. The interpenetration or distortion seems to increase with molecular weight. However, since the assumption that a polymer molecule is adsorbed as a slightly distorted random coil is probably a gross oversimplification, too much emphasis must not be placed on this model; and further analysis of this sort appears unwarranted.

A possibly more fruitful approach is based on the Silberberg theory (43). Silberberg defines a quantity, Γ, as the number of segments adsorbed per surface site. If A_o is the amount of polymer adsrobed in milligrams per gram of adsorbent, then

$$\Gamma = 6.023 a_o A_o / M_o S_m \qquad (100)$$

where a_o = area of an adsorption site (Anstroms^2);

M_o = molecular weight of a polymer segment;

S_m = specific surface area of the adsorbent (m.^{2}/g.).

In order to evaluate Γ, it is necessary to know a_o. One may estimate the area of a segment of a polystyrene segment at 50 A.^{2} assuming it to be slightly less than the sum of the areas (obtained from vapor adsorption

studies) of benzene (32.3 $A.^2$) and ethane (22.5 $A.^2$) (93). It is not necessarily true, however, that this is a reasonable value for a_o since the segment may be sterically hindered from lying flat on the surface. If the plane of the benzene ring is inclined with respect to the surface, a_o will probably be less than this simple estimate. Silberberg (43) suggests that values of 20 or even ten square Angstroms may be appropriate for a_o. Table 20 shows the calculated values of Γ based on these three values for a_o.

Clearly the results are compatible with either a two-dimensional or a three-dimensional model, depending on the choice of the value of a_o. Unfortunately, the values of Γ that are obtained from this calculation are proportional to A_o which may be influenced by other factors than the number of adsorption sites on the surface. Thus a randomly coiled molecule might be adsorbed at relatively few sites, yet make many other sites inaccessible to other molecules. This situation is indistinguishable, by means of this calculation, from that in which a molecule is extended on the surface and adsorbed at many sites, without interfering significantly with adsorption at unoccupied sites. In the former case one should use very large values for a_o, but there seems to be no way to predict what these values should be (22). The plateau values of A have been related by other workers to the molecular weight by the empirical equation

$$A = K\bar{M}_w^{\,a} \qquad (101)$$

where K and a are constants (13, 16). In this study the intercepts, A_o,

were used in place of A in Equation 101. The plot of log A_o versus log M_w should give a straight line having slope a and intercept log K. Figure 42 shows the plot; values of K and a for 34.8° and 50° C. are shown in Table 21 along with representative values obtained by other workers for the adsorption of polymethyl methacrylate (PMMA) and polydimethyl siloxane (PDS).

The values of K and a are seen to fall within the range of previous results. The higher value of a at the higher temperature does not agree with the Silberberg theory (43) which predicts a diminished molecular weight dependence with improvement in solvent. However, the experimental error is such that any distinction between these two numbers may be illusory, and no conclusions should be drawn.

The anomalous behavior of fraction B presents a problem in interpretation, particularly in view of the very regular behavior of this fraction when adsorbed on aluminum oxide (cf. next section) and the close agreement between results for fraction B and those for other fractions based on values of A_o. More data were obtained using this fraction than any other. In all cases, the isotherm for adsorption on aluminum had a relatively steep rise with increasing concentration and an intercept around three milligrams adsorbed per gram of aluminum. Also, in all cases the scatter in the measured points was substantially greater than that observed with the other fractions. A further comment concerning this problem will be made in connection with the adsorption of polystyrene on aluminum oxide.

The desorption studies support Silberberg's assertion that desorption does not take place in the presence of a poor solvent but can be

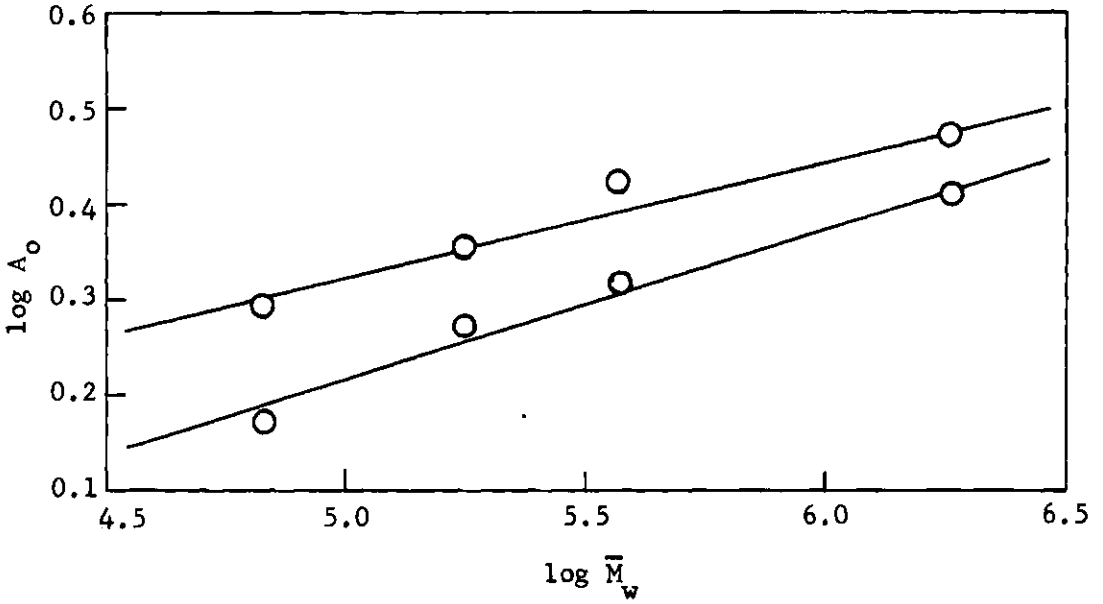

Figure 42. Relation Between Specific Adsorption on Aluminum at Zero Concentration and Molecular Weight

Table 21. Parameters K and a in Equation 101

System	K	a	Ref.
Pst, Cyclohexane, Al, 34.7° C.	0.39	0.13	--
PSt, Cyclohexane, Al, 50° C.	0.20	0.16	--
PDS, Benzene, Glass, 30.4° C.	0.97	0.40	13
PDS, n-Heptane, Glass, 30.4° C.	2.94	0.35	13
PDS, Benzene, Fe, 30.4° C.	0.34	0.43	13
PDS, n-Heptane, Fe, 30.4° C.	4.9	0.23	13
PMMA, Benzene, Fe	0.35	0.04	16
PMMA, Benzene, Glass	2.00	0.00	16
PMMA, 1,2-Dichloroethane, Fe	0.14	0.08	16

accomplished using a good solvent (43). Any desorption that may take place with increasing temperature is evidently very slow since none was observed within four days.

The results of the very cursory investigation of adsorption of polyisobutylene from benzene, a theta system thermodynamically similar to the polystyrene-cyclohexane system, indicate a strong relationship between adsorption and the relative interaction energy of solute and solvent with the surface. Qualitatively one would expect a stronger interaction between an aromatic molecule and an ionic surface than between an aliphatic molecule and the same surface because of the existence of charge-transfer forces in the former case. This is borne out in the results of Kipling and Peakall (94), who observed selective adsorption of benzene by alumina from solutions of benzene and cyclohexane at all solution compositions from nearly pure benzene to nearly pure cyclohexane. The apparent non-adsorption of polyisobutylene from benzene seems to indicate preferential adsorption of the solvent. Although the experimental error in this experiment was greater than that in the polystyrene experiments, the adsorption of polyisobutylene appears to be at least an order of magnitude less than that of polystyrene. The results suggest that the solute-surface interactions are of greater importance than the thermodynamic properties of the solutions in determining adsorption behavior of polymers.

Adsorption on Aluminum Oxide

Kinetic Effects

The kinetic studies of adsorption on aluminum oxide differ from

those on aluminum in that adsorption continues at a measurable rate for much longer periods of time. Apparently two stages are involved: an initial fast stage followed by a slower stage that appears to be first order with respect to the bulk concentration of polymer (see Figure 34). A possible mechanism involves initial saturation of the "superficial" surface, that is, the surface inside pores whose radii are much greater than molecular dimensions. Since the superficial surface is readily accessible to the polymer, this is a fast process, comparable to adsorption on aluminum; and saturation of the superficial surface is quickly reached.

Adsorption on the "interior" surface, the surface inside pores having radii only slightly greater than molecular dimensions, is controlled by diffusion of solute into these pores. The rate of diffusion should be approximately first order with respect to polymer concentration if the cross-sectional area of the pores into which diffusion takes place is assumed constant.

According to Figure 34, the rates of adsorption of fractions F and L are approximately equal in the first stage, but the rate of adsorption of fraction L is greater in the second. This result is to be expected since the smaller molecules should have a higher rate of diffusion than the larger ones. Other adsorption kinetics measurements (summarized in Figure 32) also indicate more rapid adsorption of low molecular weight fractions.

Adsorption Isotherms

The most striking result of the experiments in which aluminum oxide was used as the adsorbent is the highly preferential adsorption of the low molecular weight fractions (see Figures 38-40). This

result, in contrast with those obtained with aluminum, agrees with the results of the early workers in the field (4-7). In form, the isotherms are quite similar to that obtained by Kangle and Pacsu (17) for adsorption of polyvinyl acetate on porous charcoal.

The difference between the results with aluminum and those with aluminum oxide is ascribed to the porosity of the latter. A rather crude calculation will show how the pore structure affects adsorption. Assume that the area occupied by a given quantity of adsorbed polymer is the same on aluminum oxide as on aluminum at the same temperature. Using the value of A_o obtained by extrapolating the isotherm to zero concentration, it is then possible to calculate the area of the adsorbed film of a given fraction on the aluminum oxide surface by the equation

$$S(\text{film}) = S(\text{Al})A_o(Al_2O_3)/A_o(\text{Al}) \qquad (102)$$

where S(film) = area of adsorbed film per gram of aluminum oxide;

S(Al) = specific surface area of the aluminum;

A_o = specific adsorption at zero concentration of the indicated adsorbent.

The area of the adsorbed film so calculated may then be assumed to be the area of the aluminum oxide surface that is accessible to polymer molecules of the given fraction. Access to the remainder of the area of the adsorbent is denied by the inability of the polymer molecules to pass through the small pores. Figure 26 is a plot of the area in pores of radius greater than R_c versus R_c. From this graph the limiting pore size is readily estimated. Table 22 shows the values of the

Table 22. Results of Adsorption Measurements

Fraction	$\bar{M}_w$ x 10^{-5}	$\bar{M}_w/\bar{M}_n$	Specific Adsorption at Zero Concentration: Aluminum 34°	Aluminum 50°	Aluminum Oxide 34°	Aluminum Oxide 50°
B	18.2	1.22	2.70	2.18	3.33	2.36
F	3.70	1.05	2.40	1.89	7.44	5.90
J	1.77	1.22	2.05	1.70	10.23	9.00
L	0.67	1.15	1.77	1.36	11.69	11.08

Fraction	S(film) 34°	S(film) 50°	Pore Radius (R_{cm}) 34°	Pore Radius (R_{cm}) 50°	R_{cm}/R_G 34°	R_{cm}/R_G 50°
B	1.36m.^{2}	1.23m.^{2}	240 A.	260 A.	0.61	0.59
F	3.53	3.12	177	188	1.03	0.99
J	5.79	5.29	102	112	0.86	0.86
L	7.54	8.15	94	92	1.28	1.15

limiting pore radius R_{cm} and the ratios R_{cm}/R_G so obtained.

There is no reason a priori to expect that the ratio R_{cm}/R_G should be exactly unity, though one would not expect it to be greatly different from unity if pore size is the only limiting factor in accessibility of the interior surface. One might expect the ratio to be the same for all fractions or to show a consistent trend in molecular weight. Either condition might be applied to the results in Table 22 except for the remarkable agreement in every case between the values of R_{cm}/R_G measured at the two different temperatures with the same fraction.

In view of the considerable experimental error in the measurements and the approximations involved in the calculations, this agreement may be fortuitous, even though it occurs in four cases. There is, however, another possible explanation for the observed results. The fractions used are not perfectly sharp, and so contain a great many molecules having molecular weights, and hence radii of gyration, considerably smaller than the average. More of the interior surface is accessible to these molecules than is accessible to those of average size, so their presence would tend to increase the value of A_o and thus decrease R_{cm}. The value of R_{cm}/R_G is smallest for the broad fraction, B, almost exactly unity for the sharp fraction, F, and less than unity for the broad fraction, J. The high value for fraction L remains unexplained, but another process may be operative in this case.

Since diffusion into pores has been postulated as a slow process that controls the rate of adsorption, and since diffusion presumably becomes slower as pores become deeper and smaller, the high value of R_{cm}/R_G for fraction L may be explained by failure of the molecules to penetrate

the pores as deeply as possible, either because the smaller pores were obstructed by adsorbed molecules or simply because even 25 days was insufficient time to allow for maximum penetration.

The steep slopes of the aluminum oxide isotherms may be explained by diffusion of polymer molecules in and out of pores. A molecule may be trapped inside a pore even though not adsorbed. This may take place by any of several mechanisms: plugging of the pore by adsorption of another molecule, entanglement with pendent loops from adsorbed molecules, low probability of diffusing out of a pore after entering because of reduced mobility in a confined space, etc. Thus, even after the surface is saturated, more polymer may be trapped and apparently adsorbed within the pore structure. This may be put in semi-quantitative terms by considering rates of diffusion in and out of pores.

Let s_1 be the rate at which polymer molecules diffuse into the pores. Then s_1 can be represented by

$$s_1 = k_1 c \tag{103}$$

where c = bulk concentration of polymer in solution;

k_1 = a proportionality constant.

By "into the pores" we mean into the region referred to above as the "interior surface." The rate of diffusion out of the pores, s_2, is given by

$$s_2 = k_2 c' \tag{104}$$

where c' = concentration of unadsorbed polymer inside the pores;

k_2 = a proportionality constant.

The constant k_2 is an average for pores of all shapes and, in a given sample of adsorbent, depends on the size distribution as well as on the sizes themselves. It should also depend somewhat on the amount of polymer inside the pores, since obviously the presence of a large quantity of polymer in the pores changes the effective size and shape of the pores. However, so long as the concentration of polymer inside the pores does not become too large, k_2 should be approximately independent of it.

After establishment of a steady state, s_1 and s_2 are equal and we have

$$k_1 c = k_2 c'; \quad c' = (k_1/k_2)c. \tag{105}$$

We have assumed that a polymer molecule is less likely to diffuse out of a pore than in, so that k_1/k_2 is greater than unity. Now the apparent adsorption, A, is given by

$$A = A_o + (c' - c)v_p \tag{106}$$

where A_o = specific adsorption at zero concentration;

v_p = volume of pores accessible to polymer molecules. Hence we have

$$A = A_o + (k_1/k_2 - 1)v_p c. \tag{107}$$

Qualitatively, Equation 107 predicts an increase in the slope of the isotherm with decreasing molecular weight, in general agreement with experimental results.

This same analysis might explain the steep slope of the isotherm for fraction B adsorbed on aluminum. The aluminum powder tended to form a cake inside the adsorption tubes that was not readily broken up, even by vigorous shaking. It is possible that the interstitial spaces within this cake were of the same order of magnitude as the dimensions of the large molecules, so that the cake acted as a porous adsorbent. The scatter in the data would arise from dissimilarities in the stability, compactness, and porosity of the cake from one tube to the next.

Adsorption of Ethylbenzene

The measurements of the adsorption of ethylbenzene on aluminum oxide were made in order to obtain an estimate of the heat of adsorption per segment of polystyrene. An adsorbed film may be treated as a separate phase, and the limiting slope of the isotherm at very low concentration of adsorbate as an equilibrium constant for the distribution of solute between the bulk phase and the adsorbed phase. The heat of adsorption may then be determined from the van't Hoff equation,

$$d\ln K/dT = \Delta H/RT^2 \qquad (108)$$

where K = equilibrium constant;

T = absolute temperature;

ΔH = heat of adsorption;

R = gas constant (94).

The limiting slopes of the isotherms at 34° and 50° C. are determined from Figure 41. Equation 108 may then be written in the integrated form

$$\Delta H = R(\ln K_2 - \ln K_1)/(1/T_1 - 1/T_2). \qquad (109)$$

The calculation is shown in Table 23. The resulting value of $-\Delta H$, about 4220 calories per mole, is equal to about 3.3 RT, almost sufficient to cause collapse of the adsorbed molecules and bring about two-dimensional adsorption, even according to the Simha-Frisch-Eirich theory (37). However, it should be pointed out that the adsorption of ethylbenzene may be very different from that of polystyrene. The small molecules are adsorbed independently of one another and are able to assume low-energy orientations with respect to the surface. Polystyrene segments, being connected to other segments, are not free to assume an arbitrary orientation on the surface, and may be adsorbed in configurations of significantly higher energy, thus reducing the effective heat of adsorption per segment. Thus, the heat of adsorption of ethylbenzene must be regarded as only a crude estimate of the heat of adsorption of polystyrene.

Table 23. Heat of Adsorption of Ethylbenzene

T(°K.)	$1/T \times 10^3$	K	ln K
307	3.245	1.687	0.523
323	3.098	0.870	-0.139

$\Delta H = 1.987(0.532 + 0.139)/(3.098 - 3.245) \times 10^3$

$= 1.987(0.671)/(-1.57) \times 10^4$

$=$ -4220 calories per mole

CHAPTER V

CONCLUSIONS

1. The adsorption behavior of polystyrene on aluminum powder is qualitatively similar to that observed previously for other polymers on non-porous adsorbents. In most cases the isotherms are nearly-horizontal straight lines down to the lowest concentrations that can be determined experimentally. Adsorption increases with increasing molecular weight and decreases with increasing temperature. Desorption is not observed within a period of days in the presence of a poor solvent, even when the temperature is increased, but is readily effected through the use of a good solvent.

2. Within experimental error, polyisobutylene is not adsorbed from benzene, a poor solvent, onto aluminum. This result is attributed to preferential adsorption of the solvent. Other investigators (14, 16, 17) have observed that other things being equal, adsorption is greater from a poor solvent than from a good one. An exception to this rule was the case of polyvinyl acetate in acetonitrile, a relatively poor solvent (14). Preferential adsorption of the solvent, attributed to the high polarity of acetonitrile, altogether excluded adsorption of the polymer. In this case, non-adsorption of the polymer from a poor solvent must be attributed to the existence of pi bonds in the solvent, making possible charge transfer forces. Polystyrene, on the other hand, is strongly adsorbed, probably through its aromatic side chains, in preference to

cyclohexane which has no pi bonds.

3. The adsorption of polystyrene on the porous adsorbent alumina is limited by the ability of the polymer molecules to penetrate the pore structure. Such penetration appears to be limited, at least in a poor solvent, by the dimensions of the polymer molecule in solution. Further work in this area is indicated, but if this result proves to be general, it should provide a method for determining molecular dimensions in sharp fractions. If porous adsorbents can be prepared with narrow pore-size distributions, it could also provide the basis of a simple method of selective fractionation.

APPENDIX

ADSORPTION DATA

Fraction: B
Number-Average Molecular Weight (M_n): 15.0×10^5
Weight-Average Molecular Weight (M_w): 18.4×10^5
Ratio M_w/M_n: 1.22
Adsorbent: Aluminum Powder

Vial	Weight of Adsorbent (grams)	Weight of Solution (grams)	Initial concentration (mg./100 g.)	Final Concentration (mg./100 g.)	Specific Adsorption (mg./g.)
	Temperature:	34.8° C.	Adsorption Time:	6 Days	
1a	1.0308	7.5655	98.7	34.7	4.69
2a	1.5097	7.5506	98.7	17.5	4.06
3a	2.0074	7.5453	98.7	17.1	3.06
4a	3.0254	7.7844	98.7	0	2.54
5a	4.2320	7.5680	98.7	1.3	1.74
				A_o:	--
	Temperature:	34.8° C.	Adsorption Time:	25 Days	
1b	0.4613	7.4502	111.1	62.6	7.83
2b	0.9813	7.4657	111.1	39.3	5.46
3b	1.4922	7.4555	111.1	21.1	4.50
4b	1.9913	7.4843	111.1	11.0	3.76
5b	2.9760	7.4864	111.1	1.5	2.76
				A_o:	2.70
	Temperature:	50° C.	Adsorption Time:	25 Days	
1c	0.4926	7.4906	110.2	81.6	4.35
2c	1.0212	7.4779	110.2	59.3	3.73
3c	1.5267	7.5126	110.2	44.8	3.22
4c	2.0094	7.4929	110.2	28.3	3.05
				A_o:	2.18

ADSORPTION DATA

Fraction: B
Number-Average Molecular Weight (M_n): 15.0×10^5
Weight-Average Molecular Weight (M_w): 18.4×10^5
Ratio M_w/M_n: 1.22
Adsorbent: Aluminum Oxide

Vial	Weight of Adsorbent (grams)	Weight of Solution (grams)	Initial Concentration (mg./100 g.)	Final Concentration (mg./100 g.)	Specific Adsorption (mg./g.)
	Temperature:	34.8° C.	Adsorption Time:	6 Days	
1d	0.5228	7.5571	98.7	72.3	3.81
2d	1.0152	7.5462	98.7	52.2	3.46
3d	1.5528	7.5558	98.7	36.1	3.04
4d	2.1247	7.5371	98.7	23.1	2.68
5d	3.0992	7.5277	98.7	3.9	2.31
					A_o: --
	Temperature:	34.8° C.	Adsorption Time:	25 Days	
1e	0.2399	7.4353	111.1	94.9	5.02
2e	0.7144	7.4877	111.1	68.3	4.49
3e	0.9390	7.5041	111.1	58.5	4.20
4e	1.8933	7.4699	111.1	17.1	3.71
					A_o: 3.33
	Temperature:	50° C.	Adsorption Time:	25 Days	
1f	0.2468	7.4909	110.2	102.4	2.37
2f	0.4665	7.5074	110.2	95.9	2.30
3f	0.7032	7.4771	110.2	87.2	2.45
4f	0.9441	7.5001	110.2	77.7	2.58
5f	1.8818	7.4950	110.2	54.7	2.21
					A_o: 2.36

ADSORPTION DATA

Fraction: F
Number-Average Molecular Weight (M_n): 3.54×10^5
Weight-Average Molecular Weight (M_w): 3.70×10^5
Ratio M_w/M_n: 1.05
Adsorbent: Aluminum Powder

Vial	Weight of Adsorbent (grams)	Weight of Solution (grams)	Initial Concentration (mg./100 g.)	Final Concentration (mg./100 g.)	Specific Adsorption (mg./g.)
	Temperature: 34.8° C.		Adsorption Time: 6 Days		
11a	1.0438	7.5490	100.9	65.3	2.57
12a	1.5191	7.5537	100.9	52.4	2.41
13a	2.0295	7.5362	100.9	37.4	2.36
14a	3.0045	7.5620	100.9	13.5	2.20
15a	4.0150	7.5451	100.9	0.1	2.03
					A_o: --
	Temperature: 34.8° C.		Adsorption Time: 25 Days		
11b	0.4898	7.5169	108.9	86.5	3.44
12b	1.0231	7.5024	108.9	70.0	2.85
13b	1.5017	7.4962	108.9	55.0	2.69
14b	1.9847	7.5088	108.9	39.3	2.63
15b	2.9623	7.4957	108.9	12.6	2.44
					A_o: 2.40
	Temperature: 50° C.		Adsorption Time: 25 Days		
11c	0.4674	7.4929	110.3	96.6	2.20
12c	1.0443	7.5023	110.3	81.4	2.08
13c	1.5292	7.4910	110.3	68.7	2.04
14c	2.0179	7.5167	110.3	52.3	2.16
15c	3.0390	7.4956	110.3	32.0	1.93
					A_o: 1.89

ADSORPTION DATA

Fraction: F
Number-Average Molecular Weight: 3.54×10^5
Weight-Average Molecular Weight: 3.70×10^5
Ratio M_w/M_n: 1.05
Adsorbent: Aluminum Oxide

Vial	Weight of Adsorbent (grams)	Weight of Solution (grams)	Initial Concentration (mg./100 g.)	Final Concentration (mg./100 g.)	Specific Adsorption (mg./g.)
	Temperature:	34.8° C.	Adsorption Time:	6 Days	
11d	0.5159	7.5620	100.9	47.7	7.96
12d	1.0220	7.5572	100.9	15.3	6.33
13d	1.5191	7.5584	100.9	1.7	4.94
14d	2.0419	7.5824	100.9	0	3.74
15d	3.0805	7.5815	100.9	0	--
				A_o:	--
	Temperature:	34.8° C.	Adsorption Time:	25 Days	
11e	0.1243	7.4749	108.9	91.3	10.58
12e	0.2496	7.4940	108.9	75.6	10.00
13e	0.3508	7.4975	108.9	64.8	9.43
14e	0.4852	7.5005	108.9	50.2	9.07
15e	0.7000	7.5005	108.9	29.5	8.51
				A_o:	7.44
	Temperature:	50° C.	Adsorption Time:	25 Days	
11f	0.1466	7.5208	110.3	90.1	10.36
12f	0.2733	7.5371	110.3	78.3	8.82
13f	0.3660	7.5314	110.3	69.8	8.33
14f	0.4778	7.5487	110.3	60.0	7.95
15f	0.9522	7.5171	110.3	24.2	6.80
				A_o:	5.90

ADSORPTION DATA

Fraction: J
Number-Average Molecular Weight (M_n): 1.45×10^5
Weight-Average Molecular Weight (M_w): 1.77×10^5
Ratio M_w/M_n: 1.22
Adsorbent: Aluminum Powder

Vial	Weight of Adsorbent (grams)	Weight of Solution (grams)	Initial Concentration (mg./100 g.)	Final Concentration (mg./100 g.)	Specific Adsorption (mg./g.)
	Temperature: 34.8° C.		Adsorption Time: 6 Days		
21a	1.0208	7.5189	98.9	72.0	1.96
22a	1.5568	7.5275	98.9	57.4	2.04
23a	2.0490	7.5183	98.9	46.7	1.92
24a	3.9952	7.5480	98.9	9.1	1.68
				A_o:	--
	Temperature: 34.8° C.		Adsorption Time: 25 Days		
21b	0.5096	7.5049	111.8	91.8	2.95
22b	0.9922	7.4951	111.8	76.7	2.65
23b	1.5194	7.4959	111.8	60.7	2.52
24b	1.9419	7.4925	111.8	51.5	2.33
25b	3.0472	7.7455	111.8	25.6	2.19
				A_o:	2.05
	Temperature: 50° C.		Adsorption Time: 25 Days		
21c	0.5400	7.4904	107.6	83.4	3.36
22c	1.0096	7.5089	107.6	80.1	2.05
23c	1.5826	7.4789	107.6	70.2	1.77
24c	2.0003	7.5182	107.6	60.7	1.76
25c	3.5146	7.5110	107.6	27.7	1.71
				A_o:	1.70

ADSORPTION DATA

Fraction: J
Number-Average Molecular Weight (M_n): 1.45×10^5
Weight-Average Molecular Weight (M_w): 1.77×10^5
Ratio M_w/M_n: 1.22
Adsorbent: Aluminum Oxide

Vial	Weight of Adsorbent (grams)	Weight of Solution (grams)	Initial Concentration (mg./100 g.)	Final Concentration (mg./100 g.)	Specific Adsorption (mg./g.)
	Temperature: 34.8° C.		Adsorption Time: 6 Days		
21d	0.4969	7.5167	98.9	31.1	10.24
22d	0.0109	7.5030	98.9	0	7.33
23d	1.5704	7.5279	98.9	0	--
24d	2.0609	7.7762	98.9	0	--
25d	3.0115	7.5525	98.0	0	--
				A_o:	--
	Temperature: 34.8° C.		Adsorption Time: 25 Days		
21e	0.1213	7.4962	111.8	90.7	13.04
22e	0.2437	7.5156	111.8	71.5	12.43
23e	0.3578	7.4984	111.8	54.2	12.07
24e	0.4673	7.4845	111.8	37.8	11.85
25e	0.7138	7.4885	111.8	10.4	10.64
				A_o:	10.23
	Temperature: 50° C.		Adsorption Time: 25 Days		
21f	0.1333	7.5445	107.6	85.3	12.62
22f	0.2478	7.4955	107.6	69.1	11.80
23f	0.3640	7.5158	107.6	54.6	10.94
24f	0.4788	7.4927	107.6	54.6	10.63
25f	0.7516	7.5064	107.6	12.1	9.54
				A_o:	9.00

ADSORPTION DATA

Fraction: L
Number-Average Molecular Weight (M_n): 0.58×10^5
Weight-Average Molecular Weight (M_w): 0.67×10^5
Ratio M_w/M_n: 1.15
Adsorbent: Aluminum Powder

Vial	Weight of Adsorbent (grams)	Weight of Solution (grams)	Initial Concentration (mg./100 g.)	Final Concentration (mg./100 g.)	Specific Adsorption (mg./g.)
	Temperature: 34.8° C.		Adsorption Time: 6 Days		
31a	1.0105	7.5423	99.8	78.3	1.61
32a	1.5034	7.5232	99.8	68.5	1.57
33a	1.9110	7.5412	99.8	57.8	1.66
33a	3.0615	7.6974	99.8	37.4	1.57
34a	3.9916	7.5090	99.8	23.2	1.44
				A_o:	--
	Temperature: 34.8° C.		Adsorption Time: 25 Days		
31b	0.4908	7.5119	112.7	94.5	2.79
32b	1.5151	7.4880	112.7	70.3	2.10
33b	2.0638	7.4867	112.7	56.7	2.03
34b	2.9437	7.4859	112.7	36.4	1.94
				A_o:	1.77
	Temperature: 50° C.		Adsorption Time: 25 Days		
31c	0.4875	7.4560	106.1	94.5	2.79
32c	1.0810	7.4656	106.1	84.5	1.49
33c	1.4778	7.4651	106.1	76.0	1.52
34c	2.0027	7.4708	106.1	64.7	1.54
35c	3.7075	7.4740	106.1	34.7	1.44
				A_o:	1.36

ADSORPTION DATA

Fraction: L
Number-Average Molecular Weight (M_n): 0.58×10^5
Weight-Average Molecular Weight (M_w): 0.67×10^5
Ratio M_w/M_n: 1.15
Adsorbent: Aluminum Oxide

Vial	Weight of Adsorbent (grams)	Weight of Solution (grams)	Initial Concentration (mg./100 g.)	Final Concentration (mg./100 g.)	Specific Adsorption (mg./g.)
	Temperature: 34.8° C.		Adsorption Time: 6 Days		
31d	0.5673	7.9200	99.8	15.0	11.84
32d	1.0017	7.5176	99.8	0	7.48
33d	1.5049	7.5394	99.8	0	--
34d	2.0622	7.5216	99.8	0	--
35d	3.0838	7.5551	99.8	0	--
				A_o:	--
	Temperature: 34.8° C.		Adsorption Time: 25 Days		
31e	0.1269	7.4689	112.7	86.3	15.21
32e	0.3557	7.4920	112.7	49.0	13.42
33e	0.4781	7.4864	112.7	28.9	13.12
34e	0.7092	7.4989	112.7	3.4	11.56
				A_o:	11.69
	Temperature: 50° C.		Adsorption Time: 25 Days		
31f	0.1248	7.4985	106.1	74.6	18.93
32f	0.2156	7.4872	106.1	58.5	16.53
33f	0.3455	7.4686	106.1	38.7	14.57
34f	0.4843	7.4954	106.1	18.7	13.53
35f	0.7036	7.4833	106.1	0	11.28
				A_o:	11.08

LITERATURE CITED

1. C. Tanford, Physical Chemistry of Macromolecules, John Wiley and Sons, Inc., New York, 1961, p. 189.

2. Ibid, p. 202.

3. Ibid, p. 249.

4. H. Mark and G. Saito, Monatshefte für Chemie und Verwandte Teile Anderer Wissenschaften, 68, 237 (1936).

5. I. Claesson and S. Claesson, Arkiv for Kemi, Mineralogi och Geologi, 19A, No. 5 (1945).

6. S. Claesson, ibid., 26A, No. 24 (1949).

7. I. Landler, Comptes Rendus, Academie des Sciences, Paris, 225, 234 (1947).

8. E. Jenckel and B. Rumbach, Zeitschrift für Elektrochemie und Angewandte Physikalische Chemie, 55, 612 (1951).

9. J. S. Binford, Jr. and A. M. Gessler, Journal of Physical Chemistry, 63, 1376 (1957).

10. F. Patat and C. Schliebener, Die Makromolekulare Chemie, 46, 643 (1961).

11. F. Patat and L. Estupinian, ibid., 49, 182, (1962).

12. F. Patat, E. Killmann, and C. Schliebener, ibid., 49, 200 (1962).

13. R. Perkel and R. Ullman, Journal of Polymer Science, 54, 127 (1961).

14. J. Koral, R. Ullman, and J. L. Eirich, J. Phys. Chem., 62, 541 (1958).

15. H. L. Frisch, M. Y. Hellman, and J. L. Lundberg, J. Polymer Sci., 38, 441 (1959).

16. S. Ellerstein and R. Ullman, ibid., 55, 123 (1961).

17. P. J. Kangle and E. Pacsu, ibid., 54, 301 (1961).

18. I. M. Kolthoff, R. G. Gutmacher, and A. Kahn, J. Phys. Chem., 55, 1240 (1951).

19. I. M. Kolthoff and R. G. Gutmacher, ibid., 56, 740 (1952).

20. B. J. Fontana, ibid., 67, 2361 (1963).

21. B. J. Fontana and J. R. Thomas, ibid., 65, 480 (1961).

22. R. R. Stromberg, E. Passaglia, and D. J. Tutas, Journal of Research of the National Bureau of Standards, 67A, 431 (1963).

23. W. Heller and W. Tanaka, Physical Review, 82, 302 (1951).

24. E. Treiber, G. Porod, W. Gierlinger, and J. Schulz, Makromol. Chem., 9, 241 (1953).

25. J. F. Hobden and H. H. G. Jellinek, J. Polymer Sci., 11, 365 (1953).

26. E. R. Gilliland and E. B. Gutoff, Journal of Applied Polymer Science, 3, 26 (1960).

27. H. H. G. Jellinek and H. A. Northey, J. Polymer Sci., 14, 863 (1954).

28. A. I. Yurzhenko and I. I. Maleyev, ibid., 31, 301 (1958).

29. C. Peterson and T. K. Kwei, J. Phys. Chem., 65, 1330 (1961).

30. E. L. Mackor and J. M. van der Waals, J. Coll. Sci., 7, 535 (1952).

31. L. Sarolea, Academie Royale de Belgique, Classe das Sciences Bulletin, Series 5, 40, 1131 (1954).

32. R. Simha, H. L. Frisch, and F. R. Eirich, J. Phys. Chem., 57, 584 (1953).

33. S. Chandrasekhar, Reviews of Modern Physics, 15, 1 (1943).

34. H. L. Frisch and R. Simha, J. Phys. Chem., 58, 507 (1954).

35. H. L. Frisch and R. Simha, Journal of Chemical Physics, 27, 702 (1957).

36. H. L. Frisch, J. Phys. Chem., 59, 633 (1955).

37. W. I. Higuchi, ibid., 65, 487 (1961).

38. E. R. Gilliland and E. B. Gutoff, ibid., 64, 407 (1960).

39. W. C. Forsman and R. E. Hughes, J. Chem. Phys., 38, 2118 (1963).

40. W. C. Forsman and R. E. Hughes, ibid, 38, 2123 (1963).

41. W. C. Forsman and R. E. Hughes, ibid., 38, 2130 (1963).

42. A. Silberberg, J. Phys. Chem., 66, 1872 (1962).

43. A. Silberberg, ibid., 66, 1884 (1962).

44. H. Tompa, Polymer Solutions, Butterworths Scientific Publications, London, 1956, Chapter 7.

45. G. V. Schulz, Zeitschrift für physikalische Chemie, B46, 137 (1940).

46. V. Desreux, Receuil des Travaux chemiques des Pays-Bas, 68, 789 (1949).

47. C. A. Baker and R. J. P. Williams, Journal of the Chemical Society, 1956, 2352.

48. N. S. Schneider, L. H. Holmes, C. F. Mijal, and J. D. Loconti, J. Polymer Sci., 37, 551 (1959).

49. N. S. Schneider, J. D. Loconti, and L. G. Holmes, J. Appl. Polymer Sci., 5, 354 (1961).

50. R. W. Hall, "The Fractionation of High Polymers," in Techniques of Polymer Characterization (P. W. Allen, ed.) Butterworths Scientific Publications, London, 1959, Chapter 2.

51. D. C. Pepper and P. P. Rutherford, J. Appl. Polymer Sci., 2, 100 (1959).

52. N. S. Schneider, J. D. Loconti, and L. G. Holmes, ibid, 3, 251 (1960).

53. Chu, Ju-Chin, Vapor-Liquid Equilibrium Data, J. W. Edwards, Inc., Ann Arbor, Michigan, 1956.

54. Tanford, pp. 145-147.

55. G. V. Schulz and A. Dinglinger, Z. phys. Chem., B43, 47 (1939).

56. I. C. Booth, J. Polymer Sci., 45, 443 (1960).

57. I. C. Booth and L. R. Beeson, ibid., 42, 80 (1960).

58. H. T. Hookway, "Number-Average Molecular Weights by Osmometry," in Techniques of Polymer Characterization (P. W. Allen, ed.) Butterworths Scientific Publications, London, 1959, Chapter 3.

59. J. V. Stabin and E. H. Immergut, J. Polymer Sci., 14, 209 (1954).

60. R. U. Bonnar, M. Dimbat, and F. H. Stross, Number-Average Molecular Weights, Interscience, New York, 1958, Chapter 5.

61. Tanford, Chapter 5.

62. "Brice-Phoenix Light Scattering Photometer Operation Manual, OM-1000A," Phoenix Precision Instrument Company, Philadelphia, 1957.

63. B. H. Zimm, J. Chem. Phys., 16, 1099 (1948).

64. Tanford, p. 228.

65. E. U. Condon, "Electromagnetic Waves," in Handbook of Physics (E. U. Condon and H. Odishaw, eds.) McGraw-Hill, New York, 1958. p. 6 - 9.

66. M. Gubler, C. Reiss, and H. Benoit, Journal de Chemie et Physique et de Physicochimique Biologique, 59 421 (1962).

67. American Institute of Physics Handbook, McGraw-Hill, 1957, p. 6-18.

68. "Brice-Phoenix Differential Refractometer Operation Manual," Phoenix Precision Instrument Company, Philadelphia, 1957.

69. H. Mark, Der Feste Körper, Hirzel, Leipzig, p. 103.

70. R. Houwink, Journal für Praktische Chemie, 157, 15 (1941).

71. A. R. Schultz and P. J. Flory, J. Polymer Sci., 15, 231 (1955).

72. P. Outer, C. I. Carr, and B. H. Zimm, J. Chem. Phys., 18, 830 (1950).

73. T. G. Fox, Jr., and P. J. Flory, J. Phys. and Colloid Chem., 53, 197 (1949).

74. M. L. Huggins, Journal of the American Chemical Society, 64, 2716 (1942).

75. P. F. Onyon, "Viscometry," in Techniques of Polymer Characterization (P. W. Allen, ed.) Butterworth Scientific Publications, London, 1959, Chapter 6.

76. Tompa, p. 284 ff.

77. E. C. Bingham and R. F. Jackson, Bulletin of the National Bureau of Standards, 14, 75 (1918).

78. V. L. Streeter, Fluid Mechanics, Third Edition, McGraw-Hill, New York, p. 422.

79. P. J. Flory, Principles of Polymer Chemistry, Cornell University Press, Ithaca, New York, 1953, p. 310.

80. S. Brunauer, P. H. Emmett, and E. Teller, J. Am. Chem. Soc., 60, 309 (1938).

81. C. Orr, Jr. and J. M. DallaValle, Fine Particle Measurement, Macmillan, New York, 1959, Chapter 10.

82. E. P. Barrett, L. G. Joyner, and P. P. Halenda, J. Am. Chem. Soc., 73, 373 (1951).

83. C. Pierce, J. Phys. Chem., 57, 149 (1953).

84. C. G. Shull, J. Am. Chem. Soc., 70, 1405 (1948).

85. W. J. Corbett, E. H. Burson, and R. A. Young, Clays and Clay Minerals, 10, 344 (1963).

86. Handbook of Chemistry and Physics, 33rd Edition, Chemical Rubber Publishing Company, Cleveland, Ohio, 1951, p. 448.

87. F. Danusso and G. Moraglio, J. Polymer Sci., 24, 161 (1957).

88. Tanford, p. 219.

89. Ibid., p. 162.

90. Flory, pp. 612-618.

91. W. R. Krigbaum and D. K. Carpenter, J. Phys. Chem., 59, 1166 (1955).

92. N. T. Notley and P. Debye, J. Polymer Sci., 24, 275 (1957).

93. Orr and Dallavalle, p. 185.

94. J. J. Kipling and D. B. Peakall, J. Chem. Soc., 1956, 4828.

95. K. Denbigh, The Principles of Chemical Equilibrium, Cambridge University Press, Cambridge, 1961, p. 141.

VITA

Harris Burns, Jr. was born July 14, 1933 in Birmingham, Alabama. He attended the public schools of Birmingham and, in 1950, enrolled at Harvard University. In 1952 he transferred to the Georgia Institute of Technology, where he received the degrees of Bachelor of Chemical Engineering in 1954 and Master of Science in Chemical Engineering in 1958. From 1956 through 1958 he served as an officer in the United States Army and was a member of the faculty of the U. S. Army Chemical Corps School. After working for a short while at the Lawrence Radiation Laboratory at Livermore, California, he returned to Georgia Tech in 1959 to pursue advanced study in chemistry. In 1961 he was married to Priscilla Elise Goree. At present he is a member of the staff of the Department of Chemistry and Chemical Engineering of the University of Illinois.